UNIVERSITY OF CALIFORNIA, SAN DIEGO

Business Cases for Microgrids: Modeling Interactions of Technology Choice, Reliability, Cost, and Benefit

A dissertation submitted in partial satisfaction of the
requirements for the degree Doctor of Philosophy

in

Engineering Sciences (Mechanical Engineering)

by

Ryan Hanna

Committee in charge:

Jan Kleissl, Chair
Duncan S. Callaway
Joshua Graff Zivin
William V. Torre
George R. Tynan
David G. Victor

2017

The Dissertation of Ryan Hanna is approved and is acceptable in quality and form for publication on microfilm and electronically:

_____

_____

_____

_____

_____

_____

Chair

University of California, San Diego

2017

DEDICATION

To my parents, family, and friends; and to those devoted to a better, fairer, more equitable and sustainable world.

TABLE OF CONTENTS

LIST OF FIGURES

LIST OF TABLES

ACKNOWLEDGEMENTS

First and foremost, I must acknowledge the support of my parents and family. It is only by their constant love and support that I have found myself in a position to undertake this dissertation.

I gratefully acknowledge the mentorship of my advisors Professor Jan Kleissl and Professor David Victor, as well as of William Torre and Byron Washom, over the course of my studies. To simply watch and observe has been to learn and better myself professionally.

I am thankful to my committee members, Professor Duncan Callaway, Professor Joshua Graff Zivin, Bill Torre, Professor George Tynan, and Professor David Victor for their valuable input during the preparation of this dissertation.

I acknowledge also the support of all my colleagues and collaborators throughout my years at the University of California, San Diego. I give special thanks to Oytun Babacan, Mohamed Ghonima, Vahid Disfani, Elizabeth Ratnam, Zack Pecenak, Keenan Murray, Abdulelah Habib, Andu Nyugen, Ben Kurtz, Handa Yang, Guang Wang, and Changfu Li. Those in the Solar Resource Assessment and Forecasting Laboratory made our research environment special and fun.

The friendships I made in San Diego, as people arrived, departed, and returned again, are among the closest I have. I was lucky to meet and grow close to Oytun, Mohamed, Augusta, Tina, Handa, Margherita, Amedeo, Marta, Emilia, Carlotta, Jesus Bueno, George, Kristen, Marine, Victor 1, Victor 2, Sebastian, Maxime, Coral, and Aida. The international nature of graduate school was something I did not expect, and an experience I would never wish to relinquish.

The text and data in Chapter 1, in full, is a reprint of the material as it appears in "Evaluating business models for microgrids: Interactions of technology and policy", Hanna, Ryan; Ghonima, Mohamed, Kleissl, Jan, Tynan, George, David G., Victor, *Energy*

Policy, 103 (2017), 47-61. The dissertation author is the primary investigator and author of this article.

The text and data in Chapter 2, in full, is submitted for publication of the material with the title "Reliability evaluation for microgrids using cross-entropy Monte Carlo simulation". Hanna, Ryan; Disfani, Vahid R.; Kleissl, Jan. The dissertation author is the primary investigator and author of this article.

Chapter 3, in part, is currently being prepared for submission for publication of material. Hanna, Ryan; Disfani, Vahid R.; Kleissl, Jan; Victor, David G. The dissertation author is the primary investigator and author of this article.

Chapter 4, in part, is currently being prepared for submission for publication of material. Hanna, Ryan; Kleissl, Jan; Victor, David G. The dissertation author is the primary investigator and author of this article.

VITA

2011	Bachelor of Arts, Pacific Lutheran University
2011	Bachelor of Science, Washington University in Saint Louis
2013	Master of Science, University of California San Diego
2017	Doctor of Philosophy, University of California San Diego

PUBLICATIONS

R. Hanna; J. Kleissl and D.G. Victor. "The impact of microgrids on greenhouse gas emissions in California". In: Preparation.

R. Hanna; V. Disfani and J. Kleissl and D.G. Victor. "The economic value of reliability for microgrids: Modeling reliability costs and value". In: Preparation.

R. Hanna; V. Disfani and J. Kleissl. "Reliability evaluation for microgrids using cross-entropy Monte Carlo simulation". In: Review.

R. Hanna; V. Disfani and J. Kleissl and D.G. Victor. "A new simulation model to develop and assess business cases for commercial microgrids". In: North American Power Symposium (NAPS). Morgantown, WV, September 2017.

R. Hanna; M. Ghonima and J. Kleissl and G. Tynan and D.G. Victor. "Evaluating business models for microgrids: Interactions of technology and policy". In: Energy Policy 103 (2017), pp. 47 - 61.

R. Hanna; V. Disfani and J. Kleissl. "A game-theoretical approach to variable renewable generator bidding in wholesale electricity markets". In: North American Power Symposium (NAPS). Denver, CO, September 2016.

R. Hanna; J. Kleissl and A. Nottrott and M. Ferry. "Energy dispatch schedule optimization for demand charge reduction using a photovoltaic-battery storage system with solar forecasting". In: Solar Energy 103 (2014), pp. 269 - 287.

ABSTRACT OF THE DISSERTATION

Business Cases for Microgrids: Modeling Interactions of Technology Choice, Reliability, Cost, and Benefit

by

Ryan Hanna

Doctor of Philosophy in Engineering Sciences (Mechanical Engineering)

University of California, San Diego, 2017

Jan Kleissl, Chair

Distributed energy resources (DERs), and increasingly microgrids, are becoming an integral part of modern distribution systems. Interest in microgrids—which are insular and autonomous power networks embedded within the bulk grid—stems largely from the vast array of flexibilities and benefits they can offer stakeholders. Managed well, they can improve grid reliability and resiliency, increase end-use energy efficiency by coupling electric and thermal loads, reduce transmission losses by generating power locally, and may reduce system-wide emissions, among many others. Whether these public benefits are realized, however, depends on whether private firms see a "business case", or private

value, in investing. To this end, firms need models that evaluate costs, benefits, risks, and assumptions that underlie decisions to invest.

The objectives of this dissertation are to assess the business case for microgrids that provide what industry analysts forecast as two primary drivers of market growth—that of providing energy services (similar to an electric utility) as well as reliability service to customers within. Prototypical first adopters are modeled—using an existing model to analyze energy services and a new model that couples that analysis with one of reliability—to explore interactions between technology choice, reliability, costs, and benefits.

The new model has a bi-level hierarchy; it uses heuristic optimization to select and size DERs and analytical optimization to schedule them. It further embeds Monte Carlo simulation to evaluate reliability as well as regression models for customer damage functions to monetize reliability. It provides least-cost microgrid configurations for utility customers who seek to reduce interruption and operating costs.

Lastly, the model is used to explore the impact of such adoption on system-wide greenhouse gas emissions in California. Results indicate that there are, at present, co-benefits for emissions reductions when customers adopt and operate microgrids for private benefit, though future analysis is needed as the bulk grid continues to transition toward a less carbon intensive system.

Introduction

The electric power industry, and indeed the electric power grid, are in the midst of transformation. Over the past half decade, adoption rates for utility-scale renewables have increased dramatically. State governments have set ambitious renewable energy portfolio standards of $30\%-50\%$ or more. Industry and interest groups believe much higher numbers are achievable, that we lack only concerted political will. At the distributed level, customer adoption rates for distributed energy resources have seen substantial increase as well—notably solar photovoltaics and increasingly battery energy storage, both stationary and in electric vehicles. Microgrids are finding their place in that picture. With aid in the form of government subsidies, a strong and self-sustaining industry and market for renewables and distributed energy technologies has taken hold in the United States, and in California in particular. Government support is focused, and public support for grid decarbonization is strong. Climate stabilization goals demand a long-term view, yet with immediate action.

One area of intent government focus has been to address grid modernization—especially in the wake of deadly and costly Atlantic superstorms (Sandy in 2012, Maria in 2017) that caused destruction throughout the U.S. and Caribbean. Microgrids have been a focal point of that conversation. Indeed, many states have initiated proceedings that aim to improve grid reliability and resiliency for critical public services via microgrids, among other means. While policy support has spurred public-purpose systems, in the private sector, technology, market, and social forces are enabling a nascent market for

private microgrids. In some jurisdictions today, microgrids are becoming economically viable for certain utility customers. Industry analysts see reliability as a primary driver.

The logic for support and interest lies in the many potential benefits microgrids can provide—improving power quality, bulk grid resiliency, black-start capability, electric service reliability; deferring costs of grid capacity expansion; reducing transmission losses and possibly system-wide emissions. Whether those public benefits are realized, however, depends on whether investors see *private* benefits from building microgrids. Private firms will need to develop "business models" through which they can generate revenue and/or reduce cost. To this end, firms need analytical tools that quantify revenue streams and costs, make it possible to examine risks and robustness of assumptions, and, ultimately, that inform investment decision-making.

Though the value streams available to microgrids—including improving reliability and resiliency—are well-documented (Stadler et al., 2016), the evidentiary basis for understanding when and where microgrids are cost-effective remains contested. Models that quantify the business case by which investors will make real investment decisions using realistic modeling and optimization techniques are essential.

Mathematical models for microgrid resources are the basis for such modeling. That literature is well-established and includes, e.g., micro-turbines (Ismail et al., 2013), combined heat and power systems (Gu et al., 2014), renewables (Sinha and Chandel, 2015), and energy storage (Ru et al., 2013; Nottrott et al., 2013). So too are methodologies and optimization techniques for renewable systems and hybrid energy systems that couple renewables with conventional thermal generators (Erdinc and Uzunoglu, 2012; Upadhyay and Sharma, 2014; Iqbal et al., 2014; Fathima and Palanisamy, 2015). Microgrid models, which are slightly broader in scope, use these optimization techniques to connect resource models with other technical, economic and financial parameters to inform decision-making in the design process. Decision-making typically consists of resource siting,

selection and sizing, and/or scheduling (Gamarra and Guerrero, 2015) and is aligned to support a potentially broad array of design objectives that span economic, environmental, and/or reliability criteria (Khan et al., 2016). The literature for these models, too, is well-established.

Ultimately, we are interested in a final type of microgrid model that connects technologies, economics, risk, policy constraints (or enablers), and available revenue streams to quantify, ultimately, the business case by which firms will make real investment decisions. These models report the net present value or annual revenue and cost streams of an optimal microgrid configuration as well as associated sensitivities, financial risks, and uncertainties over the lifespan of the system. Some notable modeling tools with this capability have been developed. For instance, state-of-the-art techno-economic tools include two popular commercial models, DER-CAM (Distributed Energy Resources Customer Adoption Model) from Lawrence Berkeley National Laboratory and HOMER (Hybrid Optimization of Multiple Energy Sources) from HOMER Energy LLC. Both are used widely in literature and practice to analyze a specific business model—namely, the potential for customers to reduce energy costs by shifting from utility service to a microgrid that is optimally configured to supply energy locally. While local energy provision may be a driving force for microgrid adoption, other goals may prove more important yet harder to assess quantitatively—in particular, improvements in reliability. Existing commercial tools that are deterministic are not able to assess the question of reliability realistically and systematically. Models that evaluate reliability specifically must consider reliability and cost as a trade-off in the optimization process (Zhou et al., 2016)—which is the basis for any sensible model built for business case analysis. Such reliability-based modeling has been applied to rural off-grid systems (Siddaiah and Saini, 2016), but is relatively lacking for grid-connected systems in modern grids.

Putting reliability aside for the moment, we turn now to a brief categorical sur-

vey of the modeling literature—narrowing it before returning full circle to reliability. Those models broadest in scope simultaneously optimize resource selection and scheduling. These "investment and dispatch" models evaluate microgrids by considering the interactions within them that define business cases—for instance between technology choice, cost, energy demand and supply, and emissions. They use various optimization techniques to connect individual resource models with other technical, economic, and financial parameters and constraints (Liang and Zhuang, 2014). Some include a wide array of resources like fossil generators, solar PV, wind, and storage, as well as thermal resources like boilers and thermal energy storage (Zachar et al., 2015; Zachar and Daoutidis, 2015), while others focus more narrowly and in greater detail on a single set of technologies, e.g. combined heat and power systems (Zidan et al., 2015; Zhang et al., 2015). Investment and dispatch models are often formulated as mathematical programs to minimize the net present cost, or maximize the net present value (including, typically, the capital cost of investment amortized over the lifetime of the system as well as the annual operating cost), of a microgrid that produces energy locally for sale to customers or the incumbent utility, or that avoids utility tariffs costs.

Slightly narrower in scope are models that optimize resource scheduling only, given a fixed resource configuration. These "dispatch" models too may be applied broadly to a diverse set of resources or narrowly to study specific technologies like battery storage (Hittinger et al., 2015). They determine a resource operating schedule that minimizes the annual operating cost, and may employ mathematical programming or heuristic methods. Those models reported in literature, as with the investment and dispatch models, have been designed to consider the core value streams associated with supplying energy locally. Notably, they have not yet optimized for reliability.

Nevertheless, models of this sort may readily integrate reliability via a simple extension—for instance as a constraint in the optimization. Such frameworks, while

offering some control over reliability, do not necessarily optimize it. Typically, as in Bahramirad et al. (2012), reliability constraints require that the resource configuration meet a minimum level of reliability. Ceteris paribus, this is achieved by investing in additional costly generating capacity.

By extending the model again, reliability can be monetized and formulated as an objective. The model in Ding and Lee (2015), e.g., minimizes the operating cost of a microgrid, comprised of a fuel cost and emissions cost, but includes also a reliability penalty cost for unserved load (i.e., for that portion of microgrid load that exceeds generating capacity) using a single value of lost load. Though simplistic in its use of a single value, it offers an evaluation framework which can be used to explore the trade-off between emissions and reliability, where, e.g., reliable fossil generators can incur an emissions cost but equally reduce a reliability cost. Operation models such as these have an important drawback—though they include reliability, they do not integrate it into the design process where investment decision-making is made.

The business case of reliability can only be captured by considering the cost-benefit trade-off between investing in costly generating capacity and the economic value attributable to greater reliability, while considering also the operating cost of the resource mix. Evaluation methods have been created to explore this trade-off and typically take one of two forms. The first type mandates a minimum level of reliability, uses some selection logic to determine the resource mix, and calculates the cost to supply energy (Kanase-Patil et al., 2011; Lee et al., 2014). These can produce reliability-cost curves for varying levels of reliability, and hence provide insight into that trade-off. The second assumes a pre-determined resource configuration and calculates the investment cost and reliability cost for unserved load (Georgilakis and Katsigiannis, 2009). That configuration is varied until a minimum total cost is found. This is a brute-force approach that returns the system cost-minimizing configuration. Other frameworks take the form of a resource

dispatch logic, which first dispatches resources to meet load and then calculates system cost and reliability (Lovelady et al., 2013). Though these evaluation methods present clear frameworks for reliability evaluation, their weakness is clear—they do not have optimization functionality and hence do not necessarily provide an optimal solution for investment, dispatch, reliability, or the value of reliability.

Ultimately, to analyze the business case of reliability, models must consider the economic value of reliability and optimize the cost-reliability trade-off. They must size and schedule resources to minimize a total system cost that includes, at a minimum, investment, operation, and interruption costs. The interruption cost is the value attributable to improved reliability and requires that reliability be monetized. The most comprehensive attempts to optimize microgrid design while considering reliability, such as (Meiqin et al., 2010; Khodayar et al., 2012), follow this framework. Notably, they fall short in the simplistic manner in which they monetize reliability—namely, through use of a single value of lost load. In reality, interruption costs depend on numerous factors—the duration of an outage, its timing during the day, the day of the year, and whether or not the outage was scheduled. These factors must be captured in so-called customer damage functions and convolved with reliability metrics like outage frequency and outage duration.

In sum, there is a systematic lack of optimization models that couple state-of-the-art methods for reliability evaluation with reliability worth. It is these that must underlie any honest evaluation of the reliability business case. Though many models exist which contain a subset of these elements, to the best of our knowledge, none exist that include all. Rarely are they applied to business case modeling.

The objective of this dissertation, then, is to model the business case for microgrids that provide energy services, and that then couple that analysis with one of reliability service. This has required building a new model that treats both revenue streams in a single optimization framework. Chapter 1 presents an analysis of microgrids that supply

only energy services. It uses an existing model, DER-CAM. Chapter 2-3 describes the new optimization model we have built to add the reliability value stream. Chapter 2 describes specifically the new evaluation methodology developed to assess reliability; Chapter 3 describes the new model in full. Chapter 4 then applies the new modeling framework in a study of microgrid adoption impacts on greenhouse gas emissions from the electric power sector. Lastly, concluding remarks are given in Chapter 5.

The text and data in Chapter 1, in full, is a reprint of the material as it appears in "Evaluating business models for microgrids: Interactions of technology and policy", Hanna, Ryan; Ghonima, Mohamed, Kleissl, Jan, Tynan, George, David G., Victor, *Energy Policy*, 103 (2017), 47-61. The dissertation author is the primary investigator and author of this article. The supplementary information referred to in the text is available online at doi:10.1016/j.enpol.2017.01.010.

The text and data in Chapter 2, in full, is submitted for publication of the material with the title "Reliability evaluation for microgrids using cross-entropy Monte Carlo simulation". Hanna, Ryan; Disfani, Vahid R.; Kleissl, Jan. The dissertation author is the primary investigator and author of this article.

Chapter 3, in part, is currently being prepared for submission for publication of material. Hanna, Ryan; Disfani, Vahid R.; Kleissl, Jan; Victor, David G. The dissertation author is the primary investigator and author of this article.

Chapter 4, in part, is currently being prepared for submission for publication of material. Hanna, Ryan; Kleissl, Jan; Victor, David G. The dissertation author is the primary investigator and author of this article.

Chapter 1

The Business Case for Provision of Energy Services in Microgrids

1.1 Introduction

The electric power grid may be in the midst of a transformation. Following decades of deregulatory efforts (Wilson, 2002), it may now be heading toward a more decentralized system of supply and response. We focus on grid-connected microgrids, which are widely thought to be one of the most attractive options for decentralized power networks. Indeed, forecasted growth is substantial. When compared with 2014 levels of investment, all major segments of the microgrid market are expected to grow by 2020, for example small microgrids at commercial buildings (94%), medium sized microgrids such as those in communities (199%) or in public institutions (228%) that have special requirements for reliability, and large microgrids at military installations (142%) and universities (115%). All told, one credible study forecasts the total US microgrid capacity to reach 2,854 MW in 2020 (142% percent growth over the 2014 installed capacity of 1,181 MW) (Saadeh, 2015).

Three factors are primarily driving this shift from the traditional centralized grid structure to one with perhaps a larger role for microgrids. Through technological innovation, the cost of solar photovoltaics (PV) (Kann et al., 2016) and electric storage

(Nykvist and Nilsson, 2015) have fallen precipitously. A second factor is rising rates for grid-service electricity—for decades US retail rates have risen at near the general rate of inflation, typically at 2-3% annually (US Energy Information Administration, 2016). Third, and perhaps most decisively, are concerted policy efforts to reduce global greenhouse gas emissions while also promoting decentralization of the grid through more autonomous production from distributed energy resources (DERs). These policy interventions have taken many forms, such as renewable energy mandates (some designed to favor distributed renewables), deployment quotas for distributed generation (in California nearly 2,000 MW of distributed solar through the California Solar Initiative program, 4,000 MW of combined heat and power (CHP) per AB-32, and 1,325 MW of storage through AB-2514), and an array of subsidy schemes such as Californias Self-Generation Incentive Program (SGIP). In addition, some jurisdictions have adopted whole visions for a more decentralized and reliable electric power system—notably New Yorks Reforming the Energy Vision (REV).

While there is support for microgrid deployment in some jurisdictions, in many settings the situation is quite different. Large interconnection fees, lengthy wait times, and outright bans on self-generated networks prevail in many places. Where the policy environment is attractive, the logic for support points to the many potential *public* benefits microgrids can provide, such as improved power quality through voltage and frequency support, improved macro grid reliability, deferred costs for grid capacity expansions, improved blackstart capability after macro grid failure, and possibly lower emissions from the energy system overall. Whether those public benefits are realized, however, will hinge on whether potential investors see *private* benefits from building microgrids—what we call the "business model" or "business case" through which real investors can save money by shifting from standard grid service to microgrids. Within industry and policy circles there is intense discussion about business models but relatively little systematic

quantification (Reitenbach, 2016). We aim to show ways to add quantitative methods to that important commercial and policy debate.

In the real world, business models for microgrids depend on many factors, including the potential for energy cost savings, improved reliability, and perhaps other factors such as the amenity value of self-supply. Here we focus on economic costs and benefits of self-supply as they lie at the core of any commercial proposition, and point to subsequent work that can be done to add reliability to the analysis. We model the business case for *local energy provision*—which we define as the case in which a utility customer adopts a microgrid to self-generate (partially or fully) electricity and possibly thermal energy (i.e., heating and cooling) loads. This business case, in our analysis, stems solely from the ability to supply these loads with the microgrid at a total cost lower than standard utility service. We adopt the definition of the US Department of Energy (DOE), which defines a microgrid as "a group of interconnected loads and distributed energy resources within clearly defined electrical boundaries that acts as a single controllable entity with respect to the grid and that connects and disconnects from such grid to enable it to operate in both grid-connected or 'island' mode."

The present work makes two new contributions to the modeling literature. First, we build internally consistent load data sets for three "iconic" types of microgrids based on real world electric and thermal loads—large systems sized for campuses or military bases; medium-sized systems for critical assets such as hospitals; and smaller systems for commercial buildings such as box stores, hotels, and office buildings. We build these three iconic microgrid types to align with forecasted market growth per (Saadeh, 2015) and suggest that a consistent, reality-based set of iconic microgrids can help introduce some consistency and comparability in published academic work in this field, as well as promote more systematic microgrid analysis.

Second, we calibrate these systems using real market and policy conditions in

southern California—one of the most promising locations for microgrids—and perform several types of analysis to examine how the interplay between energy prices, technology and policy affect investment decision-making for specific technology types in microgrids—what we call the "investment case" underpinning microgrid adoption. Through sensitivity analysis we identify four variables—the price of natural gas, cost of emitting carbon dioxide (CO_2), the cost of electricity and demand in the electric tariff, and the cost of energy storage—that are most important for the future of microgrid deployment, and quantify their impacts on investment and business cases. Analyses such as these are crucial, as these systems may face highly volatile electricity, gas, and technology prices. Other work on DERs has addressed this type of uncertainty directly; for example, (Maribu and Fleten, 2008) and (Maurovich-Horvat et al., 2016) explore electricity and gas prices while (Rocha et al., 2016) looks at energy and technology costs. While we have configured our analysis for conditions in southern California, we publish our parameters and assumptions (see the supplementary information to this work) to allow ready modification for other jurisdictions. In addition to our focus on the business case for investment, we give attention to important policy-relevant outcomes from that investment, such as emissions of CO_2 from small gas generators that may prove very difficult to control as policy makers aim to achieve deep decarbonization of the whole energy system.

1.2 Methodology: building a tool for assessing business models

We provide an overview of the DER-CAM model (Distributed Energy Resources Customer Adoption Model) in section 1.2.1 and present the formulation for our configured version of the model in section 1.2.2, with explicit modifications noted in section 1.2.2. The basis for our formulation is the source code for DER-CAM version 4-4.1.1, which we term the *standard model formulation*. We then present end-use load profiles for three

iconic microgrids in section 1.2.3 and policy-relevant model calibrations for present-day market settings in section 1.2.3.

1.2.1 The DER-CAM optimization model

DER-CAM is an investment support tool for DER and microgrid systems. It computes DER investment and operation to supply load over the first year of operation, and with operating and maintenance (O&M) costs and standard amortization of capital costs allows for analysis of the net present cost and benefit of microgrid configurations. DER-CAM can be configured to minimize either an economic (total cost) or environmental (CO_2 emissions) objective, or a weighted combination of these two (i.e. Pareto optimization). For our purposes, the adaptability along with extensive published record[1] and open-source[2] nature of the source code are attractive features of the DER-CAM platform for academic research.

DER-CAM selects, sizes, and schedules DERs via several decision variables. Selection is binary (technologies are either selected or not), sizing decisions are made by individual technology and may be discrete (available in select sizes only) or continuous (available in all sizes) depending on the technology, and scheduling is determined for dispatchable DERs and for purchases of electricity and natural gas from the utility. The model outputs DER capacities and operating schedules for the first year of adoption,

[1] Development of DER-CAM by the Lawrence Berkeley National Laboratory (LBNL) is well documented. Publications include initial development in Marnay et al. (2000); Siddiqui et al. (2003) as well as later enhancements, including the addition of a carbon tax (Siddiqui et al., 2005), heat recovery (Siddiqui et al., 2007), electric and thermal storage (Marnay et al., 2008), power quality and reliability considerations (Stadler et al., 2009a), CO_2 emission minimization (Stadler et al., 2009b), zero-net-energy building constraints (Stadler et al., 2011), electric vehicles (Stadler et al., 2013), and building retrofits (Stadler et al., 2014). Other groups have used DER-CAM to systematically analyze model parameters that affect microgrid economics, for example tariff structures (Firestone et al., 2006), energy storage (Stadler et al., 2013), and climate zones (Maribu et al., 2007). More recently, it has been adapted to study electric vehicle integration in microgrids (Momber et al., 2010), ancillary service provision using electric storage in microgrids (Beer et al., 2012), and reactive power provision (von Appen et al., 2011).

[2] The source code is in certain cases made available by LBNL for non-commercial collaboration after signing a collaboration license agreement.

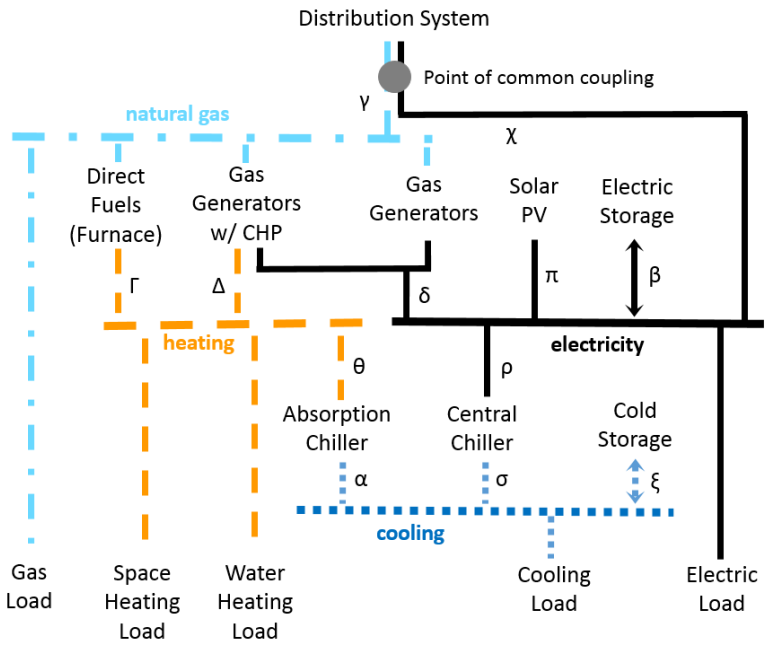

Figure 1.1. The microgrid network topology shows sources of energy demand and supply, as well as points of energy conversion, in the model. Energy balances for electricity, cooling, and heating are given by Eq. (1.2)−(1.4). The gas load is supplied trivially so the gas balance equation is omitted.

capital and operating costs, energy flows from source to end-use, fuel consumption, and CO_2 emissions from purchased and self-generated electric and thermal energy. See (Siddiqui et al., 2007) for a more detailed discussion of inputs and outputs.

For the purpose of policy oriented analysis later in this work, we classify four sets of DER technologies in DER-CAM:

1. *Fossil fuel generators*. Micro turbines, gas turbines, reciprocating engines, fuel cells—all units have discrete capacity, may or may not have heat recovery, and combust natural gas in our models.

2. *Renewable generators*. Solar PV.

3. *Thermal energy generators*. Natural gas direct-fired chillers, absorption chillers, electric central chiller, solar thermal heating, heat pumps—all units supply heating

or cooling loads directly.

4. *Flexible technologies*. Electric energy storage, heat storage, cold storage, EVs, demand response, schedulable load (i.e., load that must be met at some time during each 24-hour period).

Databases in DER-CAM are highly detailed and thus can be unwieldy to configure, but they are particularly useful in studies such as reported here because they can be adjusted to many real world conditions that are often changing quickly.

Though DER-CAM does have a simplistic demand response module, we do not consider it. It is unclear at present how to connect the real-world demand response characteristics of buildings to the generic building data modeled in this work. While including demand response may shift baseline results, we focus first on the core economic logic for microgrids considering generation and storage assets, before looking at demand-side flexibilities (which our team is planning for future work).

1.2.2 Problem formulation

Mathematically, DER-CAM is formulated as a mixed integer linear program and is coded in GAMS. (Siddiqui et al., 2005) and (Stadler et al., 2009a) provide a complete mathematical formulation. Though here we provide key highlights—decision variables, objectives, constraints, inputs and outputs, and model databases—to provide context for our modeling and analysis, and present only those elements (loads, DERs, costs, energy flows, emissions) present in our models, we give sufficient information to formulate the model and run our analyses.

Following the topology in Fig. 1.1, the microgrid is interconnected to the utility distribution system, which we call the “macro grid”. In line with common regulatory rules for electric utilities, the DERs that comprise the microgrid are installed behind

a single billing meter at the point of common coupling, lie within the boundaries of a single customer, and serve only the load of that customer.[3]

Standard model formulation and assumptions

The modeling approach is described by Eq. (1.1)−(1.4), with nomenclature summarized in Table 1.1, which we adapt from (Ghatikar et al., 2016) and (Stadler et al., 2009b). The annual modeling period is defined across three time periods: month $m \in M$, day-type $t \in T$ and hour $h \in H$, where a chosen number $N_{m,t}$ of two day-types (week-days and weekend-days) define each month. Load, supply, costs, etc. are defined or determined over these time periods. Tariff periods $p \in P$ and demand types $d \in D$ are further defined across M, T, and H.

We configure DER-CAM to select, size, and schedule DERs to minimize the year-one total cost of microgrid adoption. Selection and sizing is made for three technology sets—gas generators $i \in I$, direct-fired gas chillers $k \in K$, and DERs $q \in Q$, in addition to switchgear.[4] DERs in I and K are discrete (i.e. they have a set nameplate capacity that must be purchased), whereas those in Q are continuous (i.e. any capacity may be purchased). To enable islanding, switchgear is always selected (with $Binary_s$ and $PurchCap_s$). Scheduling is determined by month m and hour h for electricity provision $\pi_{e,m,t,h}$, cooling provision $\xi_{c,m,t,h}$, and heating provision $\chi_{g,m,t,h}$, where $e \in E$, $c \in C$, and $g \in G$ are the sources of electricity, cooling, and heating provision, respectively.

DER-CAM computes the year-one total cost c, Eq. (1.1). The total cost includes

[3]While some regulators envision futures in which unrelated customers are interconnected, we focus here on single customers because regulatory rules that constrain adoption to this framework are common to many jurisdictions (Research and Authority, 2014), and in some settings the constraints on microgrids are even more severe—for example, through public franchise laws that make it illegal for a developer to lay wires that cross public roadways.

[4]Note that the technology sets I, K, and Q do not align with the four technology sets in section 1.2.1. The distinction between I, K, and Q is a mathematical one—discrete and continuous variables are fundamentally different in the optimization formulation—while the distinction made previously is done to facilitate discussion of policy implications.

the full year-one operating cost, which includes electricity and natural gas purchases, DER fuel and maintenance, and the cost of emissions, as well as the year-one annualized capital cost for investment. Energy flows are subject to common constraints such as supply-demand balance in Eq. (1.2)−(1.4), which we show here because they depend on technology selection in our models, as well as energy storage balance, energy conversion efficiencies, and heat recovery, which we do not show because they are unmodified from the standard model formulation.

Table 1.1. Nomenclature.

Parameter	*Description*
Sets and indices	
m	Month, $M = \{1, 2, ..., 12\}$
t	Day-type, $T = \{$week, weekend$\}$
h	Hour, $H = \{1, 2, ..., 24\}$
p	Tariff period $P = \{$on-peak, mid-peak, off-peak$\}$
d	Tariff demand type, $D = \{$non-coincident, on-peak, mid-peak, off-peak$\}$
u	End-use load, $U = \{$electricity 'el', cooling 'cl', space heating 'sh', water heating 'wh', natural gas 'ng'$\}$
s	Index for switchgear
i	Generator, $I = \{$ICE, MT, ICE-HX, MT-HX$\}^a$
k	Direct-fired chiller, $K = \{$DFChiller-HX$\}$
q	Continuous DER, $Q = \{$solar PV 'pv', electric storage 'es', absorption chiller 'ac', cold storage 'cs'$\}^b$
v	All microgrid technologies, $V = \{I, K, Q,$ switchgear$\}$
e	Source of electricity, $E = \{I,$ 'pv', 'es', distribution system 'ds'$\}$
c	Source of cooling, $C = \{$K, absorption chiller 'ac', electric chiller 'ec', cold storage 'cs'$\}$
g	Source of heat, $G = \{I,$ direct fuel 'di'$\}$
Customer load	
$N_{m,t}$	Number of days of day-type t in month m

Table 1.1. Nomenclature, continued

Parameter	*Description*
$L_{u,m,t,h}$	Load profile for end-use load u, month m, day-type t and hour h, kW
Tariff parameters	
$ElecFee$	Fee for electric service, $/mo
$VChg_{m,p}$	Volumetric charge for month m and tariff period p, $/kWh
$DChg_{m,d}$	Demand charge for month m and demand type d, $/kW
$SChg$	DER standby charge, $/kW/mo
$NGFee$	Fee for natural gas service, $/mo
$NGPrice_m$	Natural gas price in month m, $/kWh
DER data	
R_v	Nameplate capacity of technology v, kW
$Cfcap_v$	Fixed capital cost of technology v, $
$Cvcap_v$	Variable capital cost for technology v, $/kW or $/kWh
$Cfom_v$	Fixed O&M cost for technology v, $/kW/yr for I, K and $/kW/mo, or $/kWh/mo for Q
$Cvom_v$	Variable O&M cost for technology v, $/kWh
A_v	Annuity factor for technology v
CO_2 parameters	
EF	Natural gas CO_2 emission factor, tCO_2/kWh
$CTax$	Tax on CO_2 emissions, $/$tCO_2$
Selection and sizing decision variables	
$PurchNum_i$, $PurchNum_k$	Number of purchased gas generators i, direct-fired chillers k
$Binary_q$, $Binary_s$	Binary decision variable to invest in DER q, switchgear
$PurchCap_q$, $PurchCap_s$	Capacity of installed DER q, switchgear, kW
Scheduling decision variables	
$\pi_{e,m,t,h}$	Electricity provision from source e, kW
$\xi_{c,m,t,h}$	Cooling provision from source c, kW
$\chi_{g,m,t,h}$	Heating provision from source g, kW
Secondary variables[c]	

Table 1.1. Nomenclature, continued

Parameter	*Description*
$\pi_{e,m,t,h}$	Electricity supplied by solar PV, kW
$\pi_{\text{'ec'},m,t,h}$	Electricity input to the central electric chiller, kW
$\chi_{\text{'ac'},m,t,h}$	Heat consumed by the absorption chiller, kW
$\gamma_{m,t,h}$	Total natural gas purchased, kW
$\gamma_{i,m,t,h}$, $\gamma_{k,m,t,h}$	Natural gas purchased for gas generator i, direct-fired chiller k, kW

[a] Notation: ICE–internal combustion engine, MT–microturbine, -HX–with heat recovery.

[b] Q does not include the electric chiller (which consumes electricity to supply the cooling load) because it is installed in every model run and hence does create differences between results.

[c] Subscript "m,t,h" denotes "in month m, day-type t, and hour h".

$$\min \quad c := c_{\text{tariff}} + c_{\text{fuel}} + c_{\text{der}} + c_{\text{carbon}}\,, \tag{1.1}$$

subject to

$$L_{\text{'el'},m,t,d} + \pi_{\text{'ec'},m,t,d} = \sum_{e \in E} \pi_{e,m,t,d}\,, \tag{1.2}$$

$$L_{\text{'cl'},m,t,d} = \sum_{c \in C} \xi_{c,m,t,d}\,, \tag{1.3}$$

$$L_{\text{'sh'},m,t,d} + L_{\text{'wh'},m,t,d} + \chi_{\text{'ac'},m,t,d} = \sum_{g \in G} \chi_{g,m,t,d} \quad \forall m,t,h. \tag{1.4}$$

We decompose c into four components: tariff costs c_{tariff} in Eq. (1.5) include a volumetric, demand, service fee, and standby component; natural gas fuel costs c_{fuel} in Eq. (1.6) include a volumetric and service fee component; DER costs c_{der} in Eq. (1.7) include capital costs as well as fixed and variable operating and maintenance costs; and carbon costs c_{carbon} in Eq. (1.8) are taxes on CO_2 emissions from on-site natural gas combustion.

$$C_{\text{tariff}} := \sum_{m\in M}\sum_{p\in P}\sum_{t\in T}\sum_{h\in H} \pi_{\text{'ds'},m,t,h}\cdot N_{m,t}\cdot VChg_{m,p}$$
$$+ \sum_{m\in M}\sum_{d\in D} DChg_{m,d}\cdot \max_{t\in T,h\in d}\{\pi_{\text{'ds'},m,t,h}\} + \sum_{m\in M} ElecFee$$
$$+ \sum_{m\in M}\left[\sum_{i\in I} PurchNum_i\cdot R_i + PurchCap_{\text{'pv'}}\right]\cdot SChg\,, \tag{1.5}$$

$$C_{\text{fuel}} := \sum_{m\in M} NGFee + \sum_{m\in M}\sum_{t\in T}\sum_{h\in H}\gamma_{m,t,h}\cdot N_{m,t}\cdot NGPrice_m\,, \tag{1.6}$$

$$C_{\text{der}} := \sum_{i\in I}\sum_{m\in M} PurchNum_i\cdot R_i\cdot\frac{Cfom_i}{12} + \sum_{i\in I}\sum_{m\in M}\sum_{t\in T}\sum_{h\in H}\pi_{i,m,t,h}\cdot N_{m,t}\cdot Cvom_i$$
$$+ \sum_{k\in K}\sum_{m\in M} PurchNum_k\cdot R_k\cdot\frac{Cfom_k}{12} + \sum_{k\in K}\sum_{m\in M}\sum_{t\in T}\sum_{h\in H}\xi_{k,m,t,h}\cdot N_{m,t}\cdot Cvom_k$$
$$+ \sum_{q\in Q}\sum_{m\in M} PurchCap_q\cdot Cfom_q\,, \tag{1.7}$$

$$C_{\text{carbon}} := \sum_{m\in M}\sum_{t\in T}\sum_{h\in H}\left(\sum_{i\in I}\gamma_{i,m,t,h} + \sum_{k\in K}\gamma_{k,m,t,h}\right)\cdot N_{m,t}\cdot EF\cdot CTax. \tag{1.8}$$

Two constraints in particular affect DER investment in our work. The first limits the area available for solar PV installations, which we term the *solar PV space constraint*. This constraint is often the factor that caps investment in solar PV. We include it nevertheless, and for comparison quantify the effect of removing it in section 1.3. This is an important variable to consider for urban microgrids in compact areas, such as office buildings and urban campuses and where other siting constraints (e.g., aesthetic considerations, shadows, or building codes) limit potential utilization of low power density renewables options.

The second, which we term the *resource adequacy constraint*, concerns the supply-demand balance of electric energy during islanded operation. This constraint requires that the model invest in sufficient generator capacity to operate in islanded mode indefinitely (assuming unaffected fuel supply), where "sufficient capacity" supplies at a minimum

the maximum critical electric load, assuming one battery charge/discharge cycle per day and an average annual solar irradiance received each day. This constraint does not guarantee perfect adequacy, nor does it guarantee the ability to island during all hours of the day or days of the year. Rather, it approximates the investment required to island generally—an outcome designed to approximate the estimated microgrid configuration with reasonable DER capacities but with full appreciation that further analysis and modeling refinement would be needed when designing any particular system. Though we require resource adequacy, we do not monetize improvement to reliability—such as from reduced interruption costs.[5]

Our model runs are built on several notable assumptions. We explicitly neglect other potential revenue streams by considering only the economic benefit derived from local energy provision (i.e., avoided utility costs). We further neglect potentially important demand-side flexibilities, such as demand response and load scheduling, which could improve microgrid economics substantially. These limitations add conservatism to our results that report the viability of business cases.

There are, conversely, two model features that likely overestimate the benefit of microgrid adoption. One, the model is deterministic. All parameters (e.g., those that are in reality stochastic such as load, solar irradiance, and DER availability) are prescribed and known. In effect this implies that operating forecasts are perfectly accurate—an advantage that likely lessens the need for and value of electric storage. Operation with real forecasts—which are imperfect—would likely require more investment in storage capacity to match results with perfect forecasts. Alternatively the same storage capacity would likely achieve less savings through reduction in demand charges—charges paid by

[5]We report in the supplementary information baseline results with the resource adequacy constraint removed. In short, for the critical asset, which has high demand for reliability, including the constraint pushes investment toward gas generators and away from solar PV and electric storage, but does not change the total cost. Results for the large commercial and campus microgrids are essentially affected because they have less demand for reliability.

most utility customers for their maximum power draw, which we explain in section 1.2.3.

Two, irradiance profiles, as is typical in planning models, are based on clear weather days—that is, they do not include diminished and/or variable solar PV output. The model captures seasonal variability across months but not day-to-day or hourly variability due to clouds. The model has a 1 h timestep and thus cannot capture sub-hourly variability either, which can be important as demand charges are based on 15 min intervals and some are calling for finer-resolution market-based tariffs. As with the deterministic assumption, this lack of variability likely overestimates demand charge savings or decreases the need for storage (depending on one's perspective), and hence the value of storage to the microgrid as well as investment cost.

We make these assumptions, which are standard in such modeling, highly transparent to help aid interpretation of results and to identify areas where future work can refine such models.

Modifications to the standard model formulation

We modify the standard model formulation in three ways to make it particularly suited for evaluating business cases. One, we remove the carbon cost *CTax* associated with electricity purchases $\pi_{\text{'ds',}m,t,h}$—a \$/tCO_2 (metric ton carbon dioxide) measure based on the marketplace generation CO_2 emission factor. Instead, we imbed *CTax* in volumetric rates $VChg_{m,p}$—noting that, ceteris paribus, wholesale electricity rates increase when the carbon cost increases. We also remove the carbon cost associated with natural gas purchases $\gamma_{m,t,h}$ and instead tax only the CO_2 emitted by gas-fired DERs (the sum of $\gamma_{t,m,t,h}$ and γ_k, m, t, h).

Second, to enable a more robust policy analysis, we remove financial parameters that cap the payback period for capital costs—as might exist, for example, for those with difficulty accessing capital—which can restrict investment in capital intensive microgrids.

Third, we neglect all revenue streams beyond those derived from local energy provision. Other revenue could come from participation in electricity markets, utility service agreements, improving reliability via islanding (i.e., reducing interruption costs), and incentives (investment incentives such as tax credits, production credits such as net energy metering and feed-in tariffs, and those with elements of both like the California SGIP). Incentives are applicable to select settings and technologies; we neglect them to build a more widely applicable analysis. Lastly, we neglect several modules within the code (e.g., zero net energy constraints, building retrofits for energy efficiency, and electric vehicles) that are not directly relevant to evaluating the business case and the particular policy aspects of interest. Our interest in neglecting these other revenue streams is to focus on one core business case for microgrids—beyond systems that might be built under special conditions such as with large subsidy or other explicit policy support.

Solution algorithm

The optimization is solved using the IBM ILOG CPLEX Optimization Studio. We vary the relative optimality gap (the gap between the best known solution and optimal solution) depending on the iconic microgrid being modeled—from 0.01 (1%) for the large commercial microgrid to 0.00001 (0.001%) for the campus microgrid. Model runtimes vary depending on this criterion—baseline and greenfield sensitivity analyses (sections 1.3.1, 1.3.4) require selection, sizing and scheduling and range from 10 minutes to 10 hours, while simple sensitivity analyses (section 1.3.3) require only scheduling and terminate in a few minutes. All model runs used a 3.40 GHz Intel Core i7-2600 processor and 16 GB of installed RAM.

1.2.3 Data

Load data for three iconic microgrids

We create data sets for three iconic microgrids—which we term the *large commercial*, *critical asset*, and *campus*. We construct data sets to align with forecasted market growth for the largest grid-tied microgrid segments (see section 1.1).[6]

In our view commercial systems supply a single building (or a small cluster of perhaps 2-3), for example large box stores such as Walmart and Costco or office buildings. Critical assets are those facilities with a particularly great need for reliability (a large portion of the load is critical and must be maintained during outages) and may include hospital complexes, community centers, critical public infrastructure, and data centers. Lastly, campus systems may include military bases, university and government campuses, and corporate parks. These are geographically large systems covering many buildings (residential, commercial, and/or industrial) but within a single ownership boundary that does not cross public rights of way.

We generate annual data sets at a 1-h timestep for five types of load—electricity $L_{\text{`el'}}$, cooling $L_{\text{`cl'}}$, space heating $L_{\text{`sh'}}$, water heating $L_{\text{`wh'}}$, and natural gas $L_{\text{`ng'}}$—using the US DOE data set of commercial reference buildings (Deru et al., 2011; Office of Energy Efficiency and Renewable Energy, 2015)—a set of 1-h resolution annual profiles for 16 building types representative of approximately 70% of all US commercial buildings, such as offices, schools, restaurants, hotels, and a hospital, among others. Thermal loads ($L_{\text{`cl'}}$, $L_{\text{`sh'}}$, and $L_{\text{`wh'}}$) are available for 16 climate zones. We use climate zone 3B-coast for southern California. Fig. 1.2 shows representative daily profiles for a weekday along with annual energy consumption; full profiles are reported in the supplementary

[6](Saadeh, 2015) distinguishes between five microgrid segments: military, university, city/community, public institution, and commercial. Each of those finer resolution categories falls into 1-2 of the three main segments in the present study: in our view, our "large commercial" category covers the commercial segment; "critical asset" includes city/community and public institution segments; and "campus" includes the military and university segments.

information. By combining the DOE data into three types of building clusters—each served by a microgrid—we hope to promote more systematic microgrid analysis.[7]

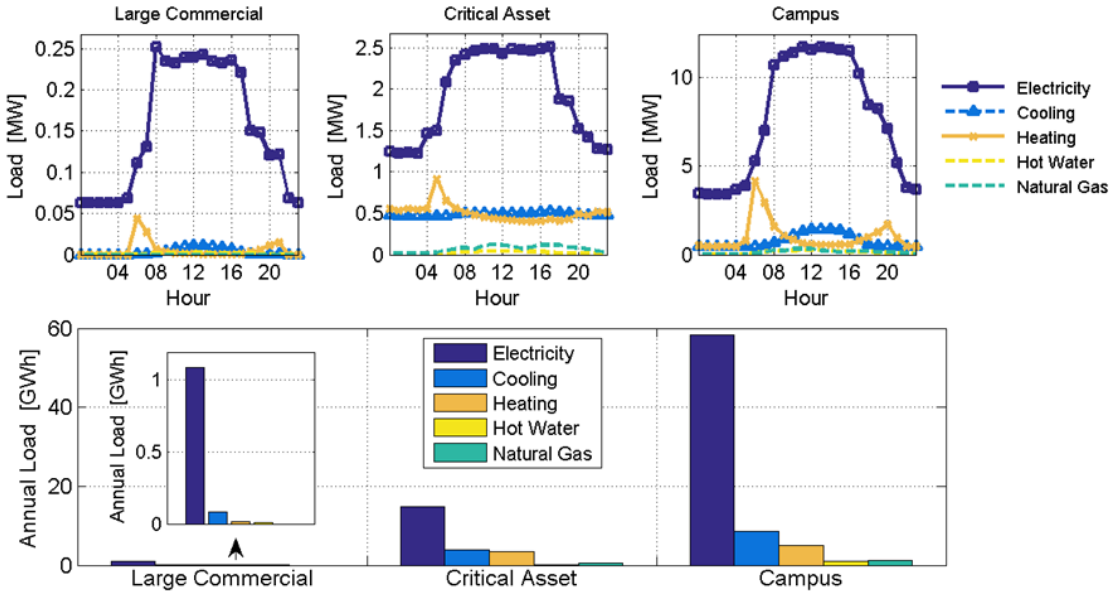

Figure 1.2. (top) Load profiles presented for a February weekday are representative of the load shape on weekdays throughout the year. (Weekend-days have a similar base load but do not peak so significantly during the day.) (bottom) Annual energy consumption for all end-use loads shows the disparity in size between the three. Note variable y-axis scaling at top and constant y-axis scaling at bottom.

We model the three iconic microgrids as an office building, hospital complex (a hospital with ancillary facilities) and university campus, and map them to the DOE commercial reference buildings as follows: the large commercial as the medium office; the critical asset as the sum of the hospital, quick-serve restaurant, and outpatient facility; and the campus as the sum of the small office, medium office, two large offices, three stand-alone retail centers, three supermarkets, four midrise apartments, two primary schools, two secondary schools, one strip mall, and one quick- and one full-serve restaurant.

[7]The Grid Integration Group at LBNL has used DER-CAM with the DOE reference building data set, which has been available since 2011, to study varying tariff structures and climate conditions (Mendes et al., 2013, 2014; DeForest et al., 2014). Systematic studies such as these are valuable because they provide insight into adoption trends for specific DERs across a range of important parameters.

Several features distinguish the three load profiles:

- *Large commercial*. Consists primarily of electric load, but also includes variable demand for heating and cooling (i.e., it has a large ratio of maximum to minimum thermal load), so CHP investments are not optimal. This class consumes the least energy of the three.

- *Critical asset*. Distinct from the other microgrids, the heating and cooling loads are relatively constant throughout the day. It has the highest electric load factor (the ratio of average to maximum load), which, with thermal loads, favors CHP investment. The peak critical electric load is large relative to the base electric load, so higher capital costs for generators are needed to reliably supply peak critical load.

- *Campus*. Of the three it has the largest demand and volumetric consumption, and in particular has large thermal demand.

Important parameters for policy analysis

We provide in Table 1.2 our parameterizations relevant to policy and that most affect investment outcomes, and leave full detail on the empirical calibration (i.e., the larger set of model parameterizations) for the supplementary information.

Table 1.2. Model calibrations important for policy analysis—costs of electricity, gas, carbon, and DERs.

Parameters	Value	Units
Tariff Parameters		
Volumetric charges		\$/kWh
Summer on-peak	0.12331	
Summer mid-peak	0.11362	
Summer off-peak	0.08287	
Winter on-peak	0.11157	
Winter mid-peak	0.09602	
Winter off-peak	0.07460	
Demand charges		\$/kW
Non-coincident	23.83	
Summer on-peak	20.93	
Winter on-peak	7.62	
Standby charge	13.76	\$/kW
Exogenous Parameters		
Interest rate	7	%
Natural gas price	8	\$/mmbtu
Carbon cost	12	$\$/tCO_2$
DER Parameters		
Solar PV capital cost	2390	$\$/kW_{ac}$
Electric storage capital cost	350	\$/kWh

The business case for local energy provision rests on avoiding utility service costs. To quantify those costs we consider the costs of interconnection to the San Diego Gas

& Electric (SDG&E) distribution system. Applicable electric tariffs are from 2015 and include the SDG&E commercial Schedule AL-TOU and Schedule S.[8]

Three other parameters (the discount rate, gas price, and carbon cost), as we will show, are also of particular importance. We assume that the cost of capital is 7%—based on the lower medium grade corporate bond rate—and use the same rate for discounting calculations. The gas price varies by region and time of year, among other factors. We use a single price of 8 $/mmbtu based on retail sales to commercial customers in California (US Energy Information Administration, 2015). We use the California Carbon Allowance futures carbon price of 12 $/t$CO_2$e (metric ton carbon dioxide equivalent), which is essentially the floor price in the carbon market ("California Carbon Dashboard", 2015). To explore the potential for future low-carbon microgrids based around solar PV and electric storage we use current costs for non-residential rooftop PV systems (Kann et al., 2016)(Kann et al., 2016) and a projected cost estimate for electric storage that aligns with estimates of current and projected costs (Bronski et al., 2015; Christiansen et al., 2015; Nykvist and Nilsson, 2015). This projected electric storage cost is the only calibration based outside of the "present day."

[8]Schedule AL-TOU imposes volumetric charges ($/kWh) and demand charges ($/kW) that vary by season and tariff period—the former are based on energy consumption and the latter on monthly maximum power draw. Schedule S codifies a standby charge, a $/kW charge on the installed generator capacity that is designed to reflect the increased load the microgrid might draw from the utility if microgrid generators were to fail. The charge can be substantial and has been debated (Darrow and Hampson, 2013) but, as we will show, is not a driving parameter of optimal configurations. In addition to these two, another schedule, Schedule E-DEPART, codifies a departing load charge—a charge on the portion of load no longer supplied by utility service (and instead supplied via self-generation). Because it is very small (approximately 0.005-0.015 $/kWh) relative to other tariff charges, and moreover specific to the three investor-owned utilities in California (Darrow and Hampson, 2013), we neglect it.

1.3 Results and discussion

1.3.1 Definitions and scenarios

We term the optimal selection and sizing of DERs the *optimal configuration* and year-one operation of DERs the *optimal dispatch*. Together they comprise the *optimal system*. We model two types of customers for each iconic microgrid, as is typical with DER-CAM—(1) a *microgrid customer*, who adopts a microgrid to supply load with some combination of self-generated electric and thermal energy and/or purchased electricity and natural gas; and (2) a *macro grid customer*, who supplies the same set of loads by purchasing electricity and natural gas services from the utility. We term the cost savings derived from microgrid adoption (i.e., the difference in total cost between the two customers) the *economic benefit* (which can be negative).

We perform three sets of analyses for each iconic microgrid and customer type (Fig. 1.3). First is a baseline analysis (section 1.3.2). Second is a simple sensitivity analysis (section 1.3.3), in which we hold constant the optimal configuration from the baseline analysis while varying individual parameters and then re-optimize the dispatch of generation technologies. These analyses explore the robustness of business cases for microgrids that might be "locked in" economically due to investment in a configuration of technologies. They also help to identify areas where more in-depth (and computationally difficult) sensitivity analysis would be needed. Third, for the four factors identified in the simple sensitivity as most important we perform a greenfield sensitivity analysis (section 1.3.4), in which we vary individual parameters before re-optimizing configuration as well as dispatch. This latter type of sensitivity analysis is most useful for unbuilt microgrid systems that might be in the planning phase.

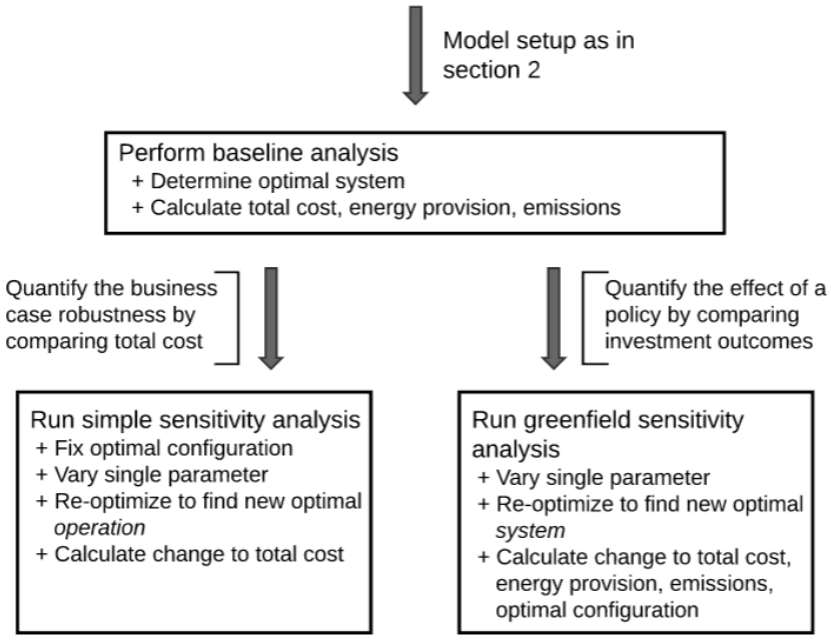

Figure 1.3. We run two types of sensitivity analysis after the baseline analysis: simple and greenfield sensitivities.

1.3.2 Baseline analysis

In the baseline optimal configurations (Table 1.3) we distinguish between investments in the four technology sets noted in section 1.2.1—conventional gas generators, renewables, thermal energy generators, and flexible technologies. We further distinguish generators with CHP—which supply both power and thermal energy within the microgrid—because they can greatly improve energy efficiency and thus can prove pivotal to establishing the business case. Detailed investment by individual unit and technology is provided in the supplementary information.

Table 1.3. Optimal microgrid configurations for the baseline model runs.

	Large Commercial	Critical Asset	Campus
Gas generators			
without CHP	150 kW	750 kW	4250 kW
with CHP	–	1650 kW	6250 kW
Renewable generators			
Solar PV	200 kW	1240 kW	3100 kW
Thermal energy generators			
Direct-fired chiller	–	200 kW	200 kW
Absorption chiller	–	340 kW	1420 kW
Flexible technologies			
Electric storage	230 kWh	20 kWh	1479 kWh
Cold storage	220 kWh	–	3340 kWh

Operationally, the DERs that comprise the microgrids supply peak and base electric load (Fig. 1.4), and hence target reduction in both demand and volumetric charges—the largest costs to the macro grid customer. The optimal configurations are sized to supply peak electric load for three reasons: to facilitate islanding per the resource adequacy constraint, to shave on-peak load (which has the highest demand charges), and to supplant electricity and fuel purchases with less costly self-generated electricity. Purchases do supply a small amount of base load in some configurations and months.

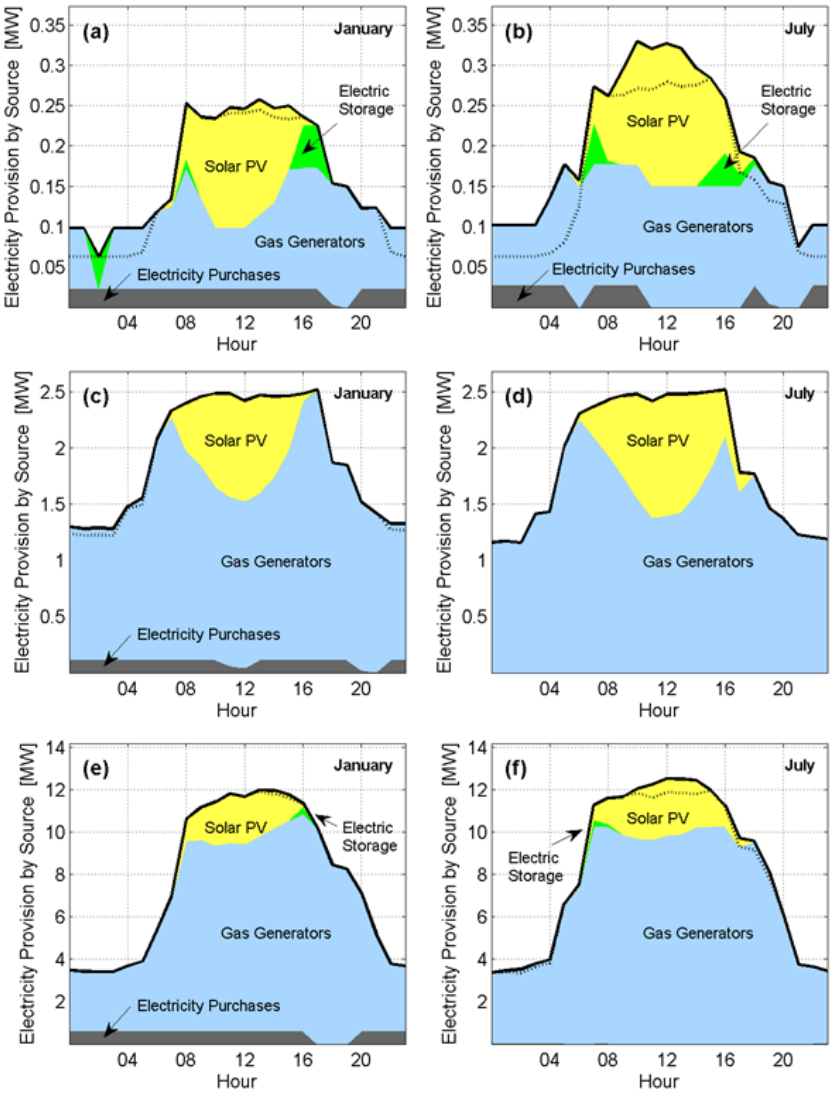

Figure 1.4. The optimal dispatch for a representative weekday in winter (left) and summer (right) for the large commercial (a, b), critical asset (c, d) and campus (e, f) microgrids shows how the microgrid supplies electric load with a combination of purchased and self-generated electricity. The microgrid electric load is denoted in solid black; for reference, the electric load for utility service is shown in dashed black. The two are different because some DERs consume electricity—see for example (a) and (b). Electric storage is shown as energy provision when discharging (green) and added to the load curve when charging. Dispatch for all 12 months of the year is in the supplementary information.

The key difference across the optimal configurations for the three iconic microgrids is not DER capacity relative to peak load, but rather the combination of DER types

(gas generators, gas generators with CHP, solar PV, and electric storage) that comprise the configuration. Those combinations we observe—and especially the variation in them when compared across sensitivity in policy variables—has the biggest implications for policy, as we will discuss in sections 1.3.4 and 1.4.

While the details of each optimal system are complex, the broad patterns are as follows:

- *Large commercial*. Gas generators supply base load and solar PV supplies peak load. Electric storage complements solar PV by supplying peak load when solar output is unavailable, as observed during winter evenings. Cold storage (i.e. chilled water) is produced during off-peak hours. The thermal demand is relatively small so the model foregoes CHP.

- *Critical asset*. Gas generators supply base load, two-thirds of which have CHP to meet the relatively large thermal load. An absorption chiller further supplies cooling. Solar PV supplies peak load and electric storage supplies an indistinguishable amount of shoulder load (i.e., load between the on- and off-peak periods, 1600-1700 LST in winter).

- *Campus*. Gas generators supply the base load, 60% of which have CHP to meet thermal demand. An absorption chiller further supplies cooling and cold storage is produced during off-peak hours. Solar PV supplies peak load and electric storage again complements when solar output is small or unavailable.

The primary driver of these investment trends is the potential to utilize natural gas to supply electricity and thermal loads at high efficiency and low cost. The models largely supplant electricity purchases with self-generated electricity, using gas generators to supply a huge fraction of the base load. The model is driven to this result because

gas prices are low, the microgrid CO_2 emission factor is comparable to that of the wholesale marketplace, and California retail electricity rates are relatively expensive. Further, the critical asset and campus integrate electric and thermal loads via CHP, thereby increasing consumption efficiencies and obviating much of the electricity and fuel purchases otherwise needed for direct heating and cooling.

All configurations include solar PV—driven in part by the coincidence of peak load and peak solar irradiance, as well as the assumption of clear weather days. The critical asset and campus invest in a maximum capacity of solar PV—that is, the solar PV space constraint caps investment.[9] The large commercial uses 33% of available space. Such large installations are cost effective because of the large daily load peak and the coincidence of peak load with peak solar.

The macro grid and microgrid customers are subject to competing costs (Fig. 1.5) per Eq. (1.1)−(1.8). The former pays only for utility electric and gas service per applicable tariffs ("tariff costs" and "fuel costs"), while the latter pays the same tariff charges in addition to "DER costs" and "carbon taxes". The total cost is the sum of these four per Eq. (1.1). We find that, for the baseline case, microgrid adoption reduces the total cost relative to the macro grid customer—that is, the economic benefit is positive.

1.3.3 Simple sensitivity analysis

Now we turn to sensitivity analysis. In this section we vary all 13 of the significant parameters in the model within ranges detailed in Table 1.4. For this "simple sensitivity" we leave the configuration of installed DERs on each iconic microgrid unchanged from the baseline. In the next section we look at a subset of the most important factors and offer full blown re-optimizations around those variables to show the deeper implications

[9] When unconstrained by available space, the critical asset and campus see investment of an additional 40% (1,750 kW constrained, 1,250 kW baseline) and 177% (8,600 kW unconstrained, 3,100 kW baseline) respectively. These results are detailed in the supplementary information.

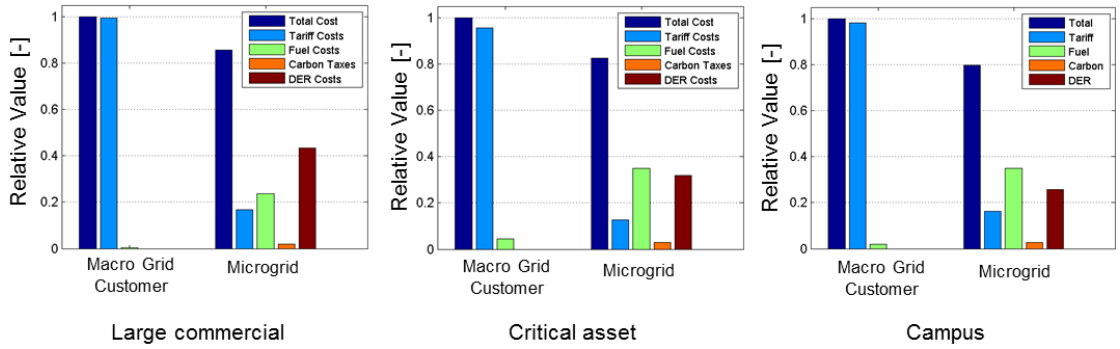

Figure 1.5. The disaggregation of the year-one total cost shows how microgrid adoption shifts the source of cost from tariff-based to DER- and fuel-based. In doing so adoption reduces the total cost—by 14, 17, and 21% for the large commercial, critical asset, and campus, respectively. Costs are normalized to the macro grid customer's total cost.

for investment decision-making.

The 13 sensitivities span the major clusters of factors that vary in ways that affect the viability of microgrid investment: technological advance, which generally lowers costs; utility tariff costs, which generally rise and vary widely with geography and regulation; carbon costs, which vary jurisdictionally; and financing and fuel costs, which reflect market conditions. We also vary the magnitude of electric and thermal loads to reflect the uncertainties omnipresent in energy service that affect load—factors such as climate zone, energy efficiency measures, and load growth.

Table 1.4. Variation of 13 parameters in the simple sensitivity analysis.

Parameter Varied	-/+ variation (nominal, range)	Justification	Reference
Interest rate	-/+25% (7, 5.25−8.75%)	Reflects a typical discount rate for lower medium grade (BBB- to BBB+) corporate bonds at the time of this work; the sensitivity range further covers high-yield and upper medium grade bonds.	

Table 1.4. Variation of 13 parameters in the simple sensitivity analysis, continued

Parameter Varied	-/+ variation (nominal, range)	Justification	Reference
Carbon cost	-100/+1000% (12, 0−132 $/tCO$_2$)	Captures the 95th-percentile cost for the out-year 2020 (129 $/tCO$_2$). At the time of this work the price of California Carbon Allowance futures is trading at 12−13 $/tCO$_2$e.	(Interagency Working Group on Social Cost of Carbon, 2013)
Natural gas price	-50/+100% (8, 4−16 $/mmbtu)	Captures the full range of AEO2015 projected Henry Hub spot prices[a] while further allowing for a range of retail prices which vary according to local natural gas infrastructure spending.	(Conti et al., 2015)
Volumetric charge	-45/+15% (multiple, varies)	Captures the wide range of US average retail electricity rates for commercial customers.[b]	Conti et al., 2015)
Demand charge	-45/+15% (multiple, varies)	For simplicity, we vary the demand charge -45/+15% to align with the variation in volumetric charge.	
Standby charge	-45/+15% (13.76, 7.57−15.82 $/kW)	As noted for the demand charge.	
Gas generator capital cost	-20/+10% (varies, see SI)	Captures cost projections for 2010−2030 for small (<1 MW) generators while allowing for emissions treatment equipment costs for compliance with potential future stringent emissions regulations. Though both capital and emissions treatment equipment costs vary by generator type and capacity, for generality we apply the sensitivity range across all generator types.	(Hedman et al., 2012)

Table 1.4. Variation of 13 parameters in the simple sensitivity analysis, continued

Parameter Varied	-/+ variation (nominal, range)	Justification	Reference
Gas generator O&M cost	-20/+10% (varies, see SI)	As noted for the gas generator capital cost.	
Electric storage capital cost	-50/+300% (350, 175−1050 $/kWh)	Captures existing and projected costs over the next 5-10 years.[d]	(Shah and Booream-Phelps, 2015)
Thermal storage capital cost	-/+20% (50, 40−60 $/kWh)	Considers potential technology advances or unforeseen policy changes affecting thermal storage.	
Solar PV capital cost	-/+50% (2390, 1195-3585 $/kW)	The sensitivity decrease nears the DOE SunShot Initiative goal of 1 $/W installed cost; the increase nears the cost of smaller rooftop solar PV systems (5−10 kW, 3,740 $/kW). The nominal cost assumes large (200 kW) rooftop installations	(Kann et al., 2016)
Electric load	-/+20% (varies)	Captures potential load growth and energy efficiency measures implemented over the microgrid lifetime. Growth assumes a 1% annual rate (per EIA forecasts) and loss a -1% growth rate.	
Thermal loads	-/+50% (varies)	Captures deviations from the nominal climate zone 3B-coast.[e]	

[a] Annual Energy Outlook 2015 (AEO2015) forecasts for 2030 range from 4 $/mmbtu in the “High Oil and Gas Resource” scenario to 8 $/mmbtu in the “High Oil Price” scenario.

Table 1.4. Variation of 13 parameters in the simple sensitivity analysis, continued

Parameter Varied	-/+ variation (nominal, range)	Justification	Reference

[b] Captures the 5th- and 95th-percentile for the average retail electricity rate for commercial customers across all 50 states and the District of Columbia over the period 2013-2033, assuming the 2013 average retail price for commercial customers in California as the baseline and an annual increase of 0.6% per AEO2015 Reference case scenario. We project the price to 2033 to capture variation over the 20-year plausible lifetime of the microgrid. See the supplementary information for detailed treatment.

[c] The EIA frequently publishes data on monthly average retail electricity prices (through the AEO) based on collected utility revenues and sales—a metric that amalgamates all utility charges—but does not report demand charges or standby charges singly. Surveying the range of demand and standby changes across utilities to generate a sensitivity range is not straightforward because those charges are closely tied to volumetric charges in the ratemaking process, and, further, it is unclear how to normalize utility charges against the volumetric charge.

[d] Today's hardware cost for battery storage ranges widely across manufacturers (and chemistries)—from 350 to $>$2000 \$/kWh (lead-acid may be as low as 200 \$/kWh while lithium-ion may be 500 \$/kWh) but are forecasted to fall sharply over the next $5-10$ years. For reference, as of 2015 Tesla Motors sells its Powerwall stationary battery storage product for 350 \$/kWh (the offering excludes inverter and soft costs).

[e] The climate of coastal southern California is moderate and requires relatively little building heating and cooling. Climate zones in the US range from 1A (hot and humid, e.g. Miami, Florida) to 8 (cold, e.g. Fairbanks, Alaska).

Fig. 1.6 shows results for the simple sensitivity analysis. While results are nuanced, several trends are common across the three microgrids:

- In general, sensitivity is greatest to four factors: gas price, carbon cost, DER costs, and tariff costs.

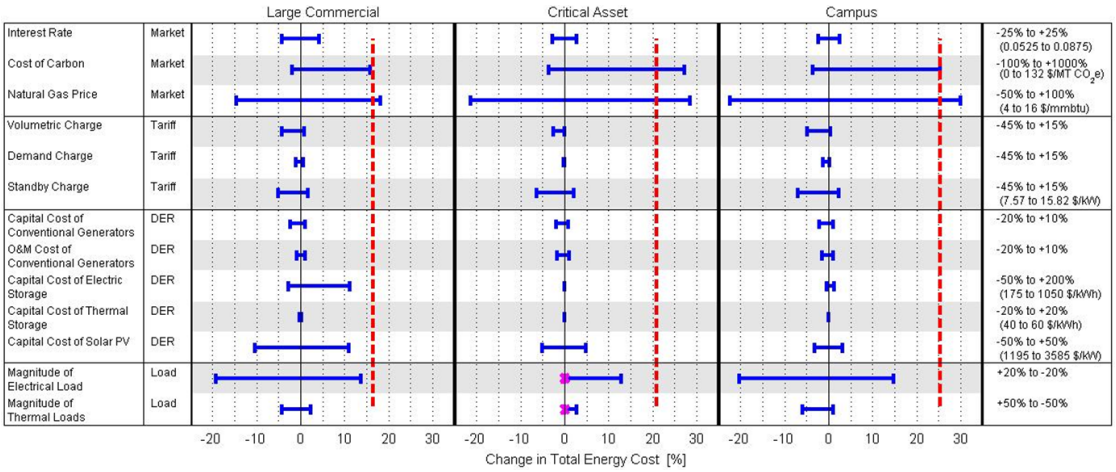

Figure 1.6. Change in total cost due to variation in the 13 simple sensitivities. The red dashed line denotes the "parity point"—the cost increase that reaches the total cost to the macro grid customer. For some market parameters (gas price, carbon cost) the parity point shifts because variation affects electricity rates for the macro grid customer, though such shifts are not noted. The models do not converge in two instances (marked in purple); in these cases the magnitude of electric and thermal load for the critical asset do not meet the resource adequacy constraint because the fixed configuration does not have sufficient capacity to supply the increase in critical load.

- Sensitivities to volumetric and demand charges are small because the microgrids primarily self-generate electricity. Put differently, once a customer invests in a microgrid, the optimal configuration reduces the cost of grid service (demand charges, volumetric charges) massively.

- Sensitivities to the carbon cost and gas price are high and exceed those to DER costs. In other words, opex can impact the total cost to a greater degree than capex (cf. the relative magnitude of DER and fuel costs in Fig. 1.5).

- The sensitivity to the electric load is large. The systems have reserve generation (gas generators are sized to meet the peak critical load and do not run at 100% output during non-peak hours). Hence the systems can supply the majority of load growth without additional capex, thereby increasing the economic benefit.

Regarding the last bullet, the means to supply load growth is highly dependent

on the volumetric charge and gas price—if volumetric charges are sufficiently low and/or gas prices high, the models instead revert to purchasing electricity. Note that variation (positive vs. negative) is reversed in Fig. 1.6 for the electrical and thermal load sensitivities—once investment is fixed, less load decreases the economic benefit.

The range of cost deviations shows that the business case for all microgrids is very robust—that is, only extraordinarily high values for the carbon cost and gas price (approaching 100-120 \$/tCO_2 and 12-16 \$/mmbtu) make microgrid adoption uneconomical. Yet high carbon taxes and gas prices would likely increase retail electricity rates commensurately and move the parity point to the right.

1.3.4 Strategically important variables: markets, technology, policy

Four variables have a large strategic effect on the business case for microgrid adoption: natural gas price, electric tariff charges, carbon cost, and electric storage cost. Gas prices are inherently variable and important because of the dominance of gas generators in the baseline optimal configurations. Carbon costs are expected to increase, while storage costs are declining rapidly. Tariff charges ultimately make it economical (or not) to invest in technologies that peak shave and/or supply base load in place of utility service; it other words, investment decisions must balance avoided costs from volumetric and demand charges while considering standby charges and fuel costs. Moreover, tariff charges and structures vary widely by utility and region. Each is a policy variable and possible pathway for policy intervention. Gas and carbon prices may push investment toward gas or renewable generators, while the magnitude of tariff charges may impose a "barrier to entry" if too low, and high storage costs may impose an analogous barrier for low-carbon configurations.

Electric storage in particular is widely seen as an important tool for integrating

renewables and facilitating deployment of low-carbon microgrids. Storage costs are decreasing rapidly, though the point at which deployment becomes cost-effective varies and is an open question, which others have investigated (Nottrott et al., 2013).

In what follows we run greenfield analyses for varying gas price, tariff charges, carbon cost, and electric storage cost (with justification for parameter variation as in section 1.3.3). For each variable, we re-determine the optimal system. We compare the total cost for the two customer types and distinguish electricity provision by resource. We present emission totals for the microgrid customer, which includes direct emissions from on-site generation as well as indirect emissions—the result of purchased electricity derived from generators in the wholesale market.

Natural gas price

We vary the gas price from $4-16$ \$/mmbtu (Fig. 1.7). Here we perform a "scenario analysis"—so-called because we vary multiple parameters to capture feedback.[10] The total cost for both microgrid and macro grid service increases with gas price because both customer types must purchase gas to meet the gas load $L_{\mathrm{n,g}}$. Across the full range of prices microgrids incur a smaller total cost when compared with utility service—with the largest differences occurring when prices are low (here the microgrids have the most flexibility to reduce costs).

Low prices drive investment in gas generators; as prices increase those are replaced with renewable sources as well as purchased electricity—a transition that decreases the economic benefit. Beyond 9 \$/mmbtu the large commercial system adopts a low-carbon configuration, and thereby maintains a positive (and increasing) economic benefit (i.e., it insulates itself from further gas price increases). The critical asset and

[10]We increase the volumetric charge with the gas price to account for a corresponding increase in natural gas-generated wholesale electricity. Marginal generators are typically gas-fired in the California wholesale market. We increase only the generation portion of the volumetric rate and scale the increase by the fraction of wholesale electricity generated from natural gas plants in California (45% at the time of this work).

campus systems, on the other hand, see a persistently diminishing economic benefit as prices increase—they do not transition to low-carbon configurations, but rather revert to purchasing electricity. Higher gas prices make it harder for these microgrids to utilize one of the chief advantages of local production: the on-site use and storage of thermal energy via CHP.

Across all three optimal systems there is a sharp transition in the source of electricity provision from gas-fired self-generation to purchased electricity. The transition points—at $7-9$, $11-13$, and $9-11$ \$/mmbtu for the large commercial, critical asset, and campus systems—have significant implications for the optimal configuration, business case, and policy decision-making if low-carbon systems are preferred. More research is needed to investigate whether these knife-edge transitions—particularly prominent in the smaller microgrids—reflect real-world conditions or are a standard discontinuity that often arises with optimization models.

Electric tariff charges

Volumetric rates are varied fractionally from $0.4-1.4$ in increments of 0.1 (Fig. 1.8), where unity is the rate in the baseline analysis. Rather than varying each element of the tariff separately, which would yield a highly complex sensitivity analysis, we vary the whole cluster of related volumetric charges so that potential investors and policy makers can understand better the fundamental impact of such charges on microgrid configuration and viability.

We find that volumetric rates greatly affect the total cost and optimal configuration. As with the gas price, sharp transition points exist in which gas-based self-generation and purchased electricity are substituted. When rates are low (<0.5), the microgrid total cost exceeds that to the macro grid customer; that is, the economic benefit is negative.

Microgrids realize an economic benefit beginning with rates >0.5 that increases

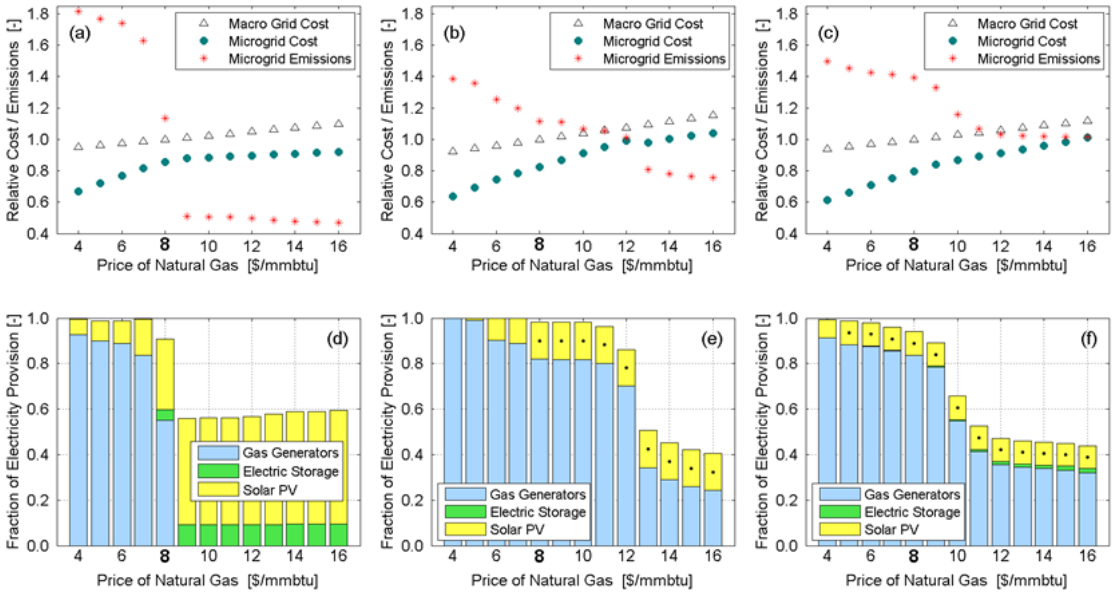

Figure 1.7. (a)−(c) The total cost and total CO_2 emissions are normalized by the total cost to and total emissions of the macro grid customer, respectively, for the nominal gas price (8 $/mmbtu; bolded); and (d)−(f) the fraction of electricity supplied by microgrid resource across variation in gas price. Each bar shows results from a single model run. The uncolored portion above a bar represents purchased electricity. A dot in the solar PV bar denotes that the solar PV space constraint has capped installations.

with rising rates. We observe scenarios with near 100% self-generation. Notably, these occur under present-day electricity rates in southern California. Purchasing electricity is the dominant mode of supply for rates near 0.6−0.9 (depending on the microgrid).

Optimal configurations fit broadly within two domains—low-carbon and gas-based configurations—separated by a transition point. The large commercial system is low-carbon for rates $<$0.9 and gas-based for rates $\geq$0.9, with gas dominant with increasing rates. Similar transitions occur for the critical asset and campus microgrids—for rates 0.6−0.8 and 0.7−0.9 respectively. For these two systems, however, gas generators remain the dominant microgrid resource over the range of rates. They are the bedrock of investment and business case for larger systems.

Demand charges are varied fractionally from 0.4−1.4 in increments of 0.1 (Fig. 1.9). As before, unity is the nominal demand charge in the baseline analysis. All demand

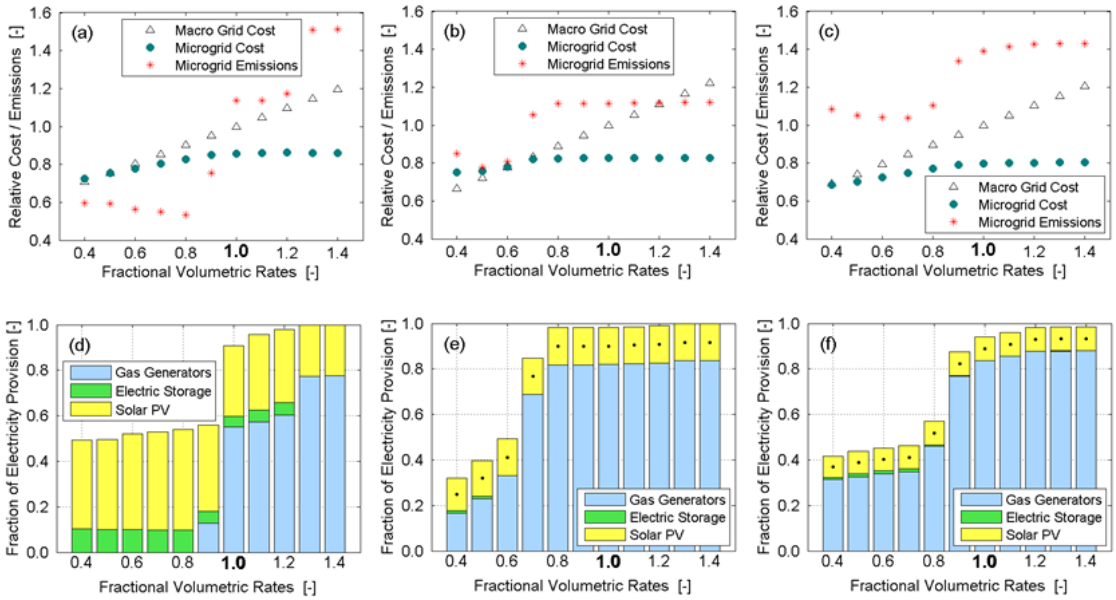

Figure 1.8. (a)−(c) The total cost and total CO_2 emissions are normalized by the total cost to and total emissions of the macro grid customer, respectively, for the nominal volumetric charge (unity; bolded); and (d)−(f) the fraction of electricity supplied by microgrid resource across variation in volumetric charges. Each bar shows results from a single model run. The uncolored portion above a bar represents purchased electricity. A dot in the solar PV bar denotes that the solar PV space constraint has capped installations.

charges are varied concurrently. We observe that peak shaving is key to the business case over the wide range of demand charges. For charges <0.6, the economic benefit is negative, while for charges >0.6 the total cost increases slightly and soon plateaus. Here the microgrids self-generate nearly 100% of electric load, and hence mitigate the demand charge to zero (or close to zero).

For present day charges (unity), it is economical to peak shave and, further, to self-generate nearly all electric load. The critical asset invests in gas generators to supply its large fraction of critical load in the event of outages independent of the demand charge, and hence sees a business case for peak shaving for demand charges 0.4−1.4. The large commercial and campus have a smaller fraction of critical load—they revert to purchasing electricity when demand charges are small. For these two microgrids, we observe a

sharp transition (0.8−1.0 and 0.7−0.9 respectively) separating two modes of electricity provision—purchased electricity when demand charges are small and gas generation when large. Present-day demand charges thus lie near this inflection point that separates two distinct investment cases—one based on renewables and partial self-generation, and another on gas generators and near 100% self-generation.

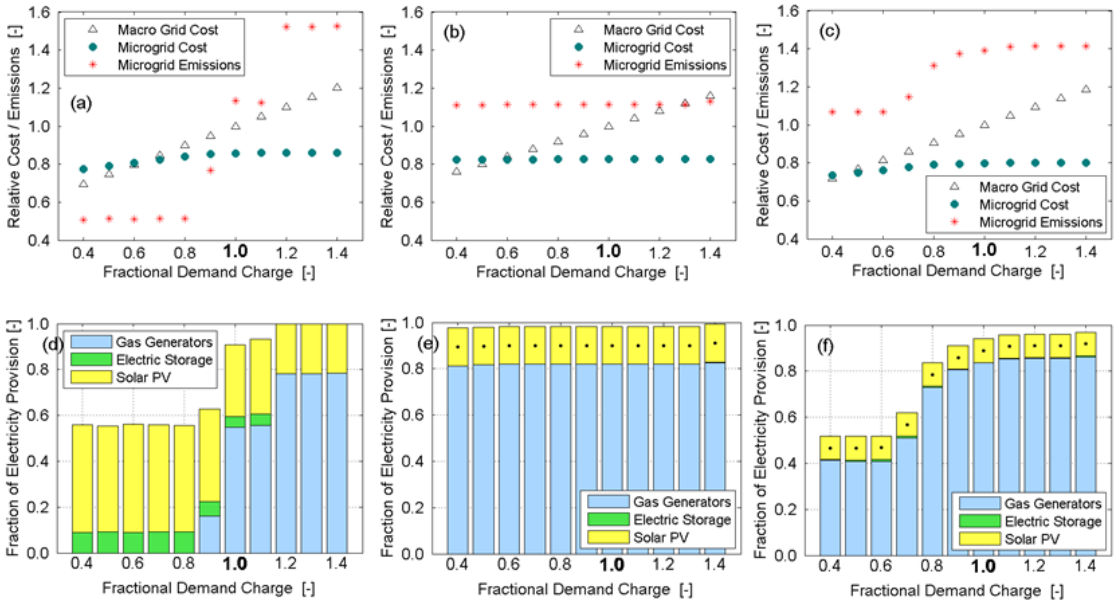

Figure 1.9. (a)−(c) The total cost and total CO_2 emissions are normalized by the total cost to and total emissions of the macro grid customer, respectively, for the nominal demand charge (unity; bolded); and (d)−(f) the fraction of electricity supplied by microgrid resource across variation in demand charges. Each bar shows results from a single model run. The uncolored portion above a bar represents purchased electricity. A dot in the solar PV bar denotes that the solar PV space constraint has capped installations.

Carbon cost

We vary the carbon cost from 0 to 132 \$/tCO_2 (Fig. 1.10) and, as with the gas price, run a scenario analysis.[11] We find that increasing carbon cost can shift investment

[11] We increase the volumetric charge with the carbon cost to account for a corresponding increase in generation costs from fossil fuel power plants and subsequently the clearing price in the CAISO wholesale market and retail rates. We use AEO 2014 projections and compare the percent difference in economy-wide electricity generation costs between the "Reference case" and "Greenhouse gas \$10" scenarios. We apply that difference as a percent increase to the generation portion of the volumetric charge (taken to be 7/16 in

from gas generators to renewables and that the onset of that shift arises at lower carbon costs for smaller microgrids (i.e. the large commercial). This is because such transitions are constrained by available space for PV in the two larger microgrids. These two, as well, make efficient use of gas with CHP—an efficiency advantage that is not offset until higher carbon prices.

The large commercial system supplies nearly 80% of electric load with gas generators at a carbon cost of 0 \$/tCO_2 and only 15% at 30 \$/tCO_2. For costs $>$36 \$/tCO_2, a low-carbon configuration with electricity purchases replaces gas generators. The critical asset and campus systems also divest in gas generators with rising carbon cost; however, they purchase additional electricity rather than transition to a low-carbon configuration. This is due in part to the solar PV space constraint.[12] This result suggests that for such configurations, decarbonizing the electricity system may best be achieved with centralized grids.

Electric storage cost

We use as the nominal turnkey electric storage cost a forecasted estimate (350 \$/kWh) that aligns with estimates of current and projected costs over the next $5-10$ years, and vary the electric storage cost $0-1150$ \$/kWh (Fig. 1.11) in increments of 50 \$/kWh.

The large commercial system adopts additional storage as costs fall. Two transitions are salient. The first occurs when storage is first adopted, at 350 \$/kWh, and the second when the microgrid reaches a low-carbon configuration, at 200 \$/kWh. With these transitions the microgrid also purchases additional electricity, eventually supplying over 30% of load. At costs $<$100 \$/kWh, further storage does not provide a benefit (i.e.,

SDG&E's service territory).

[12] We run the same greenfield analysis without the space constraint. Results show that high carbon costs do cause a shift in investment—from gas generators to solar PV and electric storage—in the larger two microgrids. Consequently, it seems a lack of space in which to install an optimal low-carbon configuration may inhibit efforts to decarbonize the grid through single-owner, single-property microgrids.

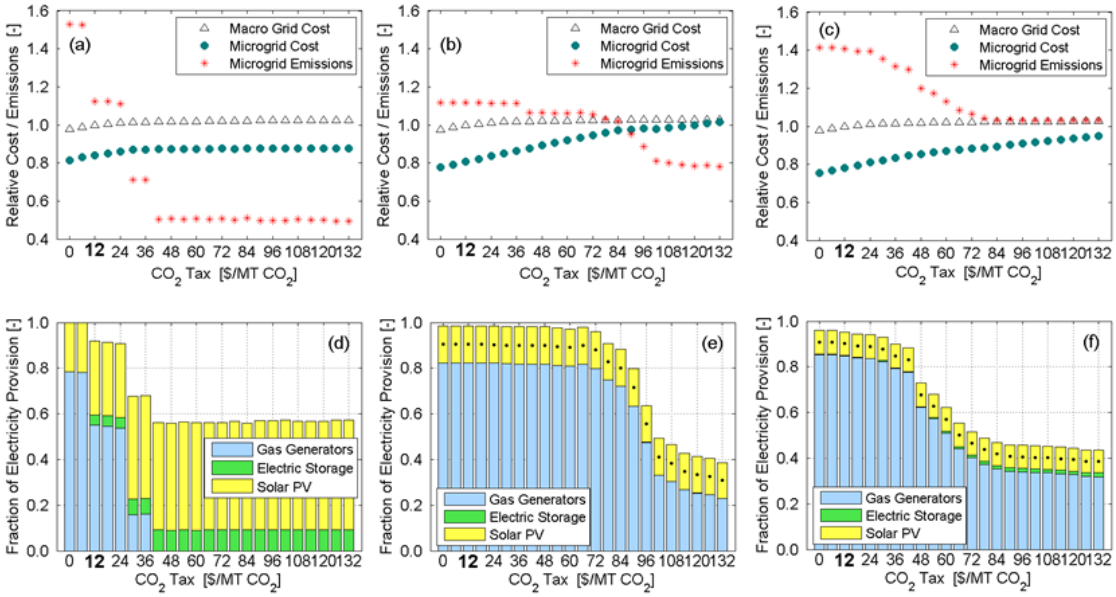

Figure 1.10. (a)−(c) The total cost and total CO_2 emissions are normalized by the total cost to and total emissions of the macro grid customer, respectively, for the nominal carbon cost (12 \$/tCO_2; bolded); and (d)−(f) the fraction of electricity supplied by microgrid resource across variation in the carbon cost. Each bar shows results from a single model run. The uncolored portion above a bar represents purchased electricity. A dot in the solar PV bar denotes that the solar PV space constraint has capped installations.

energy shifting is not needed) because the microgrid has already plateaued demand and achieved perfect on-peak/off-peak energy arbitrage.

The critical asset and campus also purchase additional storage as costs fall, but never adopt low-carbon configurations. Gas generators remain the dominant resource throughout. Even at 0 \$/kWh, storage is used only to facilitate peak shaving, as observed in the baseline results. The solar PV space constraint caps installations, thereby restricting potential low-carbon transitions, in which storage might store significant excess solar PV generation for discharging at night.

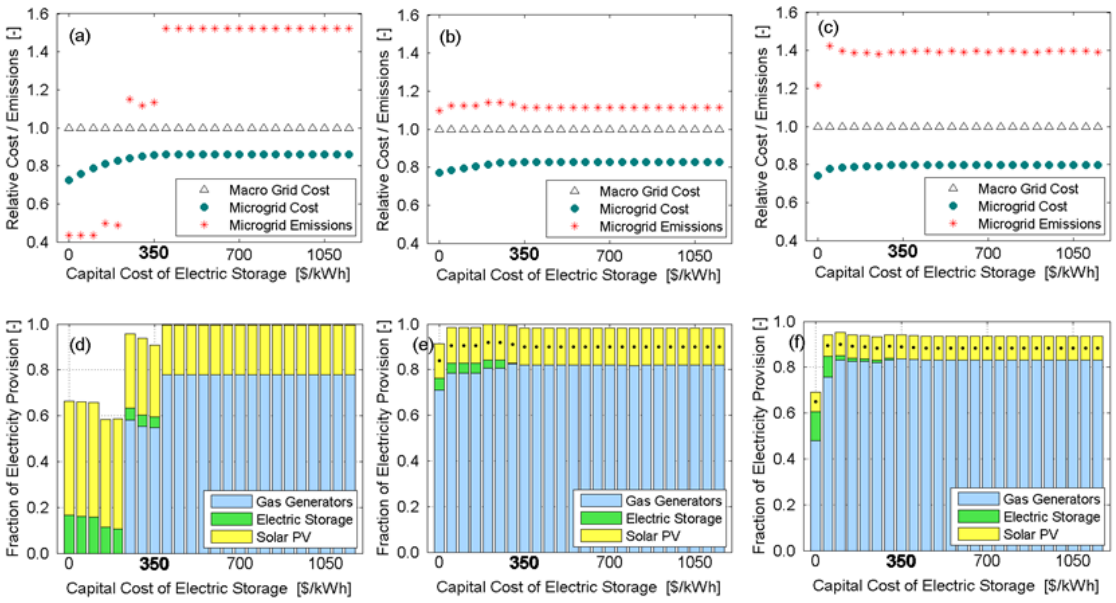

Figure 1.11. (a)−(c) The total cost and total CO_2 emissions are normalized by the total cost to and total emissions of the macro grid customer, respectively, for the nominal electric storage cost (350 $/kWh; bolded); and (d)−(f) the fraction of electricity supplied by microgrid resource across variation in the electric storage cost. Each bar shows results from a single model run. The uncolored portion above a bar represents purchased electricity. A dot in the solar PV bar denotes that the solar PV space constraint has capped installations.

1.4 Conclusion and policy implications

Under the right conditions, the supply of electric and thermal services from a microgrid can be cost-effective when compared with complete reliance upon macro grid utility service. Some of those conditions reflect changes in technology and market conditions; some are rooted in policy choices; and many reflect the interplay of technology, policy and markets.

We have focused here on the business case for investing in microgrids by focusing on the total cost of energy service for three different types of likely microgrid customers. Under prevailing conditions in southern California we find that the case for cost-effective shifts from pure utility service to microgrids is robust, and especially so

for large customers who can utilize the intrinsic advantage that local production offers in managing electric and thermal loads in tandem. Centrally, the case for microgrids is a case for natural gas fired locally that also generates significant thermal energy. Though smaller microgrids by contrast rely relatively less on gas and more on renewables, across all microgrids gas generators supply the majority of on-site electric and thermal energy. While the work presented here looks only at the economics for energy provision, future work—including that planned by our team—can enhance this analysis by adding value streams derived from increasing reliability and resiliency. We are interested, as well, in exploring these new value streams in different climate and regulatory environments, as was done in Maribu et al. (2007).

Through analyses of uncertainty we find that business cases are robust across a wide variation in parameters—costs of critical technologies, tariff rates, natural gas prices, and the price charged for carbon emissions—over which policy makers have some influence. Of particular importance for large microgrid systems is the price of natural gas, which regulators can influence only indirectly. Renewables and utility service are more attractive in a world with high gas prices, but gas remains an important player for larger systems even at 16 $/mmbtu. Preference for gas generators holds when carbon prices are independently high. In worlds where utility service costs are high and where DER technologies improve rapidly—plausibly, a world that California and other jurisdictions are now entering—the case for microgrids of all sizes is even more robust. This finding aligns with results in Firestone et al. (2006), who similarly looked at the effect of tariff charge sensitivities on DER adoption.

For policy makers, there are at least two major implications of this work. The first concerns how policy makers might guide a nascent microgrid landscape by scaling up deployment. It is one thing for a scattered number of customers to switch to grid-tied microgrids for self-supply, but another for grid operations to be structured on a new

topography of widespread distributed microgrids. Though more investigation is needed to explore how adoption may become widespread, our results indicate that microgrid deployment will likely resemble the former if left alone. Policy makers interested in the latter have the opportunity to shape deployment to align with larger social goals like reducing greenhouse gas emissions.

To this end policy makers have control over several important parameters—in particular, interconnection tariffs (which respond to regulatory decisions) and the cost of carbon (which is a policy choice). Policy makers also have the capacity to alter the cost of DER technologies—either directly with subsidies or indirectly through procurement mandates. We have been able to model some of these but the work presented here suggests the need for modelers to develop more sophisticated methods that capture both the full set of policy options available as well as of value streams policy makers might invoke to shape widespread deployment—for example as is happening in the northeast US states with resiliency-based systems. In jurisdictions such as California and New York that are actively pushing adoption of DERs it is that full set of policy options that will determine how markets could be developed.

The second implication for policy is perhaps more profound. Because the case for gas-based microgrids is so robust, policy makers may find that adoption of DER-friendly policy reforms leads to even more ubiquitous adoption of gas-based microgrids. Emissions from those systems are smaller when compared with some grids (those dominated by coal and gas generators) but they are not zero, and in many jurisdictions policy makers are setting goals for cutting emissions that probably require zero or negative emissions from electric power. California, for example, has a goal of 80% cuts in CO_2 emissions below 1990 levels by 2050. Assuming some emissions will continue to be needed from transportation, that economy-wide goal implies zero for the rest of the energy system. Policy makers who push DER and microgrids without simultaneously

adopting a carbon price (or regulatory substitute) may unwittingly encourage the creation of a long-lived microgrid infrastructure that is incompatible with zero carbon.

The text and data in Chapter 1, in full, is a reprint of the material as it appears in “Evaluating business models for microgrids: Interactions of technology and policy”, Hanna, Ryan; Ghonima, Mohamed, Kleissl, Jan, Tynan, George, David G., Victor, *Energy Policy*, 103 (2017), 47-61. The dissertation author is the primary investigator and author of this article. The supplementary information referred to in the text is available online at doi:10.1016/j.enpol.2017.01.010.

Chapter 2

Reliability Evaluation for Microgrids Using Cross-Entropy Monte Carlo Simulation

2.1 Introduction

Over the past half decade there has been growing interest in microgrids—notably, in the wake of superstorms, among grid operators and regulatory agencies seeking public grid resiliency benefits. With an expanding number of successful projects (Wilson, 2017), there is interest too among private entities (i.e., utility customers) seeking, conversely, private benefits from better reliability (Asmus, 2016).

Microgrids are aggregations of electric load and distributed energy resources (DERs) that can disconnect, or "island", from the bulk grid and provide autonomous (and potentially seamless) backup power to customers within.[1] They can increase electric service reliability beyond that provided by the local utility. When they do, customers generate value by avoiding economic losses from grid outages that they would otherwise incur as passive customers.

Analyzing reliability, as well as the economics underlying investment, requires

[1] Definition from the U.S. Department of Energy Microgrid Exchange Group. The definition we adopt is rigorous and worth noting since microgrids are often loosely defined.

reliability evaluation methods applied specifically to the case of microgrids. Sequential MCS and the cross-entropy method provide a basis. Sequential simulation (cf. analytical methods and non-sequential simulation) is widely used in studies of power system reliability (Billinton and Li, 1994) and is considered state-of-the-art because it models time dependencies in power systems and produces the broadest set of results among methods (Billinton and Allan, 1996). Simulation works by mimicking the probabilistic behavior of load, generators, climate-dependent resources, and other components of interest in the system—capturing, e.g., fluctuating load or solar PV power as well as component failures and repairs. State changes may be prescribed (such as with time series load or solar PV power) or random (such as with unit failures and repairs). The simulation repeats iterations—each with a different probabilistic outcome—until it achieves statistical convergence.

MCS has been applied in particular to small isolated power systems (Billinton and Karki, 2001; Karki and Billinton, 2001; Billinton and Bagen, 2006). These small systems resemble microgrids because of their size and resource mix—typically they use fossil fuel-fired generators, solar PV, and energy storage—but differ in their interconnection. Isolated systems are themselves bulk grids, whereas microgrids are embedded within a grid that is in many cases already highly reliable. That has huge implications for simulation methods, which can face convergence issues when running very reliable system configurations (defined as systems with loss of load probability (LOLP) $< 10^{-5}$).

Most recently, "CE-MCS" methods, which combine the cross-entropy method with MCS, have been developed and shown to greatly reduce computation times (da Silva et al., 2010; Gonzalez-Fernandez and da Silva, 2011). Cross-entropy works by distorting the unit failure rates such that failures (and hence loss of load events and convergence) occur with fewer iterations. These methods have been demonstrated successfully on large grids (e.g., tens of GW capacity) with resources including conventional generators, solar

PV, wind, and hydro power. They have not been applied to microgrids, however, and importantly have lacked a resource key to microgrids—energy storage. Storage requires unique treatment from a modeling standpoint because it is dispatchable and has a time history.

Methods therefore exist which can be tuned to analyze microgrid reliability. This work is the fist to formulate them specifically for the case of microgrids. Herein, we present a new method that combines the CE-MCS (with its fast convergence properties) with the modeling framework used for analysis of small power systems. Specifically, it extends the CE-MCS method in Gonzalez-Fernandez and da Silva (2011) by applying it to the case of microgrids (itself a topic treated rarely in power system reliability literature), by including a new energy resource (battery energy storage) that can dispatch and charge during bulk grid outages, and by including flexibility (i.e., the ability to change unit output), in addition to capacity, as a requirement in the reliability evaluation. In the context of microgrid reliability evaluation, considering flexibility is essential (as we will show). The new algorithm calculates the indices most relevant to analyzing economics—LOLP, loss of load frequency (LOLF), and what we call the loss of load cost (LOLC)—the economic loss incurred from microgrid outages, or *interruptions*.

2.2 Model and algorithm

The simulation algorithm has a period $T = 8760$ h with interval timestep $\Delta = 1$ h. T is represented by vectors of length s, where $s = T/\Delta = 8760$. We denote s-dimensional vectors of real numbers by $\mathbb{R}^s$ and use $\mathbb{R}^s_{\{\mathcal{N}\}}$ to denote vectors with all elements $1, ..., s \in \mathcal{N}$.

2.2.1 A model for grid-connected microgrids

We consider grid-connected microgrids at the distribution level, with all load and DERs at a single bus on the load side of the distribution transformer (Fig. 2.1a). The microgrid does not impact the reliability of loads outside it. Viewed from the point of common coupling (PCC), the distribution system appears to the microgrid as a single generator with sufficiently large capacity to supply peak load at all time.

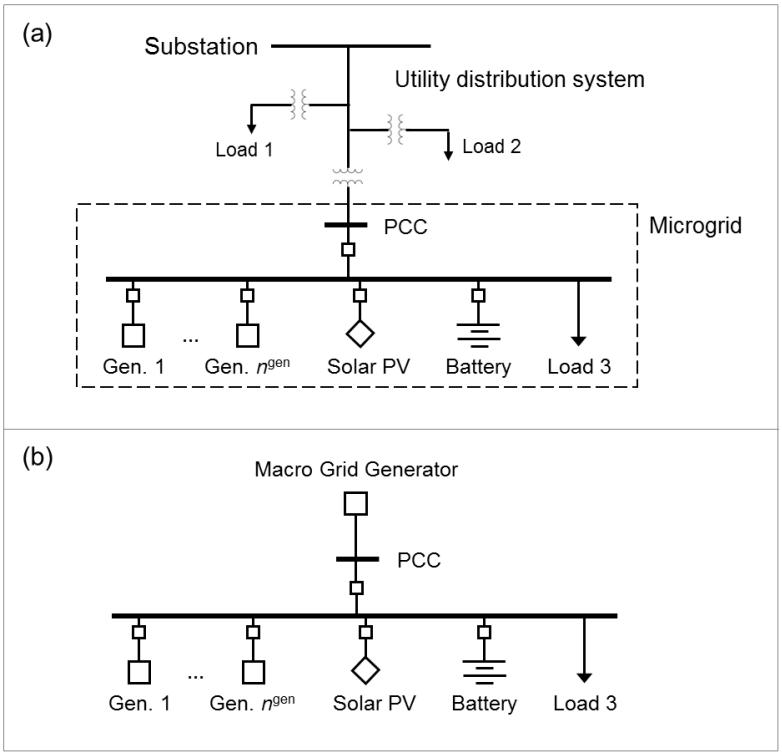

Figure 2.1. (a) Distribution system and microgrid topology and (b) modeled microgrid system topology. Adapted from (Wang et al., 2013).

Following Wang et al. (2013), the distribution system is modeled at the microgrid bus as an "equivalent" generator (Fig. 2.1b) with capacity $\overline{P}^{\text{ds}} \gg \max_k\{l_k\}$, where "ds" denotes distribution system and $l_k \in \mathbb{R}^s_{\{\geq 0\}}$ is the microgrid load time series. The

equivalent generator has failure rate λ^{ds} and repair rate μ^{ds} given by

$$\begin{aligned} \lambda^{\mathrm{ds}} &= \frac{1}{8760} \cdot \mathrm{SAIFI}, \\ \mu^{\mathrm{ds}} &= \frac{\mathrm{SAIFI}}{\mathrm{SAIDI}}. \end{aligned} \tag{2.1}$$

where the utility metrics SAIFI (system average interruption frequency index) and SAIDI (system average interruption duration index) have units of occurrences/year and hours/year, respectively, and are reported by the utility.[2]

We include three resources that contribute to improving reliability: conventional fossil generators, solar PV, and battery energy storage. DERs are modeled with failure rate $\lambda^{(\cdot)}$ and repair rate $\mu^{(\cdot)}$, which are known empirically, and defined by their operating specifications: generators have nameplate capacity $\overline{P}^{\mathrm{gen}}$ and maximum ramp rate $\overline{R}^{\mathrm{gen}}$; battery storage has maximum and minimum capacity $\overline{E}^{\mathrm{bs}}$ and $\underline{E}^{\mathrm{bs}}$, respectively, maximum discharge and charge rating $\overline{P}^{\mathrm{bs}}$ and $\underline{P}^{\mathrm{bs}}$, and discharge and charge efficiencies $\eta^{\mathrm{bs}}_{\mathrm{dchg}}$ and $\eta^{\mathrm{bs}}_{\mathrm{chg}}$. Any solar PV power time series can be input from an external source.

We consider generators as discrete units, all solar PV capacity as a single system, and all battery storage capacity as a single system, since storage capacity is often connected modularly in a single housing. We assume buses, cables and other grid devices are 100% reliable—and thereby give focus to the DERs that increase reliability, but which themselves are not 100% reliable.

2.2.2 Simulation algorithm

The algorithm is developed for microgrids specifically, and considers features which distinguish microgrids from the larger bulk grids to which they are interconnected—

[2]Utility data on MAIFI (momentary average interruption frequency index), when available, can be considered by setting the failure rate $\lambda^{\mathrm{ds}} = \frac{1}{8760} \cdot (\mathrm{SAIFI} + \mathrm{MAIFI})$, where the availability sequence h^{ds}_k is then created by considering down-times for both outage types. Momentary outages have duration <5 minutes and last one timestep in the algorithm.

specifically, resource mix and islanding capability.

Microgrids can disconnect from the bulk grid and operate autonomously by balancing load with power generated on-site—and may do so seamlessly depending on resource mix. The ability to maintain service continuity during transitions can be essential to load within. From the standpoint of reliability analysis, it is critical to model this dynamic; we do so by adding a flexibility constraint—in addition to the analysis of capacity that is standard in reliability evaluation.

Capacity requires that available microgrid generating capacity exceed load during grid outages to avoid interruptions—without regard to operation. The flexibility component, as an extension, further requires that resources be dispatched to meet changes in load during outages, including at the moment of outage, and considers resources as either slow ramping (generators) or fast ramping (battery storage).

In practice, generators like combustion engines and microturbines require several minutes to reach peak output, whereas batteries require milliseconds. Because detection and control equipment can recognize impending grid outages with sufficient lead-time to island and supply load with fast ramping resources, we require that generators use one simulation timestep to increase power, whereas battery storage can respond instantaneously.[3] Thus, in a practical sense, storage is critical for maintaining continuous power at the moment of outage, whereas generators are critical for supplying bulk load during extended outages. Because the timestep $\Delta = 1$ h, which is standard in reliability evaluation, the algorithm likely overestimates the need for storage kWh capacity (though not kW rating).

Flexibility is an important addition to the standard formulation for reliability evaluation. In other regards, the algorithm functions similarly to CE-MCS methods. As

[3]It may also be possible to model generators as fast ramping and instead apply post-processing corrections to interruption sequences (to capture, e.g., a 15-minute interruption while generators turn on and increase power).

with such methods, it has two components—optimization and simulation (Fig. 2.2). Each are discussed in turn.

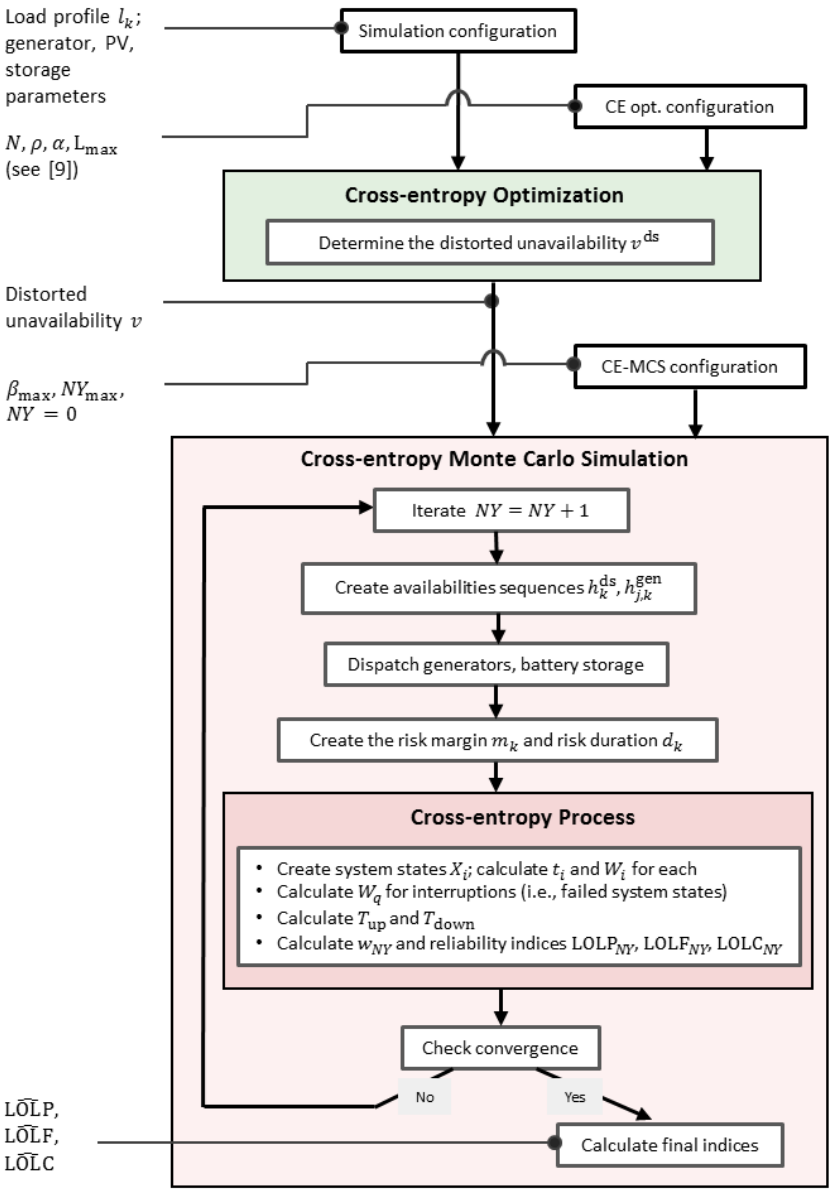

Figure 2.2. The simulation algorithm consists of two parts: optimization (green box) and simulation (red box). The optimization process finds the near-optimal distortion for unit unavailabilities, which the simulation then uses to calculate reliability indices.

2.2.3 Cross-entropy optimization

The goal of cross-entropy optimization generally is to find a set of new (near-optimal) reference parameters that increase the likelihood of events of interest. In reliability evaluation, these are the "distorted" unit unavailabilities v—found from the original availabilities $u = \lambda/(\lambda+\mu)$—that increase the probability of loss of load events and hence speed simulation convergence. Explication of the cross-entropy method is out of the scope of this paper; see Rubinstein and Kroese (2004) for detailed treatment.

In the algorithm, we distort the failure rate for the distribution system λ^{ds} since it is the primary source of reliability in the system, but leave generators, solar PV and storage undistorted.[4] Repair rates $\mu^{(\cdot)}$ are not distorted; as such, only the periods between interruptions are compressed. Interruption sequences remain completely undistorted (repair rates $\mu^{(\cdot)}$, and hence the mean times to repair $\mathrm{MTTR}^{(\cdot)} = 1/\mu^{(\cdot)}$, are unchanged), including the power supplied by generators and battery discharging and charging. Distorted unavailabilities are given by $v = \lambda^{\star}/(\lambda^{\star}+\mu^{\star})$, where "star" denotes the distorted quantity and $\mu^{\star} = \mu$.

Because the use of distorted parameters affects the frequency and duration of system states in the simulation, quantities (e.g., state duration and, ultimately, reliability indices) must be compensated via a *compensation factor* W to avoid biased estimates. Following Eq. 8 in Gonzalez-Fernandez and da Silva (2011), it is given by

$$W = \frac{\prod_{j=1}^{n^{\mathrm{units}}} (1-u_j)^{x_j} (u_j)^{1-x_j}}{\prod_{j=1}^{n^{\mathrm{units}}} (1-v_j)^{x_j} (v_j)^{1-x_j}}\,, \tag{2.2}$$

where u_j and v_j are the original and distorted unavailabilities, respectively, x_j is the state (1–not failed, 0–failed) of unit j in system state i, and n^{units} is the total number of distorted units.

[4] For very reliable configurations, generator failure rates $\lambda_j^{\mathrm{gen}}\ \forall\ j = 1,\ldots,n^{\mathrm{gen}}$ could also be distorted.

The principal steps in the cross-entropy optimization used here are standard and identical to those in Gonzalez-Fernandez and da Silva (2011); see steps 1a-10a in Gonzalez-Fernandez and da Silva (2011).

2.2.4 Cross-entropy Monte Carlo simulation

Cross-entropy simulation—the second stage of two in the CE-MCS—is a sequence of five steps (Fig. 2.2).

Step 1. First, unit states are initialized for the simulation period T by creating sequences of up-times when a unit is operational and down-times when it is failed. Sequences are created using

$$\begin{aligned} \textit{up-time} &= -\frac{1}{\lambda_j}\ln(r_1)\,, \\ \textit{down-time} &= -\frac{1}{\mu_j}\ln(r_2)\,. \end{aligned} \tag{2.3}$$

where λ_j and μ_j are the failure rate and repair rate of unit j, respectively, and r_1 and r_2 are uniformly distributed random numbers between 0 and 1. Series of up- and down-times are drawn successively and independently for all units until they form *availability sequences* $h_k \in \mathbb{R}^s_{\{0,1\}}$. As is standard, unit failure and repair rates are assumed exponentially distributed (Billinton and Allan, 1996).

Step 2. Next, dispatchable units (generators, battery storage) are scheduled during grid outages using **Algorithm 1**. In the context of reliability analysis, they act as reserve units, attempting to maintain continuous electric service. The new constraint on flexibility is considered here: at the moment of outage, generators cannot immediately change output to supply load, but instead require one timestep to ramp up power output. Battery storage, however, can ramp instantaneously to meet load imbalance at the moment of outage.

Step 3. Third, distribution system and DER output are combined to form two time series vectors—the risk margin $m_k \in \mathbb{R}^s$ and risk duration $d_k \in \mathbb{R}^s_{\{0,1\}}$—that define interruption sequences (i.e., *microgrid* outages). The risk margin is the difference between total generation, including from the distribution system, and microgrid load:

$$m_k := p_k^{\text{ds}} + \sum_j p_{j,k}^{\text{gen}} + p_k^{\text{pv}} + p_k^{\text{bs}} - l_k \,, \tag{2.4}$$

where $p_k^{\text{ds}} = \overline{P}^{\text{ds}} \cdot h_k^{\text{ds}}$ is the power provided by the distribution system, $p_{j,k}^{\text{gen}}$ is the power output of generator j, p_k^{pv} is the solar PV output, and p_k^{bs} is the battery storage output (by convention >0 denotes discharging), $\forall k = 1, ..., s$. The risk duration then denotes interruption sequences, or loss of load states:

$$d_k := \begin{cases} 1, & m_k < 0 \\ 0, & \text{otherwise}\,. \end{cases} \tag{2.5}$$

Step 4. Next, reliability indices for the simulation iteration are calculated via the cross-entropy process, which is initialized with a maximum number of allowed iterations $NY_{\max}$, the simulation length s, and a convergence criteria $\beta_{\max}$ (typically $0.01 - 0.1$, where the coefficient of variation $\beta = \sigma[E(\cdot)]/E(\cdot)$ for each reliability index is the ratio of the standard deviation of the sample mean to the sample mean). Also, NY is set to 0. The process has several substeps. First, we create the explicit list of system states $X_i = [x_i^{\text{ds}}, x_{i,1}^{\text{gen}}, ..., x_{i,n^{\text{gen}}}^{\text{gen}}, d_i]$ for all states i, where states are the steady-state periods between system transitions. Transitions are defined by any change in a unit availability sequence $h_k^{(\cdot)}$ and/or the risk duration d_k. Each state is defined by a residence time t_i and a compensation factor W_i. The former is the duration the system resides in the state; the latter is given by Eq. (2.2).

Each state i is either in a loss of load state (i.e., $d_i = 1$, in which case the microgrid is "failed") or it is not. For failed states, a group compensation factor $\tilde{W}_q$ is calculated following Eq. 17 in Gonzalez-Fernandez and da Silva (2011):

$$\tilde{W}_q := \frac{P\{X_1\} \cdot P\{X_2|X_1\} \cdots P\{X_{n_q}|X_{n_q-1}\}}{P^\star\{X_1\} \cdot P^\star\{X_2|X_1\} \cdots P^\star\{X_{n_q}|X_{n_q-1}\}}\,, \tag{2.6}$$

where $P^\star$ denotes probability using the distorted unavailabilities. The group compensation factor accounts for the entire interruption sequence—which must be captured to quantify the economic loss of interruption c_q. The use of conditional probabilities, which give the probability of the entire sequence, is therefore needed.

Next, two quantities, T_{up} and T_{down}, are calculated for the set of system states X_i. T_{up} is the compensated duration of non-failed states over the simulation period and T_{down} gives the same quantity for failed states:

$$\begin{aligned} T_{\text{up}} &= \sum_{i \in NF} t_i W_i\,, \\ T_{\text{down}} &= \sum_{i \in F} t_i W_i\,. \end{aligned} \tag{2.7}$$

where NF is the set of non-failed microgrid states and F is the set of failed states.

Lastly in the cross-entropy process, a weight w and reliability indices for the iteration NY are calculated:

$$w_{NY} = \frac{T_{\text{up}} + T_{\text{down}}}{s} \tag{2.8}$$

$$\text{LOLP}_{NY} = \frac{T_{\text{down}}}{T_{\text{up}} + T_{\text{down}}} \cdot w_{NY} \tag{2.9}$$

$$\text{LOLF}_{NY} = \sum_q \tilde{W}_q \cdot w_{NY} \tag{2.10}$$

$$\text{LOLC}_{NY} = \sum_q c_q \tilde{W}_q \cdot w_{NY}\,, \tag{2.11}$$

where q indexes interruption sequences and c_q is the cost, or economic loss, of interruption q. A weighted approach using w_{NY} is necessary because T_{up} and T_{down} vary across iterations.

Step 5. The fifth and final step in the CE-MCS is to check convergence, and if converged (or if $NY = NY_{\max}$) to calculate final indices for the simulation:

$$\hat{\text{LOLP}} = \frac{\sum_{y=1}^{NY} \text{LOLP}_y}{\sum_{y=1}^{NY} w_y}, \tag{2.12}$$

where $\hat{\text{LOLF}}$ and $\hat{\text{LOLC}}$ can be similarly estimated. Further, the loss of load duration $\hat{\text{LOLD}} = \hat{\text{LOLP}}/\hat{\text{LOLF}}$. If not converged, the algorithm returns to the updating step and advances to a next iteration. The final CE-MCS indices are the expected values for each, respectively, given the probabilistic nature of the system.

Algorithm 1. Scheduling dispatchable units

for timestep $k = 1, ..., n_q^{\text{int}}$ in outage q **do**
  calculate the load deficit: $\tilde{l}_k = l_k - p_k^{\text{pv}}$
  if $k = 1$ **then**
    dispatch storage: $p_k^{\text{bs}} = \Delta \cdot \min\{\eta_{\text{dchg}}^{\text{bs}} \cdot \overline{P}^{\text{bs}}, \tilde{l}_k, \eta_{\text{dchg}}^{\text{bs}} \cdot (E_k^{\text{bs}} - \underline{E}^{\text{bs}})\}/\eta_{\text{dchg}}^{\text{bs}}$
  else
    for generator $j = 1, ..., n^{\text{gen}}$ **do**
      schedule generator j: $p_{j,k}^{\text{gen}} = \min\{p_{j,k-1}^{\text{gen}} + \overline{R}_j^{\text{gen}} \cdot h_{j,k} \cdot \Delta\ , h_{j,k} \cdot \overline{p}_j^{\text{gen}}\}$
    end for
    re-calculate load deficit: $\tilde{l}_k = l_k - p_k^{\text{pv}} - \sum_j p_{j,k}^{gen}$
    if $\tilde{l}_k > 0$ **then**
      dispatch storage as for $k = 1$
    else
      charge storage: $p_k^{\text{bs}} = \Delta \cdot \min\{\underline{P}^{\text{bs}}/\eta_{\text{chg}}^{\text{bs}}, \text{-}\tilde{l}_k, (\overline{E}^{\text{bs}} - E_k^{\text{bs}})/\Delta/\eta_{\text{chg}}^{\text{bs}}\} \cdot \eta_{\text{chg}}^{\text{bs}}$
    end if
  end if
end for

2.2.5 Example

To illustrate, Fig. 3.4 shows how generators and battery storage in a sample system are dispatched in response to a grid outage. A 100 kWh/50 kW storage system with 90% bi-directional efficiency discharges maximum power at the moment of outage, $k = 1$, but cannot supply the entire load deficit. Three 60 kW generators turn on and ramp up to meet load at $k = 2$, and further recharge the battery. They supply load deficit again at $k = 3$ before shutting down at $k = 4$ when the grid is repaired. Because the battery is undersized (relative to peak load), microgrid customers experiences loss of load at $k = 1$. For outages during nighttime hours, the battery may prevent interruptions.

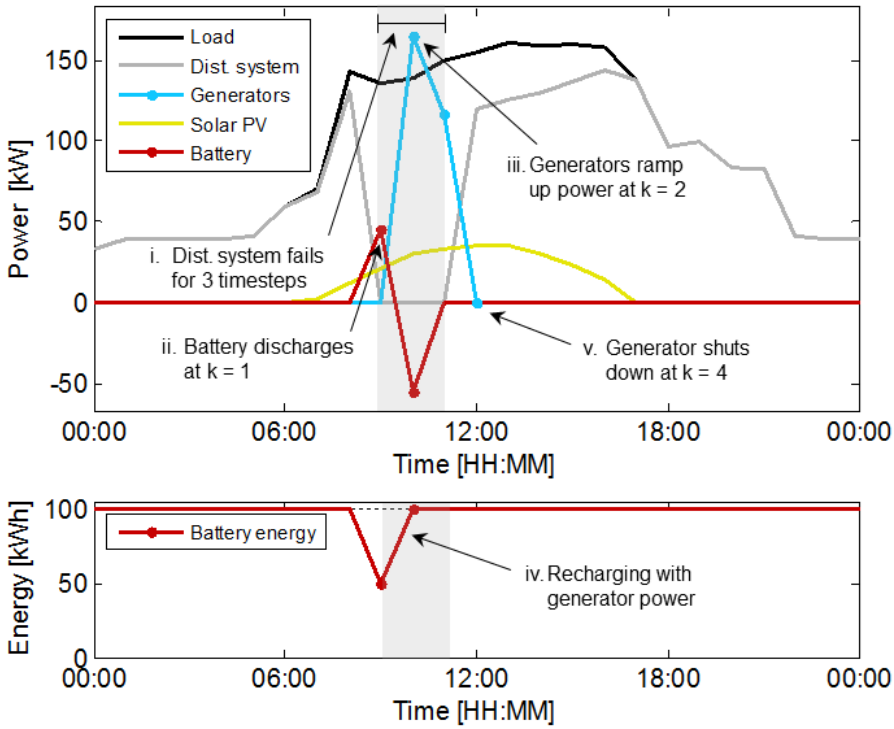

Figure 2.3. Generator and storage dispatch during a grid outage.

2.3 Validation and discussion

We validate the algorithm on four microgrid configurations (Table 2.1). As in Billinton and Bagen (2006), we use the hourly chronological load shape of the IEEE Reliability Test System (IEEE Committee Report, 1979) with a peak load of 40 kW. Solar irradiance time series data is from the TMY3 data set.[5]

Table 2.1. Microgrid system configurations run for validation.

System	Resource	No.	Rating (kW)	FOR (%)	Failure rate (occ/yr)
A	Dist. system	-	-	0.0135	1.018
B	Dist. system	-	-	0.0135	1.018
	Generator	2	20	5	9.2
C	Dist. system	-	-	0.0135	1.018
	Generator	2	20	5	9.2
	Solar PV	1	20	-	-
D	Dist. system	-	-	0.0135	1.018
	Generator	2	20	5	9.2
	Solar PV	1	20	-	-
	Battery	1	20	-	-

The distribution system has a combined SAIFI and MAIFI of 1.018 occurrences/year and a SAIDI of 71 min/year. Its failure and repair rates are calculated using Eq. (2.1). Generators have a 20 kW nameplate capacity and a forced outage rate (FOR) of 5%. The storage system is rated at 40 kWh/20 kW with 100% round-trip efficiency. Solar PV and battery storage are assumed failure-free—for simplicity and to give focus to incremental differences from adding microgrid DERs. Lost load is valued at 1000 $/kWh, though more realistic and accurate estimates are possible using customer damage functions, e.g. in Sullivan et al. (2015).

We validate against the standard sequential MCS (i.e., without cross-entropy),

[5] See http://rredc.nrel.gov/solar/old_data/nsrdb/1991-2005/tmy3/. We use global horizontal irradiance (GHI) data for Chula Vista Brown Field NAAS in California (site number 722904) and the PV power module in the microgrid model DER-CAM to compute power output.

which is considered the most accurate sequential method. However, it can face slow convergence times for very reliable systems. In all simulations, $\beta_{\max} = 0.05$ for all indices.

Two sets of validation are done. In the first (Section 2.3.1), we use the conventional definition of resource adequacy in reliability evaluation, which includes only capacity. In the second set (Section 2.3.2), we include in addition the flexibility constraint.

2.3.1 Conventional reliability evaluation

Reliability indices for the new algorithm—the CE-MCS—match those of the MCS closely for all configurations, with a mismatch of $1.2-3.9\%$ for LOLP, $1.7-3.4\%$ for LOLF and $0.4-5.6\%$ for LOLC (Table 2.2). Those differences are comparable to the $0-3.03\%$ range in Gonzalez-Fernandez and da Silva (2011). The CE-MCS further improves computational time by a factor of $5-10$ over the MCS, with larger speed-ups of 140 times for the most reliable configuration.

Across systems, there are two large improvements in reliability: adding generators (A to B) reduces the LOLP by 93%, and adding storage (C to D) reduces LOLP another 92% (or a factor of 13). The addition of solar PV improves reliability, but to a lesser degree (30% decrease in LOLP).

Table 2.2. Results and validation without considering flexibility.

System	Method	LOLP (-)	LOLF (occ/yr)	LOLC ($/yr)	CPU Time (s)
A	MCS	2.59E-04	1.032	56 160	1.9
	CE-MCS	2.49E-04	0.999	53 040	0.3
B	MCS	1.78E-05	0.079	1179	91.3
	CE-MCS	1.80E-05	0.077	1174	13.3
C	MCS	1.28E-05	0.058	713	173.7
	CE-MCS	1.25E-05	0.056	681	16.5
D	MCS	9.62E-07	0.0038	77	18 795.2
	CE-MCS	9.43E-07	0.0037	74	134.0

2.3.2 Adding flexibility

Adding the flexibility constraint for slow ramping resources (i.e., requiring that load immediately following a grid outage be supplied only by fast ramping resources, and that unit output adjust to meet fluctuating load during outages) to resource adequacy decreases the reliability of microgrid systems. In other words, the same system configuration will (falsely) appear more reliable when this requirement is not in the simulation. Nevertheless, including flexibility is essential to accurately capture system dynamics.

As results show (Table 2.3), including flexibility changes results considerably. Systems are less reliable, with increases of a factor of 7-63 for LOLP, 13-139 for LOLF, and 21-39 for LOLC. Such large changes stem only from defining generators as slow ramping resources unable to meet the instantaneous load increase at the moment the bulk grid fails.

Table 2.3. Results and validation, with flexibility included as a resource adequacy constraint.

System	Method	LOLP (-)	LOLF (occ/yr)	LOLC ($/yr)	CPU Time (s)
B	MCS	1.26E-04	1.026	25 550	5.7
	CE-MCS	1.26E-04	0.989	24 990	2.5
C	MCS	1.23E-04	1.015	21 050	5.7
	CE-MCS	1.22E-04	1.001	20 720	2.5
D	MCS	6.19E-05	0.534	3036	2592.9
	CE-MCS	5.98E-05	0.507	2907	222.8

In this scenario, reliability indices calculated by the CE-MCS again match those from the MCS—to within 6% (0-3.4% for LOLP, 1.4-5.1% for LOLF and 1.6-4.2% for LOLC). As before, the algorithm produces speedups of 6-19 times, with speedups increasing with configuration reliability.

Adding storage (C to D) decreases LOLP by 50%; however, this is considerably less than when ignoring flexibility. Such is the importance of giving explicit treatment to

ramping in reliability evaluation. In practice, generators provide a redundant source of dispatchable power when the bulk grid fails, but cannot respond instantaneously. Battery storage is fast ramping and provides this latter capability. The two resources, when properly sized, together comprise a very reliable configuration—indeed, the exact purpose of building such systems—that renders standard sequential MCS methods impractical for many analytical purposes.

The primary advantage of using cross-entropy, then, is clear: as the redundancy of configurations increases (sequentially, A through D), the time to reach convergence similarly increases (and is especially so for sequential MCS). Though the CE-MCS sees that time increase as well, it produce typical speed-ups of up to 19-fold over the MCS.

2.4 Conclusion

This work presented and validated a new simulation algorithm—based on the cross-entropy method and sequential MCS—that calculates reliability indices for time-dependent load served within a grid-connected microgrid. The algorithm, which builds on previous work on cross-entropy MCS and small isolated power systems, extends and tailors those methods specifically for analysis of microgrids. It does so by including the distributed resources that provide power and reliability in microgrids (generators, solar PV, energy storage) as well as unit flexibility as a resource adequacy constraint in the MCS. The result is a new reliability method that produces reliability indices in close agreement with standard sequential MCS and that, furthermore, is computationally fast. Because it calculates the loss of load cost (i.e., the economic loss of interruptions), the method can be used in larger microgrid analyses that evaluate, e.g., economics and the business case for investing in such systems.

The text and data in Chapter 2, in full, is submitted for publication of the material with the title “Reliability evaluation for microgrids using cross-entropy Monte Carlo

simulation". Hanna, Ryan; Disfani, Vahid R.; Kleissl, Jan. The dissertation author is the primary investigator and author of this article.

Chapter 3

The Economic Value of Reliability for Microgrids: Modeling Reliability Costs and Value

3.1 Introduction

3.1.1 Background

Microgrids are highly touted for the benefits they can confer to both public and private stakeholders. Publicly, many see microgrids as key to enhancing grid resiliency. Indeed, policy makers have turned to grid modernization, often via microgrids, in response to recent severe weather that caused longstanding power outages in major urban centers and exposed structural vulnerabilities in our system of power supply and transmission. Their efforts aim to reduce the impact and severity of outages, as well as maintain critical services.

Microgrids enhance resiliency because they are insular power networks embedded within the bulk grid. They are sited coincident with load and can use various distributed energy resources (DERs), such as fossil fuel generators, solar photovoltaics (PV), and energy storage, all coordinated by a network of smart controllers. Though small relative to the large centralized power plants that dominate the grid today, they offer several

advantages. Perhaps most importantly, they can disconnect, or "island", from the bulk grid during outages (potentially seamlessly) and operate independent of it—thereby keeping lights on for critical services when neighborhoods or entire cities go dark.

In addition to public resiliency benefits, technology and market forces are interacting in ways that make private microgrids an attractive option for an increasing number of electric utility customers. In contrast to public systems, which are often run by utilities and funded via extra-market sources (e.g., rate basing, government programs), private microgrids are designed to compete with traditional utility service—by providing low-cost power or perhaps through services it can offer customers, like reliability.

Interest among utility customers is rooted in both an empirical dimension, with an ever-growing list of operational systems (Wilson, 2017), as well as a theoretical one based on the diverse benefits microgrids can provide. Many of these are tied to clear revenue streams (Stadler et al., 2016). Perhaps the two largest—and our focus—are from energy services, in which microgrids provide electric service similar to a central utility (along with, perhaps, heating and cooling), and from reliability, in which microgrids improve electric service reliability for customers within beyond that provided by the utility.

Though microgrids can provide numerous other services, associated revenue streams are location or jurisdiction dependent (e.g., selling power to the local utility through a power purchase agreement or feed-in tariff or otherwise participating in an electricity market by selling energy or ancillary services) or do not exist (e.g., improving local power quality, providing bulk grid resiliency services like black-start, deferring infrastructure capacity upgrades, reducing transmission losses, and reducing greenhouse gas and criteria pollutant emissions).[1]

[1]For broad treatment of microgrids—such as on technical, financial, and regulatory aspects, among others—see the extensive reviews by Basu et al. (2011); Soshinskaya et al. (2014); Parhizi et al. (2015).

The focus of this work is private investment—on microgrids funded and developed by individual utility customers[2] for *private* benefit. These systems, in contrast to their publicly-funded counterpart, require monetizable benefits to generate revenue and profit; in other words, they must establish a "business case" for economic viability. Though benefits are well-known and documented in theory, an evidentiary basis for cost-effective commercial and industrial (C&I) microgrids is lacking. Our interest lies in understanding where and how private enterprises will actually invest in these systems; many see reliability as a key driver (Asmus, 2016).

Though far-reaching visions of future distributed grids typically include some structure of interconnected microgrids (Arefifar and Mohamed, 2014) or embedded distributed generation (Borges and Falcao, 2006; Banerjee and Islam, 2011) that each contribute to system-wide reliability (Costa and Matos, 2005, 2009; Bie et al., 2012), we set aside those systems here. Our focus lies in understanding the empirical basis for adoption today, and revenue streams for future visions are unclear. Further, the business case for public microgrids built for public resiliency benefits is neither jurisdiction agnostic nor driven by market forces. It is the C&I market—driven by technology advances, innovation, and new business models—that will likely unlock replicable use cases, and in so doing facilitate pathways to widespread adoption. Indeed, industry forecasts suggest that private C&I customers will lead growth in the nascent microgrid market—to the tune of $18 billion by 2026, or 35% of the market total (Asmus, 2017).

This work adopts the U.S. Department of Energy (DOE) definition of a microgrid—"a group of interconnected loads and distributed energy resources within clearly defined electrical boundaries that acts as a single controllable entity with respect to the grid... [and that] can connect and disconnect from the grid to enable it to operate in both

[2]Due to rules governing U.S. electric utilities in most jurisdictions, microgrids are prohibited from serving multiple adjacent customers whose properties span public spaces, such as roads. As such, private investment assumes a "single-property, single-owner" business model.

grid-connected or island mode"[3]—as the foundation for analysis herein. The islanding component in particular is essential. Microgrids are distinct power systems with redundant generating capacity that, from the standpoint of load, operate in parallel to the bulk grid.

3.1.2 The current state of reliability in microgrid modeling

Evaluating business cases, such as would be needed by private investors, requires a cost-based modeling approach. This "techno-economic" approach assesses the economics of different microgrid configurations by monetizing benefits, comparing those with costs, and examining risks, sensitivities, uncertainties, and robustness of assumptions. They gather data and account for interactions between technology choice, cost, energy demand and supply, and emissions. Ultimately, they inform decision-making in the planning and design process, where decision-making can comprise resource siting, selection, sizing, and/or scheduling (Gamarra and Guerrero, 2015) and be aligned to support a potentially broad array of design objectives that span economic, environmental, and/or reliability criteria (Khan et al., 2016).

Much of this information is now available. Mathematical models for energy resources are well-developed—e.g., for micro-turbines (Ismail et al., 2013), CHP systems (Gu et al., 2014), renewables (Sinha and Chandel, 2015), and energy storage (Ru et al., 2013; Nottrott et al., 2013). So too are optimization techniques for renewable and hybrid energy systems that couple these (Erdinc and Uzunoglu, 2012; Upadhyay and Sharma, 2014; Iqbal et al., 2014; Fathima and Palanisamy, 2015). What are still needed, however, are the techno-economic models that evaluate how these factors combine in ways that affect the business case for investing. These are largest in scope and use optimization techniques that connect resource models with other technical, economic, and financial

[3] From the U.S. DOE Microgrid Exchange Group, an ad hoc group working on deployment and research. The definition is important and worth noting since microgrids are often loosely defined.

parameters and constraints that enable or inhibit investment.

Our particular interest lies with models that treat reliability explicitly in ways needed for "business case analysis"—in which reliability is an explicit value stream and optimized by considering the trade-off between reliability and cost (Zhou et al., 2016). Such modeling has been applied to off-grid systems (Siddaiah and Saini, 2016), but is lacking for grid-connected applications.

In the latter case, models typically treat reliability either as a constraint or objective (or sometimes both) in an optimization framework. Typically, as in Bahramirad et al. (2012) and Meiqin et al. (2010), reliability constraints require that the resource configuration meet a minimum level of resource adequacy. Ceteris paribus, this is achieved by investing in costly generating capacity. The widely-used DER-CAM model (Distributed Energy Resource Customer Adoption Model)[4] is one such example. Though offering some control over reliability, such frameworks do not necessarily optimize it. Doing so requires treating reliability as an objective. Bernal-Agustín and Dufo-López (2009), e.g., does this via a multi-objective framework without placing a value on reliability, thus requiring the system designer to select a desired configuration from a Pareto optimal set. Monetizing reliability can obviate this step, e.g. as in Khodayar et al. (2012) and Moradi et al. (2014), which convolve unmet load with a value of lost load to calculate an interruption cost.

Consideration to reliability might also be given via a penalty factor or indirectly. Ding and Lee (2015), e.g., minimizes the operating cost of a microgrid, comprised of fuel and emissions costs, but includes also a reliability penalty cost for unserved load (i.e., for the portion of load that exceeds generating capacity) using a single value of lost load. And Cardoso et al. (2013) treats reliability indirectly—calculating increases in investment and operating costs due to fuel cell failures in the microgrid.

[4] See https://building-microgrid.lbl.gov/projects/der-cam.

Yet another lens is that of survivability, the metric of interest for which is the duration a system can sustain power once an outage occurs. The National Renewable Energy Laboratory (NREL) has adopted this framework with its REopt tool (Cutler et al., 2017). Anderson et al. (2017), e.g., calculates this time measure for a configuration optimized for a life-cycle cost that excludes reliability. Simpkins et al. (2016) further integrates outage costs in the objective function—via a pre-processing step that attributes survivability to various solar PV and battery capacities using regression analysis—and performs analysis on a configuration limited to solar PV and battery storage.

Though all these frameworks for including reliability are, in their own ways, effective, none include all components needed for business case analysis. Some serve only to schedule DERs (and hence do not integrate reliability into investment decision-making), others do not monetize reliability, while others make simplifications to access reliability costs (e.g., by using a single point estimate for the value of lost load). Though they offer frameworks that allow one to explore the effects of adding reliability to an analysis, they fall short in different ways. The business case of reliability can only be captured by considering the cost-benefit trade-off between investing in costly generating capacity and the economic value attributable to greater reliability, while considering also system operating costs.

Existing frameworks that consider that trade-off are simple "evaluation" methods, which do not have optimization functionality. They typically take one of two forms. The first type mandates a minimum level of reliability, uses some selection logic to determine the resource mix, and calculates the cost to supply energy (Kanase-Patil et al., 2011; Lee et al., 2014). These can produce reliability-cost curves for varying levels of reliability, and hence provide some insight into that trade-off. The second prescribes a resource configuration and then calculates operating cost and reliability indices (Daneshi and Khorashadi-Zadeh, 2012; Lovelady et al., 2013) or investment

cost and reliability cost for unserved load (Yokoyama et al., 2008; Georgilakis and Katsigiannis, 2009). In Georgilakis and Katsigiannis (2009), that configuration is varied via a brute-force approach until a system cost-minimizing configuration is found. Though these evaluation methods offer clear frameworks for reliability evaluation, they too have clear shortcomings if applied to business case analysis. Some are built for off-grid settings only, some include only investment costs, while others include only operating costs. None have optimization functionality.

Ultimately, to analyze the business case of reliability, models must consider the economic value of reliability and optimize the cost-reliability trade-off. They must size and schedule resources to minimize a total system cost that includes, at a minimum, investment, operating, and interruption costs. The interruption cost is the value attributable to improved reliability and requires that reliability be monetized.

This work offers a new optimization model that does so, and further integrates the two core revenue streams for private adoption—that of providing energy services and reliability. Though numerous models in literature assess the former, few couple that analysis with one of reliability. Those that do treat it do so simplistically and without the heterogeneity in interruption costs that customers report. We have built our model specifically to address this gap. We are also motivated, as investors would be, to analyze revenue "stacking" (e.g., in Hanna et al. (2017b)). As we will show, combining revenue streams changes outcomes significantly—for investment decision-making as well as the cost-benefit outlook.

The new model is bi-level and built on heuristic optimization. Its core contribution is its explicit treatment of reliability in the objective function, alongside the investment and operating costs that are standard features of mathematical programming approaches. The upper level uses a heuristic method—particle swarm optimization (PSO)—to select and size the DERs that contribute to reliability, while the lower level integrates the widely-

used DER-CAM model to schedule them, along with sequential Monte Carlo simulation (MCS) to evaluate reliability. A heuristic approach is needed for the reliability-based sizing/scheduling problem because the reliability cost is non-linear and, further, the most accurate reliability evaluation methods are simulation-based.

3.2 Model formulation: Building a new model to integrate value streams

3.2.1 Modeling framework

We consider grid-connected microgrids at the distribution level, with all load and resources in the microgrid located at a single bus on the load side of the distribution transformer (Fig. 3.1a). The microgrid does not impact the reliability of loads outside it and, at the point of common coupling (PCC), sees the distribution system as a single generator with sufficiently large capacity to supply peak microgrid load (Wang et al., 2013). As such, the distribution system is modeled at the microgrid bus as an "equivalent" generator (Fig. 3.1b) with a nameplate capacity much larger than peak load and failure rate and repair rate based on the utility metrics SAIFI (system average interruption frequency index) and SAIDI (system average interruption duration index). Utility data on MAIFI (momentary average interruption frequency index), when available, can be considered as well.

Within the microgrid, technologies available for investment fall broadly into four categories:

1. *Natural gas-fired generators*: internal combustion engines and microturbines with fixed capacity and that, optionally, can include heat recovery.

2. *Renewables*: solar PV.

3. *Flexible resources*: stationary battery energy storage.

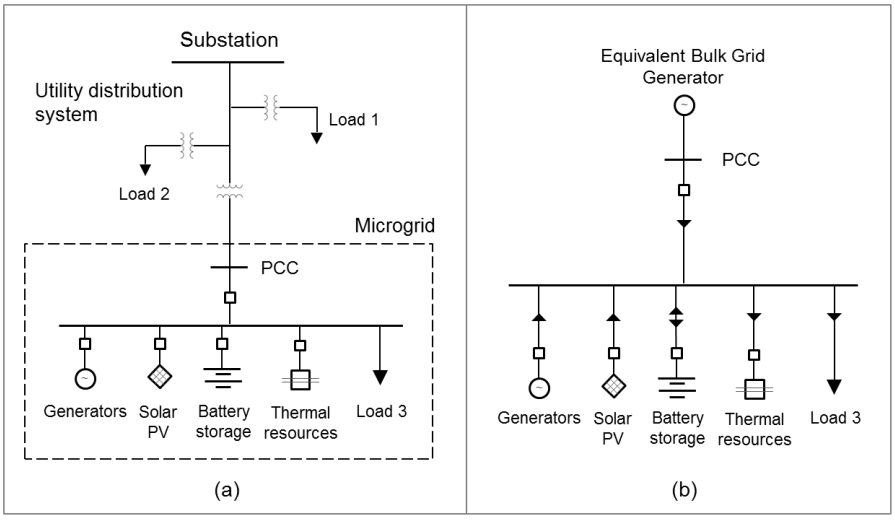

Figure 3.1. (a) Distribution system topology with a microgrid, and (b) the modeled microgrid topology. Microgrid resources comprise the four categories shown.

4. *Thermal resources*: absorption chillers that affix CHP systems, direct gas-fired chillers, electric chillers, heat storage, cold storage.

Technologies are modeled considering technical specifications (capacity, dispatch, ramping, and efficiency ratings) as well as those for cost (fixed and variable costs, lifetime) and reliability (availability, failure rate).

Fig. 3.1b shows directional power flow, which does not include back-flow to the utility grid. Though some revenue streams are derived from energy sales (e.g., utility contracts, market participation), we do not consider them in this work and prohibit back-flow.

3.2.2 Model overview

The central motivation for building a new model is to integrate the value stream for energy services, which is well-studied, with one for reliability. To that end, the model connects the DERs that enable microgrids and quantifies reliability, matches energy supply with demand, and calculates costs and emissions over the first year of operation at

a 1 h timestep.

The model is bi-level (i.e., it has two objective functions with distinct decision variables) with heuristic optimization in the upper level (PSO) and analytical optimization in the lower (DER-CAM). The four modules that comprise the model (Fig. 3.2) each serve a distinct purpose:

1. *PSO*: selects and sizes generators, solar PV, and battery storage, which it passes to DER-CAM and the MCS.

2. *DER-CAM*: sizes thermal resources, solves the scheduling problem, which it passes to the MCS, and calculates the investment cost and operating cost.

3. *MCS*: simulates microgrid and distribution system operation to determine the expected set of interruptions (timing, duration) over the year, considering the stochastic nature of the system—which it passes to the regression model.

4. *Regression model*: calculates the economic loss from interruptions.

DER-CAM returns the complete DER fleet, total investment cost, and total operating cost. The MCS iterates until it converges to a mean (i.e., expected) total interruption cost, which it then returns to the PSO. The PSO controls the total cost.

At the highest level, we use the PSO framework and give it the selection/sizing task specifically because PSO has flexibility to embed within it other methods (like mathematical programming and simulation). This is essential because simulation methods such as MCS provide the most accurate and robust estimates for reliability. Models built on mathematical programming (such as DER-CAM) are more restricted and cannot.[5]

[5]DER-CAM treats reliability via a constraint on investment—what we called the "resource adequacy constraint" in our previous work (Hanna et al., 2017d). Specifically, it requires that the sum of investment in generator capacity, average solar PV output, and capacity of one discharge cycle from electric storage exceed critical (i.e., non-deferrable) load. As we noted in Hanna et al. (2017d), "this constraint does not

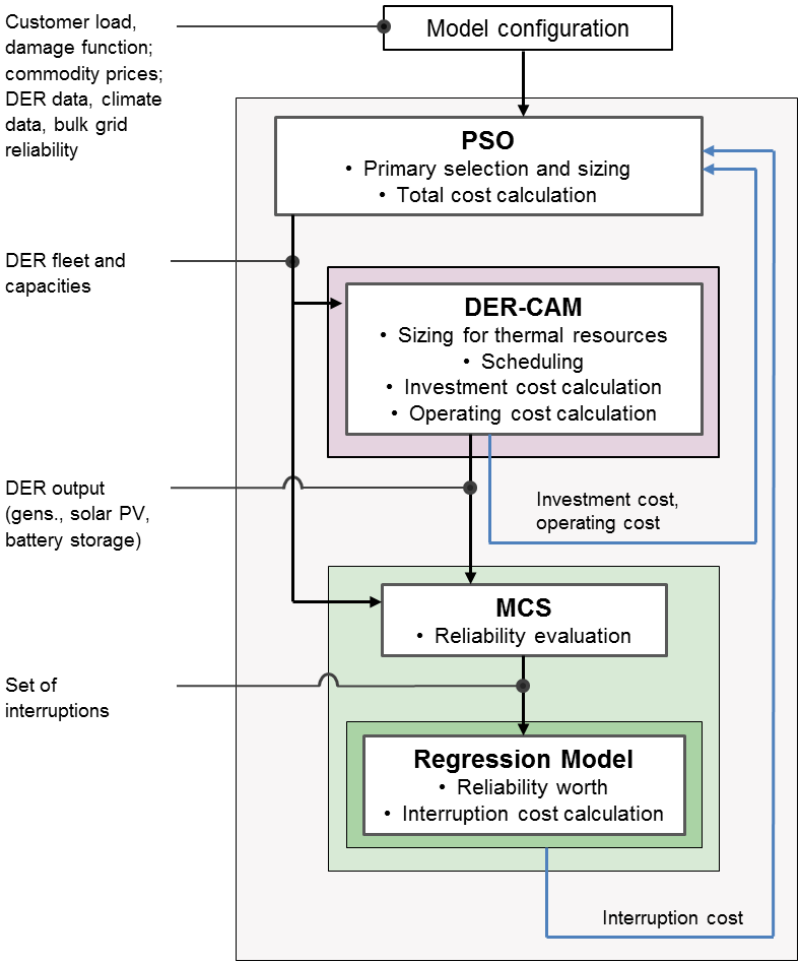

Figure 3.2. Modules comprising the bi-level model, and their functionality. The PSO solves the sizing problem; DER-CAM solves the scheduling problem; MCS evaluates reliability; and the regression model calculates the cost of interruptions. Shading shows where modules are embedded within one another. The outer gray box represents the PSO.

The modeling approach is described by Eq. (3.1)−(3.16), with nomenclature in Table 3.1.

guarantee...the ability to island during all hours of the day or days of the year. Rather, it approximates the investment required to island generally—an outcome designed to approximate the estimated microgrid configuration...but with full appreciation that further analysis and modeling refinement would be needed when designing any particular system." In one sense, then, this work extends the DER-CAM model, which has similar functionality, by adding reliability via MCS along with the PSO layer. Though newer versions of DER-CAM can assess reliability costs by prescribing grid outage scenarios, that is fundamentally different than solving the reliability-based sizing/scheduling problem.

Table 3.1. Nomenclature.

Parameter	*Description*
Sets and indices	
m	Month, $M = \{1, 2, ..., 12\}$
t	Day-type, $T = \{$week, weekend$\}$
h	Hour, $H = \{1, 2, ..., 24\}$
p	Tariff period $P = \{$on-peak, mid-peak, off-peak$\}$
d	Tariff demand type, $D = \{$non-coincident, on-peak, mid-peak, off-peak$\}$
u	End-use load, $U = \{$electricity 'el', cooling 'cl', space heating 'sh', water heating 'wh', natural gas 'ng'$\}$
s	Index for switchgear
i	Generator, $I = \{$ICE, MT, ICE-HX, MT-HX$\}^a$
k	Direct-fired chiller, $K = \{$DFChiller-HX$\}$
q	Continuous DER, $Q = \{$solar PV 'pv', electric storage 'es', absorption chiller 'ac', heat storage 'hs', cold storage 'cs'$\}^b$
v	All microgrid technologies, $V = \{I, K, Q,$ switchgear$\}$
e	Source of electricity, $E = \{I,$ 'pv', 'es', distribution system 'ds'$\}$
c	Source of cooling, $C = \{K,$ absorption chiller 'ac', electric chiller 'ec', cold storage 'cs'$\}$
g	Source of heat, $G = \{I,$ direct fuel 'di'$\}$
Customer load	
$N_{m,t}$	Number of days of day-type t in month m
$L_{u,m,t,h}$	Load profile for end-use load u, month m, day-type t and hour h, kW
Tariff parameters	
$ElecFee$	Fee for electric service, \$/mo
$VChg_{m,p}$	Volumetric charge for month m and tariff period p, \$/kWh
$DChg_{m,d}$	Demand charge for month m and demand type d, \$/kW
$SChg$	DER standby charge, \$/kW/mo
$NGFee$	Fee for natural gas service, \$/mo
$NGPrice_m$	Natural gas price in month m, \$/kWh

Table 3.1. Nomenclature, continued

Parameter	*Description*
DER data	
R_v	Nameplate capacity of technology v, kW
$Cfcap_v$	Fixed capital cost of technology v, $
$Cvcap_v$	Variable capital cost for technology v, $/kW or $/kWh
$Cfom_v$	Fixed O&M cost for technology v, $/kW/yr for I, K and $/kW/mo, or $/kWh/mo for Q
$Cvom_v$	Variable O&M cost for technology v, $/kWh
A_v	Annuity factor for technology v
CO_2 parameters	
EF	Natural gas CO_2 emission factor, tCO_2/kWh
$CTax$	Tax on CO_2 emissions, $/$tCO_2$
Selection and sizing decision variables	
$PurchNum_i$, $PurchNum_k$	Number of purchased gas generators i, direct-fired chillers k
Bin_q, Bin_s	Binary decision variable to invest in DER q, switchgear
$PurchCap_q$, $PurchCap_s$	Capacity of installed DER q, switchgear, kW
Scheduling variables[c,d]	
$\pi_{e,m,t,h}$	Electricity provision from source e, kW
$\xi_{c,m,t,h}$	Cooling provision from source c, kW
$\gamma_{m,t,h}$	Total natural gas purchased, kW
$\gamma_{i,m,t,h}$, $\gamma_{k,m,t,h}$	Natural gas purchased for gas generator i, direct-fired chiller k, kW

[a] Notation: ICE–internal combustion engine, MT–microturbine, -HX–with heat recovery.

[b] Q does not include the electric chiller (which consumes electricity to supply the cooling load) because it is installed in every model run and hence does create differences between results.

[c] Subscript "m,t,h" denotes "in month m, day-type t, and hour h".

3.2.3 Objectives and constraints

The model seeks the least-cost configuration and operation of DERs in a microgrid. *Least-cost* implies least total cost, which has three components: an investment cost (annualized and amortized for year one); operating cost (full year-one operating costs); and interruption cost from electric service disruptions (the expected cost for an average year, given the random nature of grid outages and DER failures).

The bi-level framework is hierarchical. The upper level is the sizing problem and seeks to minimize the total cost:

$$\min \quad C_{\text{total}} := C_{\text{investment}} + C_{\text{operating}} + \mathbf{E}[C_{\text{interruption}}], \tag{3.1}$$

where the investment cost $C_{\text{investment}}$ is a function of the configuration (i.e., of chosen DERs), the operating cost $C_{\text{operating}}$ is a function of DER operation convolved with a host of operating parameters, and where the interruption cost $C_{\text{interruption}}$ depends on both and is an expected value calculated via simulation.

Upper-level decision variables size those resources that contribute to reliability: generators, solar PV, and battery storage. Sizing for thermal resources, which do not contribute, is left to the lower level. Upper-level constraints offer much flexibility in defining particular problems and may include, e.g., minimum and maximum bounds on DER capacities, a minimum level of reliability, and caps on investment capital and operating expenditure.

The lower level sizes thermal resources and solves the scheduling problem, which seeks a minimum operating cost for the full configuration:

$$\min \quad C_{\text{operating}}, \tag{3.2}$$

which is then returned to the upper level in Eq. (3.1). The scheduling problem consists of scheduling all units, as well as purchasing electricity and natural gas from the local utility. Lower-level constraints enforce hourly energy balances for electricity, heating, cooling, and natural gas loads, as well as other physical constraints standard in DER-CAM (e.g., energy conversion, energy efficiencies). See Siddiqui et al. (2005) for detailed exposition of the DER-CAM model.

3.2.4 Investment and operating costs

The investment cost returned by DER-CAM is the amortized capital cost of investing in switching equipment ('switch'), which facilitates islanding, as well as all DERs (generators 'gen', solar PV 'pv', battery storage 'es', and thermal resources 'thermal'):

$$C_{\text{investment}} := C_{\text{switch}} + C_{\text{gen}} + C_{\text{pv}} + C_{\text{es}} + C_{\text{thermal}}\,. \tag{3.3}$$

The generator investment cost is the sum of individual generator costs; investment costs for solar PV and battery storage are costs of single systems (sized in any continuous capacity); and the thermal resource investment cost is the sum of investment costs for direct-fired chillers, absorption chillers, heat storage, and cold storage:

$$C_{\text{switch}} := Binary_s \cdot (Cfcap_s + Cvcap_s \cdot PurchCap_s) \cdot A_s \tag{3.4}$$

$$C_{\text{gens}} := \sum_{i \in I} PurchNum_i \cdot R_i \cdot Cvcap_i \cdot A_i \tag{3.5}$$

$$C_{\text{pv}} := Binary_{\text{pv}} \cdot Cfcap_{\text{pv}} + PurchCap_{\text{pv}} \cdot Cvcap_{\text{pv}}) \cdot A_{\text{pv}} \tag{3.6}$$

$$C_{\text{es}} := Binary_{\text{es}} \cdot Cfcap_{\text{es}} + PurchCap_{\text{es}} \cdot Cvcap_{\text{es}}) \cdot A_{\text{es}} \tag{3.7}$$

$$\begin{aligned} C_{\text{thermal}} := & \sum_{k \in K} PurchNum_k \cdot R_k \cdot Cvcap_k \cdot A_k \\ & + \sum_{q \in Q} (Binary_q \cdot Cfcap_q + PurchCap_q \cdot Cvcap_q) \cdot A_q\,, \end{aligned} \tag{3.8}$$

where q in this case indexes absorption chillers 'ac', heat storage 'hs', and cold storage 'cs'. The annuity factor for technology v is given by

$$A_v = \frac{IntRate}{1 - \frac{1}{(1+IntRate)^{Lifetime_v}}}. \tag{3.9}$$

The operating cost covers all other costs incurred from system operation—from electricity purchases C_{tariff}, natural gas purchases C_{fuel}, resource maintenance C_{der}, and from emitting carbon dioxide C_{carbon}:

$$C_{\text{operating}} := C_{\text{tariff}} + C_{\text{fuel}} + C_{\text{der}} + C_{\text{carbon}}. \tag{3.10}$$

where,

$$C_{\text{tariff}} := \sum_{m\in M}\sum_{p\in P}\sum_{t\in T}\sum_{h\in H} \pi_{\text{'ds'},m,t,h} \cdot N_{m,t} \cdot VChg_{m,p} \tag{3.11}$$

$$+ \sum_{m\in M}\sum_{d\in D} DChg_{m,d} \cdot \max_{t\in T, h\in d}\{\pi_{\text{'ds'},m,t,h}\} + \sum_{m\in M} ElecFee$$

$$+ \sum_{m\in M}\left[\sum_{i\in I} PurchNum_i \cdot R_i + PurchCap_{\text{'pv'}}\right] \cdot SChg \tag{3.12}$$

$$C_{\text{fuel}} := \sum_{m\in M} NGFee + \sum_{m\in M}\sum_{t\in T}\sum_{h\in H} \gamma_{m,t,h} \cdot N_{m,t} \cdot NGPrice_m \tag{3.13}$$

$$C_{\text{der}} := \sum_{i\in I}\sum_{m\in M} PurchNum_i \cdot R_i \cdot \frac{Cfom_i}{12} + \sum_{i\in I}\sum_{m\in M}\sum_{t\in T}\sum_{h\in H} \pi_{i,m,t,h} \cdot N_{m,t} \cdot Cvom_i$$

$$+ \sum_{k\in K}\sum_{m\in M} PurchNum_k \cdot R_k \cdot \frac{Cfom_k}{12} + \sum_{k\in K}\sum_{m\in M}\sum_{t\in T}\sum_{h\in H} \xi_{k,m,t,h} \cdot N_{m,t} \cdot Cvom_k$$

$$+ \sum_{q\in Q}\sum_{m\in M} PurchCap_q \cdot Cfom_q \tag{3.14}$$

$$C_{\text{carbon}} := \sum_{m\in M}\sum_{t\in T}\sum_{h\in H}\left(\sum_{i\in I}\gamma_{i,m,t,h} + \sum_{k\in K}\gamma_{k,m,t,h}\right) \cdot N_{m,t} \cdot EF \cdot CTax. \tag{3.15}$$

The investment and operating cost calculations internal to DER-CAM are consistent with our previous work in Hanna et al. (2017d), though here they are re-categorized slightly. Previously, all DER costs (investment and operating) were combined because the total DER cost was of interest; here, they are separated since we are now interested in trade-offs between investment and reliability.

3.2.5 Reliability and the cost of interruptions

The trade-off in any power system—between providing electricity that is at once economical and reliable—can be optimized by considering two measures: the probability that the system can sustain load without interruption, given random factors like grid and generator failures, fluctuating load, and intermittent renewable output; and the monetary value attributable to uninterrupted electric service. Assessments of the first, referred to as *reliability evaluation*, quantify the amount of reliability using metrics for expected outage frequency and duration. Assessments of the second are the purview of *reliability worth* and quantify the value of reliability by reporting interruption costs in dollars per interruption. The two assessments are complements and together produce the economic value of reliability, given as a total interruption cost in dollars per year. Together, they are the basis for quantifying and valuing reliability in any power system, including microgrids.

In this context, we model customer interruption costs as the means to assess the value of reliability. Microgrids generate value by islanding and avoiding economic losses that passive customers otherwise incur from power outages. This interruption cost, over the one-year modeling period, is given by

$$\mathbf{E}[C_{\text{interruption}}] := \sum_i d_i \cdot c_k(d_i)\,, \tag{3.16}$$

where d_i is the duration of interruption i and $c_k(d_i)$ is the cost function for interruptions for customer type k. In the bi-level model, the MCS determines the set of interruptions and passes it to the regression model, which calculates the associated cost of interruptions.

We have reported the full formulation for the MCS reliability evaluation module, along with validation, in our previous work in Hanna et al. (2017a) and direct the reader there. Reliability evaluation methods are well-developed and validated; our MCS method in Hanna et al. (2017a) extends those to the case of grid-connected microgrids.

Estimates of reliability worth, by contrast, undergo constant revision. Of the approaches to assess worth, customer surveys most directly assess interruption costs and historically have been the favored approach.[6] With surveys, customers estimate their own losses by reporting direct and indirect costs for different outage scenarios that might vary in duration, time of day, and season. Though surveys have some downsides (e.g., unknown human elements, survey bias, inaccurate predictions), they are widely considered an appropriate approach.

The most comprehensive set of work on the topic, from LBNL from 2001-2017 (Sullivan et al., 2009, 2010, 2015), has standardized numerous survey results spanning several U.S. utilities and decades. These were used to build new statistical and econometric models to estimate regression functions, known as customer damage functions (CDFs), that estimate interruption costs as a function of interruption type and customer type; hence, CDFs capture variation in costs across the variables that are important for analyzing business cases. It is these regression functions, in Sullivan et al. (2015), that are used in the bi-level model.

[6]Utilities and other groups have completed dozens of comprehensive interruption cost surveys over the past three decades; see Tollefson et al. (1991); Woo and Pupp (1992); Kufeoglu and Lehtonen (2016), which list studies, as well as Tollefson et al. (1994) for detailed discussion on an early survey.

3.2.6 Implementation of the particle swarm optimization

The upper level is built on PSO, a metaheuristic optimization method that is population-based, iterative, and stochastic (Eberhart and Yuhui Shi, 2001). The population consists of individual particles $i \in \{1, ..., n_{\text{particles}}\}$, each defined by a position x_{id} and velocity v_{id}, that move through the solution space, solve the problem for a location in the space (a candidate solution), and store and share the solution value, or "fitness" f_i. By interacting, particles exploit areas around better solutions, where "better" solutions are those that minimize the objective—here, the total cost of investing in and operating a microgrid.

The solution space is comprised of n_{dim} dimensions, where each dimension $d \in \{1, ..., n_{\text{dim}}\}$ defines a single decision variable. In their search, particles thus move through an n_{dim}-dimensional solution space, with x_{id} and v_{id} updated on a dimension-by-dimension basis. In the bi-level model, the dimensionality includes numbers of discrete generators and battery storage systems, and solar PV capacity. The upper and lower bounds for each dimension encompass the solution space. Though the exact set of dimensions and bounds may vary depending on the customer analyzed (e.g., larger customers in principle have more space in which to install DERs), it always includes those resources. The maximum velocity is set as the dimension range to allow particles to traverse the entire solution space in a single iteration. When velocities carry particles outside the solution space, we apply the absorption boundary method, which returns escaped particles to the position from which they exited.

As with any metaheuristic, PSO is advantageous because it requires few or no assumptions about the problem (e.g., about continuity and differentiability) and little parameter tuning, but disadvantageous because it requires some configuration and cannot guarantee global optimality. It allows one to define a tractable problem, but with the

caveat that a global best solution cannot be guaranteed. We choose the PSO over other metaheuristics because it finds application primarily in non-linear continuous-discrete optimization problems (Clerc, 2006), of which the reliability-based selection/sizing problem is one.

Mathematically, the PSO is implemented via two steps. The first updates particle velocity and the second updates position based on the new velocity. For each dimension d,

$$\begin{aligned} v_{id}^{(t+1)} &= w v_{id}^{(t)} + c_1 R_1 (p_{id} - x_{id}^{(t)}) + c_2 R_2 (p_{gd} - x_{id}^{(t)}), \\ x_{id}^{(t+1)} &= x_{id}^{(t)} + v_{id}^{(t+1)}, \end{aligned} \tag{3.17}$$

where i, d, and t denote particle, dimension, and iteration, respectively, v is velocity, x is position, p_{id} is the best position found by particle i, and p_{gd} is the best position found by the entire population. R_1 and R_2 are uniformly distributed random numbers in the interval $[0,1]$.

The three weighting coefficients w, c_1, and c_2 define the update process. The inertia weight w balances local and global search (Shi and Eberhart, 1998)—where higher values (e.g., 0.9) maintain particle motion and facilitate global exploration and lower values (e.g., 0.4) cause exploitation of local optima found so far (Poli et al., 2007). The terms c_1 and c_2—what are sometimes called the cognitive and social attraction parameters, respectively—pull particle trajectories toward local and global best positions, respectively. As is typical, we tune and select coefficient values based on experience with the problem to provide an acceptable balance between global and local exploration. To this end, we set the swarm size to four particles, inertia w to 0.8, and attraction parameters c_1, c_2 to the standard value 2.9922.

We use a global best particle topology, in which particles communicate the global

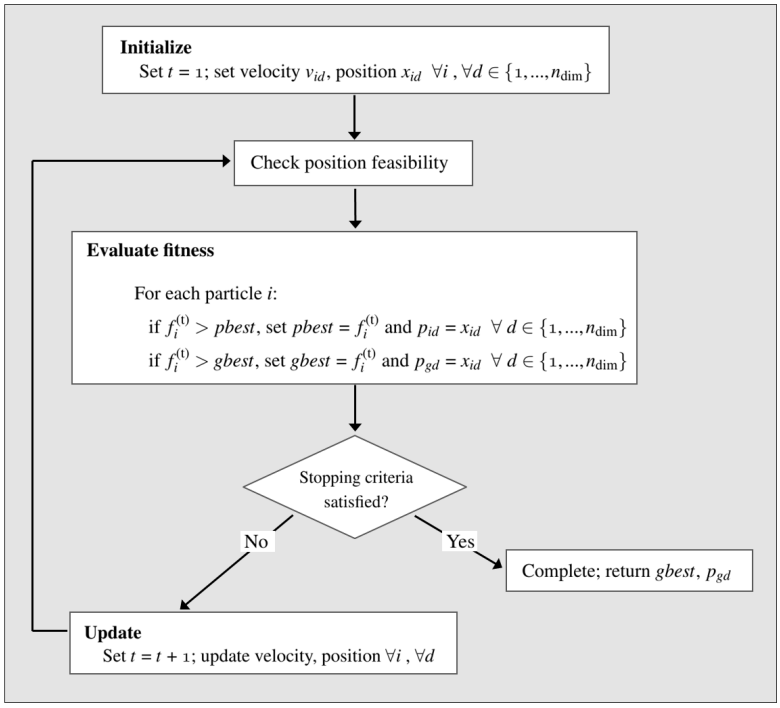

Figure 3.3. PSO implementation consists of steps for initialization/updating, fitness evaluation, and termination.

best position p_{gd}. The algorithm for this topology consists of three main steps (Fig. 3.3). The first is initialization, or updating for later iterations. The algorithm is stochastic, so initialization and updating are partly random (hence, particle motion is guided in part by randomness). After checking position feasibility and applying corrections if necessary (via boundary absorption), the PSO evaluates particle fitness $f_i^{(t)}$—the measure of the solution quality and analogous to an objective function—in the second step. Each particle maintains a record of its best solution found so far, $pbest_i$, as well as of the best solution found by the population, *gbest*, both of which guide particle trajectories. The final step is a check on termination criteria. The PSO completes either when it reaches a maximum number of iterations or when it fails to improve the best solution for a succession of iterations, both of which are prescribed.

3.2.7 Example

Fig. 3.4 illustrates characteristic behavior of the PSO on a sample customer who has the option to invest in six types of DERs: large and small generators (250 kW and 60 kW) with and without CHP, solar PV, and battery storage (units of 100 kWh/50 kW). Fitnesses converge as individual particles track to the best solution *gbest* over iterations (Fig. 3.4a)—the result of the PSO finding better combinations of DER capacities (Fig. 3.4b).

As is typical, swarm movement throughout the solution space fits two distinct epochs: one defined by exploration (approx. iterations 1-19), where particles search the solution space widely, and a second defined by exploitation (approx. iterations 20-35), where particles attempt to improve the best solutions found during exploration. In this example, the PSO terminates after eight consecutive iterations without improvement to *gbest*.

The PSO finds (nearly) the best solution relatively quickly—in this example, after three iterations. Improvements to the *gbest* fitness thereafter are marginal by comparison. Such behavior is common in our analyses, and is likely a function of a very discontinuous, and steep, solution space. Under-investment in DERs begets very high interruption costs, whereas over-investment adds to the total cost without benefit. This suggests simple rules of thumb for total unit sizing (especially for generators) may be mostly successful, though optimization does add value by determining the precise combinations of units, including less-obvious capacities for ancillary DERs like thermal resources, along with clear operating costs. Here, for example, the optimal configuration includes a single 250-kW generator without heat recovery. Because the bi-level model includes operating costs, the PSO finds that energy efficiency gains via a CHP generator do not offset the extra cost.

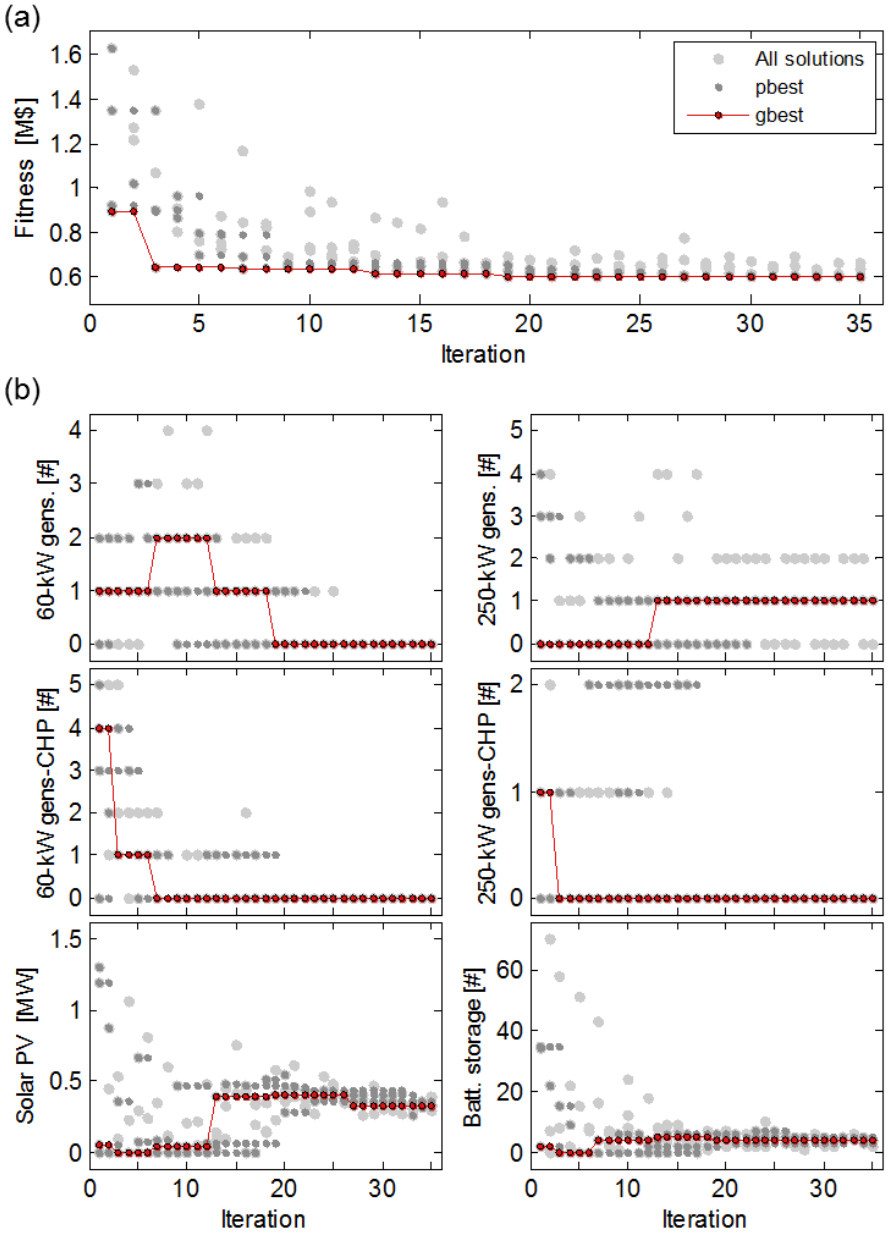

Figure 3.4. (a) Comparing the fitness returned by all solutions (light gray), as well as the best solution found by each particle *pbest* (dark gray) and the swarm *gbest* (red), shows how the PSO converges over iterations. (b) Sizing for DERs that underlie fitness values. All particle positions are shown in light gray, with *pbest* positions in dark gray. As individual particles converge in the solution space around p_{gd} (red), so to do fitness values.

3.3 Validation and discussion

3.3.1 Validation against DER-CAM without reliability

The goal of the validation is to calculate the relative match between solutions found by the bi-level model and by DER-CAM. Classical validation would require data on actual system adoption, with known solution and annual costs. Because we know of no such existing data, we compare solutions to those made by DER-CAM. We are interested in the PSO fitness *gbest*, and the solution underlying it p_{gd}, relative to the objective and solution found by DER-CAM. Because the two are inherently different models in their full form—due to their treatment of reliability—validation must neglect it. As such, we remove all reliability aspects from DER-CAM (the resource adequacy constraint) and from the bi-level model (interruption cost, MCS, regression model). What remains are models with identical objective functions (investment plus operating cost), though with different engines that size DERs. The goal, then, is to compare sizing decisions made by the PSO to those made by DER-CAM.

We perform validation on three customers that vary in size and load shape—a hospital (large C&I customer with 1414 kW peak electric load, 9.3 GWh annual consumption), medium-sized office building (small C&I with 174 kW, 0.6 GWh), and secondary school (medium C&I with 927 kW, 3.1 GWh)—and consider adoption in southern California (specifically, the TMY3 location for Camp Pendleton MCAS, site number 722926). Load data is from the DOE commercial reference building stock[7] and includes electric, cooling, heating, and natural gas loads. Climate data is from the TMY3 data set for the same location.[8] Each setup with DER-CAM is run six times, with an increasingly restrictive solution tolerance.[9] Each setup with the bi-level model is repeated

[7] See http://energy.gov/eere/buildings/commercial-reference-buildings

[8] See http://rredc.nrel.gov/solar/old_data/nsrdb/1991-2005/tmy3/

[9] I.e., the GAMS parameter OPTCR, which is the gap between the best integer solution and the best estimate for the optimal solution and an indicator of integer solution quality.

six times because the particle search is stochastic.

Fig. 3.5a compares costs and configurations. Total cost values are remarkably precise, with average differences of 0.1%, 10.3% (1.7% when excluding the outlier), and 3.9% for the hospital, office, and school, respectively. Configurations match closely as well (Fig. 3.5b), though sizing decisions with the bi-level model show wider variation, most saliently for solar PV for the hospital. Nevertheless, variable sizing produces similar fitnesses; hence, bi-level model results indicate that the optimal solution to the least-cost sizing/scheduling problem is non-unique. Indeed, the use of heuristic optimization in this problem provides a rich set of solutions that offer varying microgrid configurations with very similar total cost.

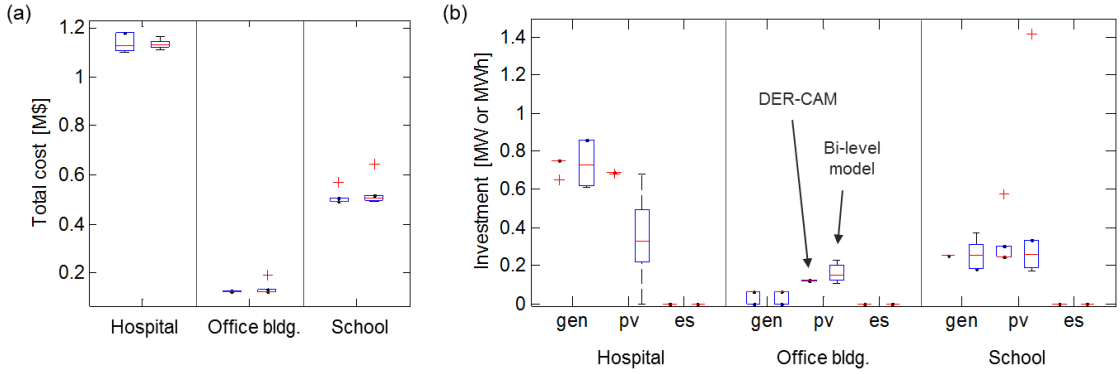

Figure 3.5. Bi-level model validation against DER-CAM with reliability removed. (a) The fitness returned by the PSO (right boxplot in each pair) closely matches the minimum total cost found by DER-CAM (left boxplot). (b) The average configuration for generators ('gen'), solar PV ('pv'), and battery energy storage ('es') aligns as well, though with greater variance; nevertheless, the *gbest* fitnesses remain precise.

Results confirm that this lean version of the bi-level model—without reliability—is consistent with a reputable model that does not treat reliability directly. We therefore claim that the lean version provides a proper basis for adding the reliability value stream. In the following section, we add reliability and report changes to investment and the cost-benefit outlook.

3.3.2 Comparison against DER-CAM considering reliability

It is intuitive that adding a reliability cost to the objective function in this optimization-based analysis should change outcomes. Our purpose here is to show those changes with the bi-level model, and further explore why differences emerge between the two models. We expect differences because the two models treat reliability differently; hence, this is a comparison and not validation. For runs with DER-CAM, we add back the resource adequacy constraint; for those with the bi-level model, we add back the interruption cost to Eq. (3.1), the MCS, and interruption cost regression model.

Herein, we use the more general tabular estimates from the regression model (Table 3.2), which averages data across customer classes, because we are still considering the question of how to classify customers in the context of a future systematic study on customer demand for reliability.

Table 3.2. Customer damage functions in $/avg-kW.

Interruption duration	*Customer type*	
	Medium/large C&I	*Small C&I*
Momentary	15.9	187.9
30 min	18.7	237.0
1 h	21.8	295.0
4 h	48.4	857.1
8 h	103.2	2138.1
16 h	203.0	4128.3

As is typical with cost-benefit analyses of this type, which requires comparison against a baseline, we model a *utility customer* and *microgrid customer*. The two are identical in all regards except investment in DERs. The utility customer represents the

pre-investment case and supplies load by purchasing electricity and natural gas from the local utility. The microgrid customer represents the post-investment case. We define the *economic benefit* of investing as the difference in total cost between the two. To demonstrate, we choose the hospital building type from the validation and again run the setup six times with each model.

Distribution system reliability metrics are taken for the north coast district in the San Diego Gas & Electric territory, which has SAIFI of 0.461 occurrences per year (occ/yr), MAIFI of 0.239 occ/yr, and SAIDI of 50 min/yr (Kurtovich and Zafar, 2016). We assume the hospital customer is an early adopter with a particular need for reliable service and increase the average interruption costs in Table 3.2 by a factor of twenty. This is not an unreasonable assumption given the LBNL meta-database reports variation in costs across several orders of magnitude. We linearly interpolate tabular data for outage durations not explicitly given and cap costs at the 8 h duration (i.e., costs for outages $>$8 h equal the 8 h datum) because LBNL cautions against using them.

Fig. 3.6 compares results for the two models. As in the validation, the individual costs that comprise the solutions, from both models, are very precise. We expect that from DER-CAM since it is a mixed integer linear program and we apply a small relative gap. For the PSO, the small variation in the *gbest* fitness underlines its success and utility on discrete selection problems such as this.

In DER-CAM there is no interruption cost. For the utility customer, then, the operating cost is the total cost. The trade-off in DER-CAM, as the model seeks the least-cost configuration of DERs, is one between investment cost and operating cost. In other words, DER-CAM seeks configurations that produce power, heat, and cooling services on-site to reduce the electricity and fuel costs of the utility customer.

With the bi-level model, reliability is considered directly in the objective function. Its inclusion markedly changes the cost-benefit analysis (made relative to the bi-level

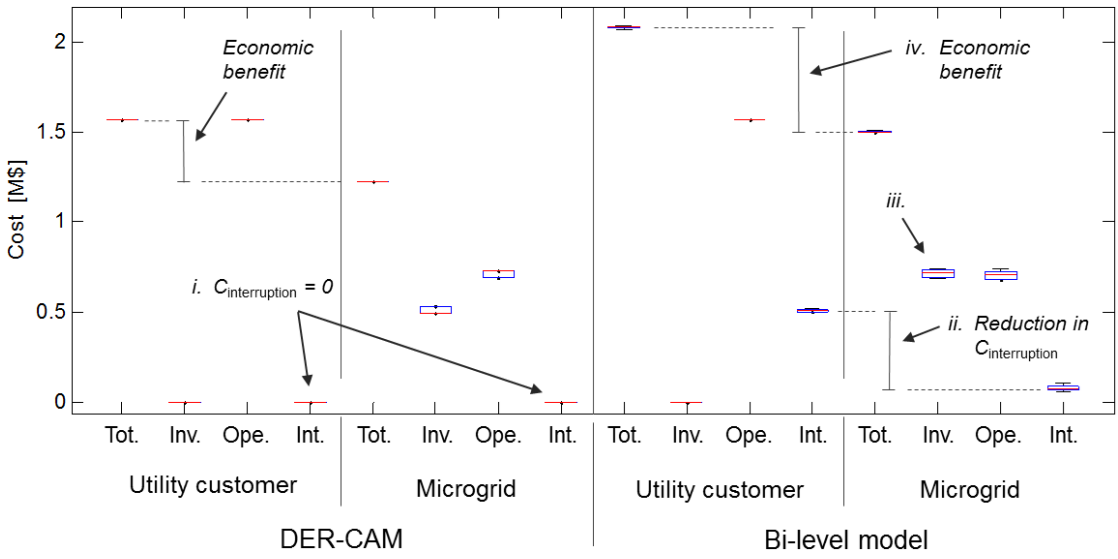

Figure 3.6. We show the effect of adding reliability to the analysis by comparing the cost breakdown (total 'tot', investment 'inv', operating 'ope', and interruption cost 'int') for the utility customer and microgrid customer for both models. Without an interruption cost (i), DER-CAM reports a lower total cost for both customer types. In the bi-level model, by contrast, the utility customer has an interruption cost; if sufficiently large, the PSO finds solutions that reduce it (ii), at the expense of a higher investment cost relative to DER-CAM (iii). The cost-benefit analysis from the bi-level model thus reports a greater total microgrid cost, but also a greater economic benefit from investing (iv).

model utility customer). Here, the utility customer has an interruption cost that is about $1/3$ of the operating cost, and hence a larger total cost than its equivalent in DER-CAM. The trade-off sought by the bi-level model, as it sizes DERs, now includes an interruption cost. As such, relative to the DER-CAM solution, it finds a least-cost configuration that has a larger investment cost, nearly equal operating cost, and larger total cost—yet the economic benefit of investing is greater. Such is the effect of adding—and optimizing against—the reliability value stream.

Although their cost-benefit analyses differ, the underlying least-cost configuration found by the two models is similar, albeit with one critical difference: investment in battery storage is 220% greater in the bi-level model solution (Fig. 3.7). This difference is a product of integrating sequential MCS—the most accurate reliability evaluation

method—in the bi-level model. The MCS assesses reliability directly by checking resource adequacy and ramping flexibility on an hourly basis. As explained in Hanna et al. (2017a), battery storage is required to island seamlessly and maintain service continuity at the moment outages occur on the bulk grid; hence it is often sized to (nearly) match peak load. Generators, by contrast, are considered a slow-ramping resource and cannot adjust output to meet instantaneous changes in net load at the moment of outage.

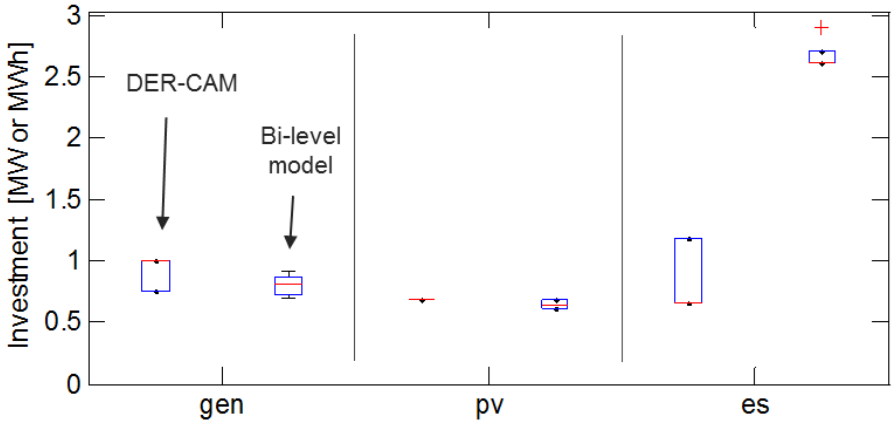

Figure 3.7. The range of investment in the optimal solution found by DER-CAM and the bi-level model. Though each treats reliability in a different manner, configurations match closely, with the exception of battery storage. The addition of the reliability value stream, along with a proper reliability evaluation method, leads to greater investment in battery storage—which is necessary and sufficient for the microgrid to ride through power outages on the bulk grid.

3.3.3 Consistency amongst PSO solutions

The success of the bi-level model depends in part on its ability to consistently find the best solution independent of initial conditions and search randomness. Fig. 3.8 shows that the model finds a consistent minimum total cost, though it does so by arriving at slightly different solutions (most saliently for solar PV for the school), which again indicates the solution is non-unique. In this regard, the bi-level model has added utility relative to mathematical programming approaches because it can return a wealth of solutions with similar total cost. Though the mathematical implications of this are

clear, the physical meaning is perhaps more profound given current discourse on the role microgrids may play in decarbonizing the electric grid.

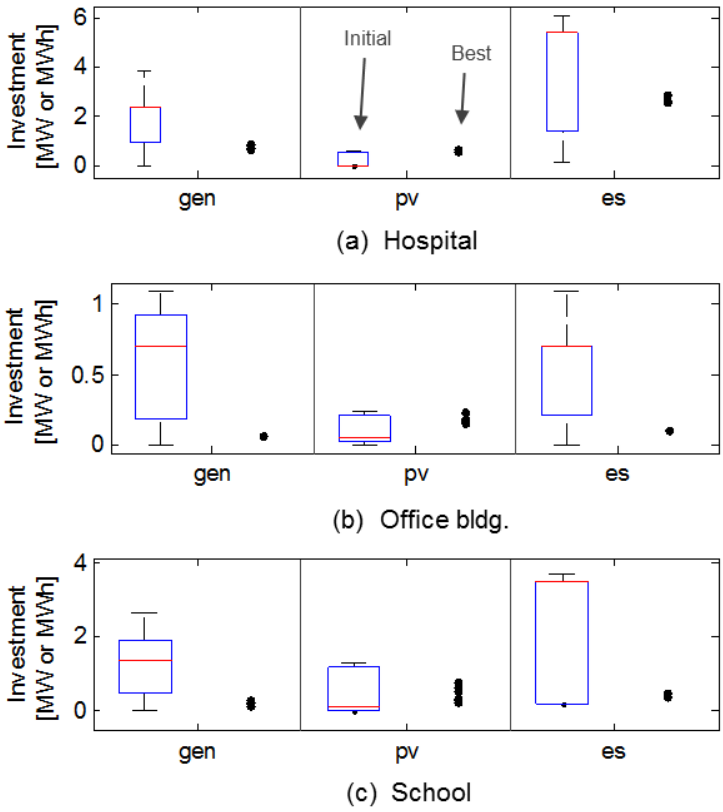

Figure 3.8. Consistency check between initial particle position and final *gbest* position in the PSO for the three building types. Boxplots show the range of investment from initial positions $p_{id}^{(1)} \forall i$, while individual dots show investment for the *gbest* solution p_{gd}. Results indicate that the PSO is successful in finding precise solutions despite wide variation in initial position.

3.4 Conclusion

This work has presented and validated a new optimization model, built on the widely-used DER-CAM platform, that quantifies the economics of microgrids by sizing and scheduling DERs in a microgrid. It extends that platform, as well as the modeling literature generally, by including an explicit value stream for reliability, in addition to

the value stream for energy services that is central to DER-CAM. Units are sized and scheduled via PSO and DER-CAM, respectively, while reliability is quantified using a state-of-the-art method based on sequential MCS.

By including the value of reliability (through a cost on electric service interruptions) directly in the objective function, the new model offers a strategic advantage over existing models that treat reliability indirectly or crudely. The model can be used to study, e.g., how customer demand for reliability drives investment in combinations of DERs, and vice versa. Because it uses heuristic optimization, it returns numerous competing solutions that, when compared, can show how incremental modification to a system configuration improves reliability and system cost. Ultimately, the model works as a robust and flexible analytical tool that can be used to study the business case for investing in microgrids that procure energy services and improve reliability for customers within.

A final note concerns risk. The bi-level model provides a core economic analysis based on energy costs and *mean* interruption costs, given the random nature of the grid. In reality, investors may be wary of various elements of risk inherent in analysis of grid outages, and, further, may consider factors outside of an energy analysis (e.g., risk, financing, insurance) when deciding to invest. Though herein we have not considered variation in assessments of risk, which may be subjective or perhaps part of the standard investment protocol of a firm, the model can integrate this information if known. Because it is based in simulation, the bi-level model can equally use the tails of outage distributions (e.g., outcomes with low probability but high cost) in place of mean values. But this requires specific insight into the ways investors think about risk. Indeed, a large future contribution to literature may lie in systematizing real-world investor appetite for risk in such reliability-based business cases.

Chapter 3, in part, is currently being prepared for submission for publication of material. Hanna, Ryan; Disfani, Vahid R.; Kleissl, Jan; Victor, David G. The dissertation

author is the primary investigator and author of this article.

Chapter 4

The Impact of Microgrid Adoption on Greenhouse Gas Emissions From the Electric Power Sector

4.1 Introduction

Technology, policy and market forces are interacting in ways that make insular power networks an attractive option for an increasing number of electric utility customers. Such "microgrids"[1]—which are customer-sited and use small-scale distributed energy resources (DERs), in contrast to the large centralized power plants that dominate grids today—may play a large role in shaping the future structure of the electric power industry. Some industry observers think these resources at the "edge of the grid" will come to dominate and perhaps even replace standard grid service. Already, grid operators in some jurisdictions are accommodating these new distributed resources—in particular solar photovoltaics (PV) and battery energy storage. There is policy support as well for small fossil fuel generators that function as combined heat and power (CHP) systems, capturing waste heat to increase end-use energy efficiency.

Interest in microgrids stems in part from the flexibility they provide. Managed

[1] See Basu et al. (2011), Soshinskaya et al. (2014), and Parhizi et al. (2015) for broad treatment of microgrids—such as on technical, financial and regulatory aspects, among others.

well, they can increase reliability and reduce energy costs for customers within them, as well as provide a host of other benefits to the local utility to which they are interconnected (Bahramirad et al., 2015). Though benefits are well-known and documented in theory, the evidentiary basis for understanding when and where microgrids are cost-effective is lacking. One of the central missing elements is a robust understanding of where and how private enterprises will actually invest in these systems. Models that quantify such "business cases" using state-of-the-art methods are essential.

There are numerous revenue streams available to developers that can underpin business cases (Stadler et al., 2016). The two largest are perhaps from energy services, in which the microgrid provides electric service similar to a central utility (along with, perhaps, heating and cooling services), and from reliability, in which the microgrid improves electric service reliability for customers within beyond that provided by the local utility. Industry observers believe early adopters in the nascent market will be customers that can realize multiple benefits and that can implement systems under the auspices of current regulatory rules[2]—such as private businesses, hospitals and public infrastructure like schools.

This work adopts the U.S. Department of Energy (DOE) definition of a microgrid—"a group of interconnected loads and distributed energy resources within clearly defined electrical boundaries that acts as a single controllable entity with respect to the grid...[and that] can connect and disconnect from the grid to enable it to operate in both grid-connected or island mode"[3]—as the foundation for analysis herein. The islanding component in particular is essential. Microgrids are distinct power systems with redundant generating capacity and, with respect to supplying load, operate in parallel to the

[2]Rules governing U.S. electric utilities in most jurisdictions would, e.g., prohibit microgrids from serving multiple customers whose properties span public spaces, such as roads. As such, market growth typically assumes a "single-property, single-owner" business model.

[3]From the U.S. DOE Microgrid Exchange Group, an ad hoc group working on deployment and research. The definition is important and worth noting since microgrids are often loosely defined.

bulk grid. Though in many cases utilities provide customers with highly reliable power, microgrids can improve reliability still further by islanding seamlessly when grid outages occur upstream. Such capabilities underlie a core business case for those with high demand for reliable power.

In addition to a lack of systematic analysis on business cases (e.g., on potential customer types, on jurisdictions where adoption is likely to occur, and on enabling technologies), there is little analysis too on impacts—notably on how microgrids affect the local balance of energy supply and demand and hence system-wide emissions. This is, in part, because so few of these systems are in operation today. Nevertheless, many proponents of a future grid built on ubiquitous microgrids often assume complementary emissions reductions; the evidence for this is lacking, however. In reality the impact on emissions is unknown and depends on numerous connected parameters—e.g., commodity prices for electricity and natural gas, technology innovation, and policy prescriptions. It is therefore important and worthwhile to attempt to track these impacts, especially to marginal greenhouse gas emissions and in the larger context of climate stabilization goals. This work is the first study to do so, and has required building a new model that connects investment and operation decision-making in microgrids to value streams (notably reliability), costs, energy flows and emissions.

4.2 Study setup and data

4.2.1 Model

Models that evaluate microgrid economics along with technical aspects are the basis for microgrid planning studies as well as microgrid analysis generally. One type in particular—what might be called “investment and dispatch” models—evaluate microgrids by considering the interactions within them that define business cases, for instance

between technology choice, cost, energy demand and supply, and, ultimately, emissions. These models use various optimization techniques to connect individual resource models (e.g., for fossil fuel-fired generators, thermal energy resources, solar PV, battery energy storage, etc.) with other technical, economic, and financial parameters and constraints (Liang and Zhuang, 2014). Ultimately, they inform decision-making in the design process to support a potentially broad array of design objectives that span economic, environmental, and/or reliability criteria (Ahmad Khan et al., 2016).

Many such models have been built—e.g., the well-known DER-CAM (Distributed Energy Resources Customer Adoption Model) and HOMER (Hybrid Optimization Model for Multiple Energy Resources) models. These evaluate the economics of local energy provision, in which the microgrid functions similarly to a utility, providing electric and perhaps thermal energy services to customers within it. Critically, few models couple that analysis with one of reliability, which industry forecasts consider a primary market driver for the commercial and industrial segment. Our primary motivation is to understand how an emerging market for microgrids—adopted by private firms and operated for private benefit—might impact emissions from the electric power sector. We are therefore interested in capturing investment trends which stem from reliability. As such, we use the new bi-level optimization model developed in Hanna et al. (2017a) and Hanna et al. (2017c). That model connects the DERs that are key enablers of microgrids—such as gas generators, CHP, solar PV, energy storage, and thermal resources—to quantify least-cost investment, reliability, cost, energy demand/supply, and emissions for microgrid systems. The model does not treat emissions reductions as a goal. The emissions impact of systems are a by-product of firms' pursuit of private benefits.

4.2.2 Setup

With technology, policy, and market forces interacting to make microgrids economically attractive for utility customers, and as industry forecasts point to significant future growth, it is important to understand how greenhouse emissions from these systems compare with standard utility service. The goal of the study, then, is to systematically quantify carbon emissions from microgrids for likely first adopters who would seek private benefits like greater reliability and lower utility bills.

This has two main parts. First, to qualify the prevailing conditions (which might be rooted in technology, markets, or policy—or some combination) under which microgrid adoption is economically viable, and second to quantify microgrid emissions for comparison against marginal emissions from wholesale market generators. The logic is that modeled shifts in emissions (if any) from microgrid adoption are irrelevant if systems are uneconomical.

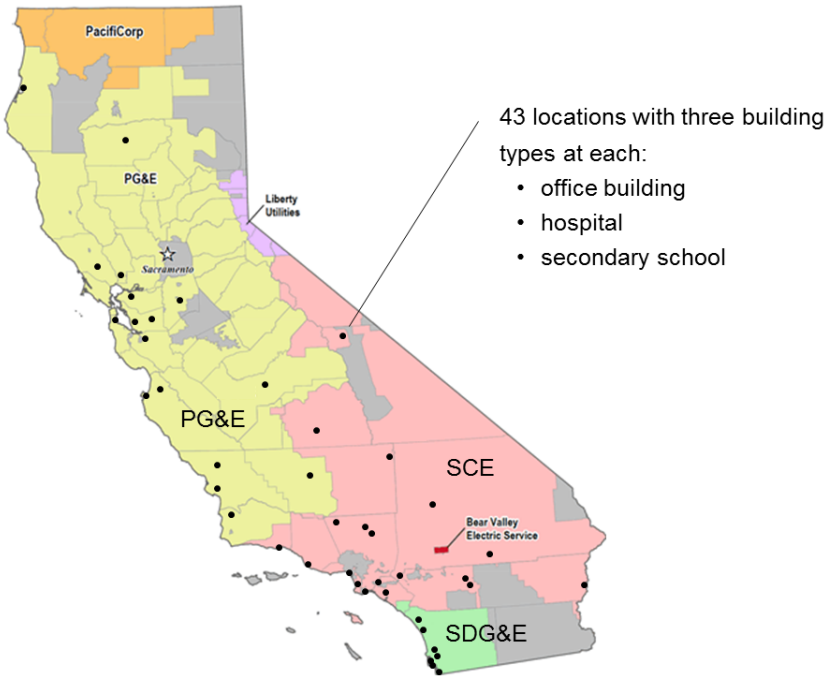

Figure 4.1. Locations modeled throughout California for microgrid adoption.

To this end, customers and locations were selected across the state of California (Fig. 4.1) to capture variation across the key parameters that drive outcomes. Locational parameters—such as climate, irradiance, and utility of interconnection—affect solar PV output, building thermal demand, and electricity rates, as well as define bulk grid reliability. Customer-specific parameters define the size of the microgrid (physical property size, total energy demand, peak demand) as well as the value attributable to reliability. The latter stems from customer function (i.e., what the building is built to do or provide).

In total, adoption at 43 locations across California was modeled. While numerous model parameters vary by location, electricity prices and rate structures, which vary by utility, are perhaps most important. The 43 locations cover the three large investor-owned utilities (IOUs) in California and hence capture that variation, as well as differences in utility reliability, climate, and solar irradiance. Rate structures are available on utility webpages[4]; the retail natural gas price is set to 8 $/mmbtu; utility reliability data is published by the California Public Utilities Commission (Kurtovich and Zafar, 2016); and meteorological and irradiance data is from the National Solar Radiation Database from the National Renewable Energy Laboratory[5]. Climate data serves as input to an external modeling tool that produces time series load data.

In addition, three microgrid adopters (or building types)—an office building, school and hospital—are modeled at each location. These adopters are electric utility customers and defined by annual load profiles for electricity, heating, cooling and natural gas. Load profile data is from the U.S. DOE[6] and produced using the building simulation

[4]See https://www.pge.com/tariffs/index.page for Pacific Gas & Electric; https://www.sce.com/wps/portal/home/regulatory/tariff-books/rates-pricing-choices for Southern California Edison; and https://www.sdge.com/rates-regulations/current-and-effective-tariffs/current-and-effective-tariffs for San Diego Gas & Electric.

[5]The National Solar Radiation Database is maintained at http://rredc.nrel.gov/solar/old_data/nsrdb/1991-2005/tmy3/.

[6]Data sets for building load are maintained at https://energy.gov/eere/buildings/commercial-reference-

model EnergyPlus. It is location specific to the 43 locations modeled.

A last key set of inputs is bulk grid emission factors, which give the emission intensity (tCO_2/MWh) of the bulk grid. Data is available for all eight regions of the North American Electric Reliability Corporation (Siler-Evans et al., 2012).

4.3 Results

This study sought to answer three core questions: whether microgrid adoption is economical under present conditions; how microgrids configure to achieve minimum total cost; and how emissions from those systems compare against emissions from the wholesale electricity market. Ultimately, answers to these can highlight to policy makers whether microgrid adoption provides a co-benefit for emissions reductions or whether some intervention might be needed to achieve that.

To this end, several modeling sets were run. The first, a baseline set (section 4.3.1), answers the above questions for microgrids under conditions today and with no (artificial) restrictions. The second cluster then explores how groups of technologies, notably thermal resources, drive reductions (section 4.3.2).

Adopters are modeled before and after investment. A *utility customer* represents the pre-investment case. This customer supplies load by purchasing all electricity and natural gas from the utility. The post-investment case is the *microgrid customer*, who invests in a microgrid to generate electric and thermal energy on-site. The option to purchase utility power and natural gas remains. The cost savings derived from microgrid adoption (i.e., the difference in total cost between the two customers) is the economic benefit, which can be negative if adoption is uneconomical.

A similar comparison is made for CO_2 emissions. Emissions attributable to the utility customer are indirect. They result from power produced by the marginal

buildings.

generator in the wholesale market (i.e., the last generator dispatched in the market clearing process)—which is known through regression analysis of hourly market data. Microgrid emissions, which are both indirect and direct—the latter the result of on-site gas combustion in gas generators—are compared to the indirect total of the utility customer. The logic is that microgrid adoption is a market intervention, albeit indirect. Power produced at the distribution level by microgrids replaces power that would otherwise be produced by the marginal generator.

4.3.1 Baseline results

Results show, under present conditions and for all building types and locations, that microgrids are economical—i.e., microgrid adoption reduces the total cost of supplying electricity and gas services to the utility customer (Fig. 4.2). Further, the transition to microgrid service reduces CO_2 emissions relative to marginal generators in the wholesale market. For the case in which customers pursue private benefits to lower costs, there is a co-benefit for system-wide CO_2 emissions reductions from the electric power sector.

Two types of variation in the results are notable. First, utility customers for the hospital produce similar emissions totals but a wide range in total cost. The narrow spread on emissions is expected—these buildings consume, more or less, the same quantity of energy. They deviate only due to small variation in load driven by climate (e.g., buildings have different heating and cooling needs if located in the desert compared to the coast). The range is total cost is wide, however, and due to differences in the reliability of the distribution system to which the microgrid is interconnected. Reliability metrics range from $0.39-3.97$ occurrences/year for SAIFI and $19-311$ min/occurrence for CAIDI—an order of magnitude difference. The same building with nearly the same demand can incur vastly different interruption costs depending on the reliability of the local grid. Utility customers for the school and office building have a more equal spread between emissions

and cost. For these building types, which respond more reactively to climate, climate has a greater effect on energy consumption (total and peak consumption) and hence on cost and emissions.

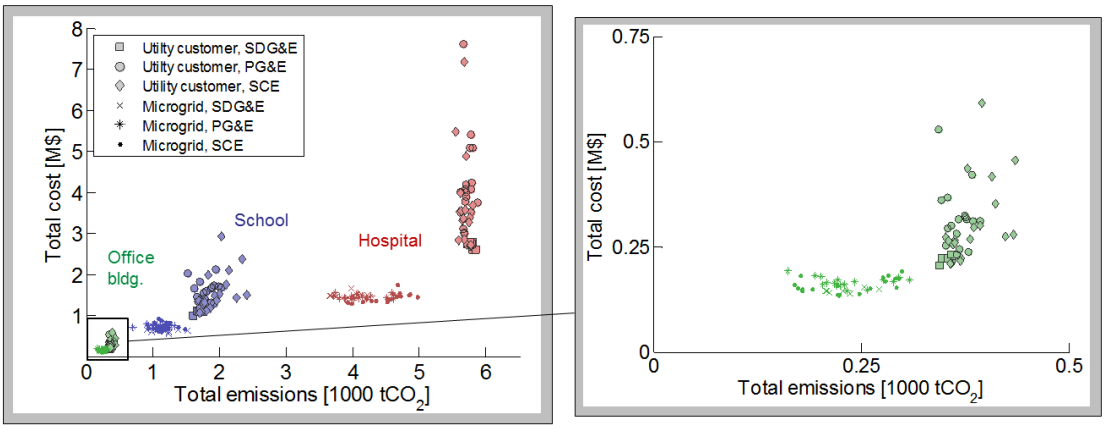

Figure 4.2. Total cost versus total emissions for all macro grid and microgrid customers.

The second type of variation is among microgrid customers, who show a wide spread in total emissions but, by contrast, a very small spread in total cost. This is the result of the modeling framework, which is built on least-cost optimization. Each microgrid seeks a configuration of energy resources that minimizes total cost, irrespective of resulting emissions—so cost totals are consistent across building types, but emissions totals need not be. This means optimal solutions are likely non-unique: there are various configuration pathways (i.e., combinations of gas generators, solar PV, energy storage, and thermal resources) to least cost, and each differs in emissions, as Fig. 4.3 shows (each result therein corresponds to a cost/emission total in Fig. 4.2). To some extent, then, regulators have room to enact policy measures that further reduce emissions without burdening customers by driving up their costs.

Interestingly, total cost results converge for microgrids adopted throughout the three utility territories. This means least-cost solutions are indifferent to differences across utilities, which are electricity rates and grid reliability. In other words, the starting

point (utility-wise) matters little because the microgrid configuration (built on technology costs and fuel costs) is cost-effective independent of outside electricity prices.

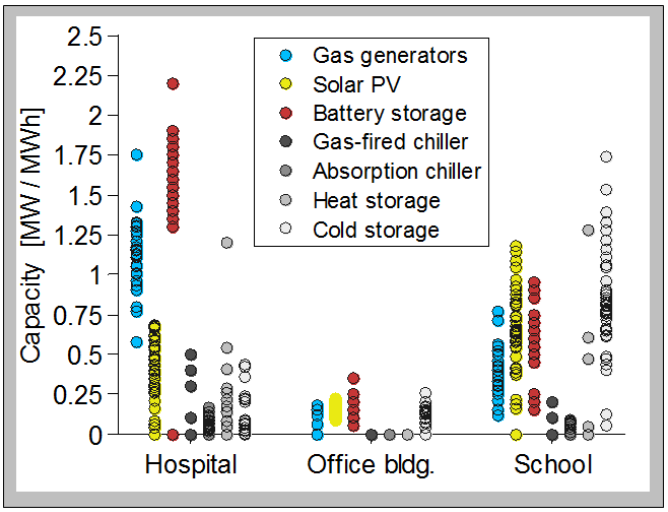

Figure 4.3. Range of microgrid configurations (i.e., technology deployment).

Results show, comprehensively, that microgrids are economical. In many cases, notably for the larger hospital microgrids, they reduce both interruption costs and energy costs (Fig. 4.4; where energy costs are the sum of investment and operating costs for DERs). In other words, investment in generating infrastructure to reduce interruption costs does not require a trade-off of increasing energy costs (which includes the cost of repaying capital). This is notable because a business case (i.e., an economic justification for investment) can then be made by pursuing either value stream (improving reliability or reducing energy costs) independently, though of course developers would pursue both. In these cases, the business case is highly robust.

By contrast, for smaller systems (the office building microgrid), there is at times a trade-off between interruption and energy costs. Size is a factor: larger microgrids (i.e., with greater electric and thermal load) are able to take advantage of CHP systems (i.e., generators that capture and re-use heat) that simultaneously improve reliability and energy efficiency (and hence cost) in the microgrid. In a sense, their electrical generation

provides free heating and cooling services that would otherwise be supplied by other means, like purchasing natural gas for chillers and furnaces. Smaller microgrids have smaller demand and therefore do not deploy the largest CHP units with the highest efficiencies; instead, they procure a greater share of energy from solar PV and battery storage and by purchasing it from the utility (Fig. 4.3).

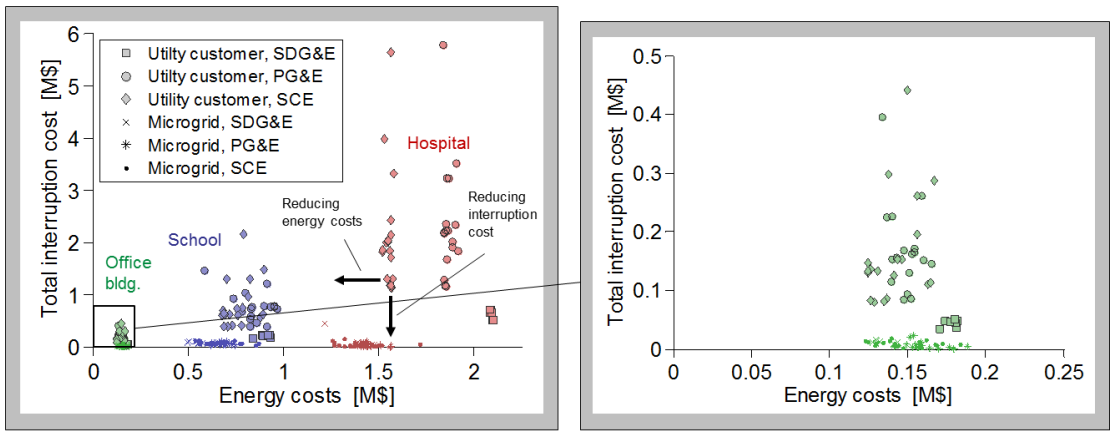

Figure 4.4. Cost shift from microgrid adoption, with interruption cost on the y-axis and all other costs (investment plus operating costs, or "energy costs") on the x-axis.

4.3.2 Technology drivers

Baseline results show that microgrids deploy a diverse set of resources to minimize cost. While each resource has a role, their contribution to meeting private goals like increasing reliability and reducing energy costs, and to meeting social goals like reducing emissions, are not necessarily equal. Those in the power industry who support grid decentralization[7] often tout associated environmental benefits, such as integrating carbon-free resources like solar PV. But the degree to which solar PV actually contributes to emissions reductions, let alone cost reductions in an industry driven by cost, is unclear.

To explore the role of technologies, a second set of models was run on top of the

[7]Grid decentralization, i.e. transitioning the grid from its current centralized paradigm of electrical generation to one built on small-scale local resources.

baseline set. In this new set, microgrid customers were re-modeled and, successively and independently, restricted from investing in solar PV and then in thermal technologies (CHP units, thermal generators, thermal storage). The subsequent shifts in cost and emissions relative to the utility customer and baseline microgrid customer show the contributions of each technology set (Fig. 4.5).

Several takeaways are clear. For larger buildings (the hospital), it is thermal resources (and not solar PV) that are the primary technology driver of emissions reductions. In some cases, hospital microgrids without thermal resources increase emissions relative to the utility customer. Solar PV does contribute to reducing emissions (emissions increase by approximately 12% on average when solar PV is restricted), but reductions are small relative to that from thermal resources (emissions increase approximately 40% on average when thermal resources are restricted). Restricting either set impacts cost little. In no case does are microgrids uneconomical when these technologies are unavailable.

For smaller microgrids (the office building and school), where CHP is less advantageous, the opposite trend is true: primary emissions reductions stem from solar PV and not thermal resources. Again, neither set of resources is independently critical to reducing cost. This is due to the fact that least-cost solutions are not unique. Restricting one technology set does not necessarily restrict all pathways to least cost, as results for the school and office building microgrids demonstrate.

4.4 Conclusion and policy implications

Supply of reliability, electricity and thermal energy services via a microgrid can be cost-effective compared to provision by a utility. There are various reasons for this. Some have to do with technology choice, others are the result of market conditions, and still others are connected to policy decisions. Those complexities aside, microgrids in California are economical and, under conditions today, produce co-benefits for system-

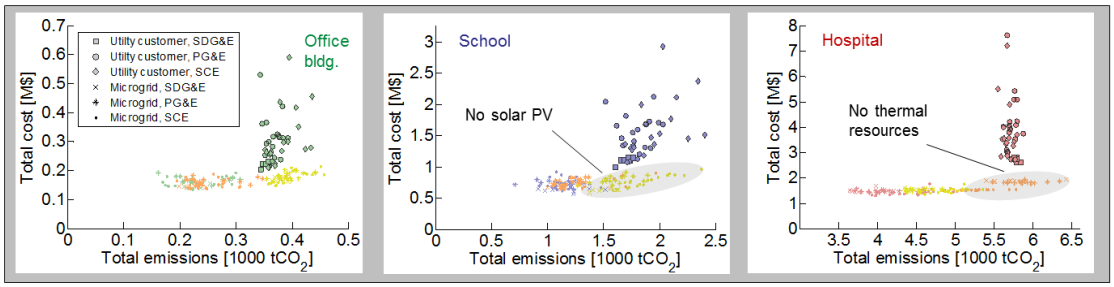

Figure 4.5. Total cost versus total emissions for selected technology sets (yellow shows the case in which solar PV is restricted; orange shows the case in which thermal resources are restricted) for the office building (left), school (middle), and hospital (right).

wide emissions reductions.

In the context of long-term climate goals, however, several points are worth nothing. Though microgrids reduce emissions now as a co-benefit, they are systems built, in part, to improve reliability—which in California means systems built on natural gas generators. Though backup operation would occur only rarely, generators could operate when grid-connected to reduce customer energy costs when sensible. California has set a goal to reduce CO_2 emissions 80% below 1990 levels by 2050. Given that the transportation sector will likely produce some emissions, such an aggressive economy-wide goal implies little carbon emissions from the rest of the energy system. Ubiquitous microgrids built on gas generators are fundamentally at odds with long-term climate goals.

Policy makers have some control over important parameters. For example, carbon taxes on direct emissions would likely shift investment to solar PV and further reduce emissions without increasing total cost (see earlier discussion regarding cost and emissions spreads in Fig. 4.2). Further modeling is needed but could show how far a carbon tax could drive down emissions before it begins simply burdening customers.

In addition, policy makers can address electric tariffs. Specific electric tariffs designed for microgrids—which are highly flexible systems that can in theory respond to

real-time pricing—could better align actual system costs, including the cost of emitting in the wholesale market, with electricity rates. Such tariffs could incentive microgrids to self-consume local renewable power when the bulk grid is carbon intensive and electricity prices are high, as well as to store renewable power when the bulk grid is producing mostly green power. It is unclear at present what those special tariffs might look like.

A final comment concerns location. The modeling in this work was set in California, with emissions comparisons made against the California Independent System Operator (CAISO) wholesale market. CAISO is a relatively green grid by comparison to others throughout the U.S. The potential for microgrids to reduce emissions is highly dependent on the bulk grid of interconnection. That microgrids reduce emissions in California therefore likely bodes well for locations across the U.S. A megawatt of microgrid-generated power in the Midwest might be worth substantially more, in the context of emissions reductions, than the same megawatt generated in California. Further modeling is needed to explore jurisdictional differences, however, as electricity rates and tariff structures also vary across the U.S. Such modeling would show both to potential investors where business cases are best, as well as to regulators where associated emissions reductions are greatest.

Chapter 4, in part, is currently being prepared for submission for publication of material. Hanna, Ryan; Kleissl, Jan; Victor, David G. The dissertation author is the primary investigator and author of this article.

Chapter 5

Concluding Remarks

This dissertation has taken place in the midst of a time of transformation in the electric power industry, and indeed to its physical embodiment the electric power grid. The adoption rate of utility-scale renewables has increased dramatically. Many state governments are calling for 30% or 50% renewable energy portfolio standards; industry and interest groups believe much higher numbers are achievable. At the customer scale, adoption rates for distributed energy resources too have seen substantial increase—notably solar PV and increasingly battery energy storage, both stationary and in electric vehicles. Over the course of this dissertation, with aid in the form of government subsidies, a strong and self-sustaining industry and market for renewables and distributed energy technologies has formed in the U.S., and in California in particular. Government support is focused, and public support for decarbonization is strong.

One area of intent government focus has been to address grid modernization—especially in the wake of multiple deadly Atlantic superstorms (notably Sandy in 2012 and Maria in 2017) that caused billions of dollars in damage throughout the Caribbean islands and northeast U.S. Microgrids have been a focal point of that conversation. Indeed, many states have initiated proceedings that aim to improve grid reliability and resiliency via microgrids, among other means. Policy support has spurred utility microgrids, while in the private sector technology, market, and policy forces are combining to make microgrids

economically viable for some utility customers.

It is in the broader context of such development that this dissertation is set. Herein, we have analyzed the business case for microgrids that provide energy services to customers within (Chapter 1). A broad review of the literature then showed that, though the number of microgrid models capable of such analysis is numerous, few touch reliability aspects at all, and those that do do so crudely or simplistically. At the same time, industry analysts maintain that reliability will be a primary driver of future investment and market growth. And so we set out to create a new model that combines the utility of existing models with new functionality that addresses reliability.

Another review of literature showed new reliability evaluation methods would be required. In Chapter 2 we present that method—cross-entropy Monte Carlo simulation applied to the case of microgrids. We have built it specifically to integrate with our larger optimization model that evaluates microgrid economics while considering reliability. In Chapter 3 we present that model. Its novelty lies in its treatment of reliability; it extends the modeling literature as the first framework that solves the sizing/scheduling problem in microgrids while treating reliability costs realistically and explicitly as an objective. The new algorithms in Chapter 2 and Chapter 3 are the core methodological contributions of this dissertation.

Lastly, in Chapter 4, we applied the new models in a systematic study of microgrid emissions throughout California. During this dissertation, many industry observers have called for widespread adoption of DERs and microgrids. Their reasoning, often predictably, includes the standard claim that adoption will reduce carbon system-wide emissions. Little empirical evidence exists on the topic, however. Our study, the first to provide these data systematically for early adopters throughout California, showed, at present, that there are indeed co-benefits for carbon emissions reductions derived from private investment in microgrids. Those reductions are not guaranteed, however, and

future analyses will be needed, especially as the bulk grid becomes less carbon intensive over time.

Over the course of this work, we have demonstrated how microgrids can provide benefits to customers by reducing costs and improving electric service reliability, as well as society at large, insofar as microgrids integrate renewables and reduce marginal greenhouse gas emissions. We have also discussed where, in the context of microgrids and decarbonization, future research is needed and how the tools we have built in this dissertation can contribute. It is our hope that the assessments presented in this dissertation would assist regulators and policy makers in their efforts to decarbonize and modernize the electric grid.

Bibliography

Ahmad Khan, A., Naeem, M., Iqbal, M., Qaisar, S., Anpalagan, A., 2016. A compendium of optimization objectives, constraints, tools and algorithms for energy management in microgrids. Renewable and Sustainable Energy Reviews 58, 1664–1683.

Anderson, K. H., DiOrio, N. A., Cutler, D. S., Butt, R. S., Richards, A., 2017. Increasing resiliency through renewable energy microgrids. Journal of Energy Management 2 (NREL/JA-7A40-69034).

Arefifar, S. A., Mohamed, Y. A.-R. I., 2014. DG mix, reactive sources and energy storage units for optimizing microgrid reliability and supply security. IEEE Transactions on Smart Grid 5 (4), 1835–1844.

Asmus, P., Mar 2016. Market Data: Microgrids. Navigant Consulting, Inc.

Asmus, P., May 2017. Microgrids without Subsidy? Check Out the C&I Market. [Online; posted 19-May-2017].
URL http://microgridmedia.com/microgrids-without-subsidy-check-ci-market/

Bahramirad, S., Khodaei, A., Svachula, J., Aguero, J. R., Mar 2015. Building Resilient Integrated Grids: One neighborhood at a time. IEEE Electrification Magazine 3 (1), 48–55.

Bahramirad, S., Reder, W., Khodaei, A., Dec 2012. Reliability-constrained optimal sizing of energy storage system in a microgrid. IEEE Transactions on Smart Grid 3 (4), 2056–2062.

Banerjee, B., Islam, S. M., 2011. Reliability based optimum location of distributed generation. International Journal of Electrical Power & Energy Systems 33 (8), 1470–1478.

Basu, A. K., Chowdhury, S. P., Chowdhury, S., Paul, S., dec 2011. Microgrids: Energy management by strategic deployment of DERs—A comprehensive survey. Renewable and Sustainable Energy Reviews 15 (9), 4348–4356.

Beer, S., Gómez, T., Dallinger, D., Momber, I., Marnay, C., Stadler, M., Lai, J., 2012. An economic analysis of used electric vehicle batteries integrated into commercial building microgrids. IEEE Transactions on Smart Grid 3 (1), 517–525.

Bernal-Agustín, J. L., Dufo-López, R., 2009. Multi-objective design and control of hybrid systems minimizing costs and unmet load. Electric Power Systems Research 79 (1), 170–180.

Bie, Z., Zhang, P., Li, G., Hua, B., Meehan, M., Wang, X., 2012. Reliability evaluation of active distribution systems including microgrids. IEEE Transactions on Power Systems 27 (4), 2342–2350.

Billinton, R., Allan, R. N., 1996. Reliability Evaluation of Power Systems. Springer US.

Billinton, R., Bagen, Apr 2006. Generating capacity adequacy evaluation of small stand-alone power systems containing solar energy. Reliability Engineering & System Safety 91 (4), 438–443.

Billinton, R., Karki, R., 2001. Capacity expansion of small isolated power systems using PV and wind energy. IEEE Transactions on Power Systems 16 (4), 892–897.

Billinton, R., Li, W., 1994. Reliability Assessment of Electric Power Systems Using Monte Carlo Methods. Springer US.

Borges, C. L., Falcao, D. M., 2006. Optimal distributed generation allocation for reliability, losses, and voltage improvement. International Journal of Electrical Power & Energy Systems 28 (6), 413–420.

Bronski, P., Creyts, J., Crowdis, M., Doig, S., Glassmire, J., Guccione, L., Lilienthal, P., Mandel, J., Rader, B., Seif, D., Tocco, H., Touati, H., 2015. The Economics of Load Defection: How Grid-connected Solar-plus-battery Systems Will Compete With Traditional Electric Service, Why it Matters, and Possible Paths Forward. Rocky Mountain Institute.
URL http://www.rmi.org/electricity_load_defection

"California Carbon Dashboard", 2015.
URL http://calcarbondash.org/

Cardoso, G., Stadler, M., Siddiqui, A., Marnay, C., DeForest, N., Barbosa-Póvoa, A., Ferrão, P., 2013. Microgrid reliability modeling and battery scheduling using stochastic linear programming. Electric Power Systems Research 103, 61–69.

Christiansen, C., Murray, B., Conway, G., 2015. Energy Storage Study: Funding and Knowledge Sharing Priorities. AECOM.

Clerc, M., 2006. Particle Swarm Optimization. Wiley.

Costa, P. M., Matos, M. A., 2005. Reliability of distribution networks with microgrids. In: 2005 IEEE Russia Power Tech. IEEE, pp. 1–7.

Costa, P. M., Matos, M. A., 2009. Assessing the contribution of microgrids to the reliability of distribution networks. Electric Power Systems Research 79 (2), 382–389.

Cutler, D., Olis, D., Elgqvist, E., Li, X., Laws, N., DiOrio, N., Walker, A., Anderson, K., Sep 2017. REopt: A Platform for Energy Systems Integration and Optimization. Tech. Rep. NREL/TP-7A40-70022, National Renewable Energy Laboratory.

da Silva, A., Fernandez, R., Singh, C., Feb 2010. Generating capacity reliability evaluation based on Monte Carlo simulation and cross-entropy methods. IEEE Transactions on Power Systems 25 (1), 129–137.

Daneshi, H., Khorashadi-Zadeh, H., 2012. Microgrid energy management system: A study of reliability and economic issues. In: 2012 IEEE Power and Energy Society (PES) General Meeting.

Darrow, K., Hampson, A., 2013. The Effect of Departing Load Charges on the Costs and Benefits of Combined Heat and Power. ICF International.

DeForest, N., Mendes, G., Stadler, M., Feng, W., Lai, J., Marnay, C., 2014. Optimal deployment of thermal energy storage under diverse economic and climate conditions. Applied Energy 119, 488–496.

Deru, M., Field, K., Studer, D., Benne, K., Griffith, B., Torcellini, P., Liu, B., Halverson, M., Winiarski, D., Rosenberg, M., Yazdanian, M., Huang, J., Crawley, D., 2011. US Department of Energy Commercial Reference Building Models of the National Building Stock. National Renewable Energy Laboratory.

Ding, Z., Lee, W.-J., 2015. A stochastic microgrid operation scheme to balance between system reliability and greenhouse gas emission. IEEE Transactions on Industry Applications, 1–1.

Eberhart, R., Yuhui Shi, 2001. Particle swarm optimization: Developments, applications and resources. Proceedings of the 2001 Congress on Evolutionary Computation (IEEE Cat. No.01TH8546) 1, 81–86.

Erdinc, O., Uzunoglu, M., Apr 2012. Optimum design of hybrid renewable energy systems: Overview of different approaches. Renewable and Sustainable Energy Reviews 16 (3), 1412–1425.

Fathima, A. H., Palanisamy, K., May 2015. Optimization in microgrids with hybrid energy systems – a review. Renewable and Sustainable Energy Reviews 45, 431–446.

Firestone, R. M., Marnay, C., Maribu, K. M., 2006. The Value of Distributed Generation under Different Tariff Structures. Lawrence Berkeley National Laboratory.

Gamarra, C., Guerrero, J. M., Aug 2015. Computational optimization techniques applied to microgrids planning: A review. Renewable and Sustainable Energy Reviews 48, 413–424.

Georgilakis, P. S., Katsigiannis, Y. A., Jan 2009. Reliability and economic evaluation of small autonomous power systems containing only renewable energy sources. Renewable Energy 34 (1), 65–70.

Ghatikar, G., Mashayekh, S., Stadler, M., Yin, R., Liu, Z., apr 2016. Distributed energy systems integration and demand optimization for autonomous operations and electric grid transactions. Applied Energy 167, 432–448.

Gonzalez-Fernandez, R. A., da Silva, A. M. L., Nov 2011. Reliability assessment of time-dependent systems via sequential cross-entropy Monte Carlo simulation. IEEE Transactions on Power Systems 26 (4), 2381–2389.

Gu, W., Wu, Z., Bo, R., Liu, W., Zhou, G., Chen, W., Wu, Z., Jan 2014. Modeling, planning and optimal energy management of combined cooling, heating and power microgrid: A review. International Journal of Electrical Power & Energy Systems 54, 26–37.

Hanna, R., Disfani, V., Kleissl, J., 2017a. Reliability evaluation for microgrids using cross-entropy Monte Carlo simulation. In: 2018 IEEE Conference on Probabilistic Methods Applied to Power Systems. *(Under review)*.

Hanna, R., Disfani, V., Kleissl, J., Victor, D., 2017b. A new simulation model to develop and assess business cases for commercial microgrids. In: 2017 IEEE North American Power Symposium (NAPS).

Hanna, R., Disfani, V. R., Kleissl, J., Victor, D. G., 2017c. The economic value of reliability for microgrids: Modeling reliability costs and value. *(To be submitted)*.

Hanna, R., Ghonima, M., Kleissl, J., Tynan, G., Victor, D. G., 2017d. Evaluating business models for microgrids: Interactions of technology and policy. Energy Policy 103, 47–61.

Hittinger, E., Wiley, T., Kluza, J., Whitacre, J., Jan 2015. Evaluating the value of batteries in microgrid electricity systems using an improved energy systems model. Energy Conversion and Management 89, 458–472.

IEEE Committee Report, Nov 1979. IEEE Reliability Test System. IEEE Transactions on Power Apparatus and Systems 98 (6), 2047–2054.

Iqbal, M., Azam, M., Naeem, M., Khwaja, A., Anpalagan, A., Nov 2014. Optimization classification, algorithms and tools for renewable energy: A review. Renewable and Sustainable Energy Reviews 39, 640–654.

Ismail, M., Moghavvemi, M., Mahlia, T., May 2013. Current utilization of microturbines as a part of a hybrid system in distributed generation technology. Renewable and Sustainable Energy Reviews 21, 142–152.

Kanase-Patil, A., Saini, R., Sharma, M., Nov 2011. Sizing of integrated renewable energy system based on load profiles and reliability index for the state of uttarakhand in india. Renewable Energy 36 (11), 2809–2821.

Kann, S., Shiao, M., Honeyman, C., Perea, A., Jones, J., Smith, C., Gallagher, B., Moskowitz, S., Baca, J., Rumery, S., Holm, A., O'Brien, K., 2016. U.S. Solar Market Insight 2016 Q2. Solar Energy Industries Association.

Karki, R., Billinton, R., 2001. Reliability/cost implications of PV and wind energy utilization in small isolated power systems. IEEE Transactions on Energy Conversion 16 (4), 368–373.

Khan, A. A., Naeem, M., Iqbal, M., Qaisar, S., Anpalagan, A., May 2016. A compendium of optimization objectives, constraints, tools and algorithms for energy management in microgrids. Renewable and Sustainable Energy Reviews 58, 1664–1683.

Khodayar, M. E., Barati, M., Shahidehpour, M., Dec 2012. Integration of high reliability distribution system in microgrid operation. IEEE Transactions on Smart Grid 3 (4), 1997–2006.

Kufeoglu, S., Lehtonen, M., Jun 2016. A review on the theory of electric power reliability worth and customer interruption costs assessment techniques. In: 2016 13th International Conference on the European Energy Market (EEM). IEEE.

Kurtovich, M., Zafar, M., 2016. California Electric Reliability Invester-Owned Utilities Performance Review 2006-2015. California Public Utilities Commission.

Lee, M., Soto, D., Modi, V., Sep 2014. Cost versus reliability sizing strategy for isolated photovoltaic micro-grids in the developing world. Renewable Energy 69, 16–24.

Liang, H., Zhuang, W., Mar 2014. Stochastic modeling and optimization in a microgrid: A survey. Energies 7 (4), 2027–2050.

Lovelady, D., Yang, B., Natti, S., Mueller, H., Tao, L., 2013. A scenario driven reliability assessment approach for microgrids. In: 2013 IEEE Power & Energy Society General Meeting. Institute of Electrical and Electronics Engineers (IEEE).

Maribu, K. M., Firestone, R. M., Marnay, C., Siddiqui, A. S., 2007. Distributed energy resources market diffusion model. Energy Policy 35 (9), 4471–4484.

Maribu, K. M., Fleten, S.-E., 2008. Combined Heat and Power in Commercial Buildings: Investment and Risk Analysis. The Energy Journal 29 (2), 123–150.

Marnay, C., Blanco, R., LaCommare, K. H., Kawann, C., Osborn, J. G., Rubio, F. J., 2000. Integrated Assessment of Dispersed Energy Resources Deployment. Lawrence Berkeley National Laboratory.

Marnay, C., Venkataramanan, G., Stadler, M., Siddiqui, A. S., Firestone, R., Chandran, B., 2008. Optimal technology selection and operation of commercial-building microgrids. IEEE Transactions on Power Systems 23 (3), 975–982.

Maurovich-Horvat, L., De Reyck, B., Rocha, P., Siddiqui, A. S., 2016. Optimal Selection of Distributed Energy Resources Under Uncertainty and Risk Aversion. IEEE Transactions on Engineering Management.

Meiqin, M., Meihong, J., Wei, D., Chang, L., Jun 2010. Multi-objective economic dispatch model for a microgrid considering reliability. In: The 2nd International Symposium on Power Electronics for Distributed Generation Systems. Institute of Electrical and Electronics Engineers (IEEE).

Mendes, G., Feng, W., Stadler, M., Steinbach, J., Lai, J., Zhou, N., Marnay, C., Ding, Y., Zhao, J., Tian, Z., Zhu, N., 2014. Regional analysis of building distributed energy costs and CO_2 abatement: A U.S.-China comparison. Energy and Buildings 77, 112–129.

Mendes, G., Marnay, C., Silva, C., Correia de Barros, M., Stadler, M., Ferrão, P., Loakimidis, C., 2013. Microgrid Adoption Patterns in Portugal and the U.S. In: Santi-

ago 2013 Symposium on Microgrids.

Momber, I., Gomez, T., Venkataramanan, G., Stadler, M., Beer, S., Lai, J., Marnay, C., Battaglia, V., 2010. Plug-in electric vehicle interactions with a small office building: An economic analysis using DER-CAM. IEEE PES General Meeting, 1–8.

Moradi, M. H., Eskandari, M., Showkati, H., 2014. A hybrid method for simultaneous optimization of DG capacity and operational strategy in microgrids utilizing renewable energy resources. International Journal of Electrical Power & Energy Systems 56, 241–258.

Nottrott, A., Kleissl, J., Washom, B., 2013. Energy dispatch schedule optimization and cost benefit analysis for grid-connected, photovoltaic-battery storage systems. Renewable Energy 55, 230–240.

Nykvist, B., Nilsson, M., 2015. Rapidly falling costs of battery packs for electric vehicles. Nature Climate Change 5 (April), 329—-332.

Office of Energy Efficiency and Renewable Energy, 2015. Commercial reference buildings.
URL http://energy.gov/eere/buildings/commercial-reference-buildings

Parhizi, S., Lotfi, H., Khodaei, A., Bahramirad, S., 2015. State of the art in research on microgrids: A review. IEEE Access 3, 890–925.

Poli, R., Kennedy, J., Blackwell, T., Aug 2007. Particle swarm optimization. Swarm Intelligence 1 (1), 33–57.

Reitenbach, G., Mar 2016. Emerging Microgrid Business Models. POWER Magazine.

Research, N. Y. S. E., Authority, D., 2014. Toward a Clean Energy Future: A Strategic Outlook. New York State Energy Research and Development Authority.

Rocha, P., Kaut, M., Siddiqui, A. S., Apr 2016. Energy-efficient building retrofits: An assessment of regulatory proposals under uncertainty. Energy 101, 278–287.

Ru, Y., Kleissl, J., Martinez, S., 2013. Storage size determination for grid-connected photovoltaic systems. IEEE Transactions on Sustainable Energy 4 (1), 68–81.

Rubinstein, R. Y., Kroese, D. P., 2004. The Cross-Entropy Method. Springer New York.

Saadeh, O., 2015. North American Microgrids 2015: Advancing Beyond Local Energy

Optimization.

Shi, Y., Eberhart, R., 1998. A modified particle swarm optimizer. In: 1998 IEEE International Conference on Evolutionary Computation Proceedings. IEEE World Congress on Computational Intelligence. IEEE.

Siddaiah, R., Saini, R., May 2016. A review on planning, configurations, modeling and optimization techniques of hybrid renewable energy systems for off grid applications. Renewable and Sustainable Energy Reviews 58, 376–396.

Siddiqui, A., Marnay, C., Edwards, J., Firestone, R., Ghosh, S., Stadler, M., 2005. Effects of carbon tax on microgrid combined heat and power adoption.

Siddiqui, A. S., Firestone, R. M., Ghosh, S., Stadler, M., Edwards, J. L., Marnay, C., 2003. Distributed Energy Resources with Combined Heat and Power Applications. Lawrence Berkeley National Laboratory.

Siddiqui, A. S., Marnay, C., Firestone, R. M., Zhou, N., 2007. Distributed Generation with Heat Recovery and Storage. Journal of Energy Engineering 133 (3), 181–210.

Siler-Evans, K., Azevedo, I. L., Morgan, M. G., May 2012. Marginal Emissions Factors for the U.S. Electricity System. Environmental Science & Technology 46 (9), 4742–4748.

Simpkins, T., Anderson, K., Cutler, D., Olis, D., Sep 2016. Optimal sizing of a solar-plus-storage system for utility bill savings and resiliency benefits. In: 2016 IEEE Power & Energy Society Innovative Smart Grid Technologies Conference (ISGT).

Sinha, S., Chandel, S., Oct 2015. Review of recent trends in optimization techniques for solar photovoltaic–wind based hybrid energy systems. Renewable and Sustainable Energy Reviews 50, 755–769.

Soshinskaya, M., Crijns-Graus, W. H. J., Guerrero, J. M., Vasquez, J. C., dec 2014. Microgrids: Experiences, barriers and success factors. Renewable and Sustainable Energy Reviews 40, 659–672.

Stadler, M., Cardoso, G., Mashayekh, S., Forget, T., DeForest, N., Agarwal, A., Schönbein, A., Jan 2016. Value streams in microgrids: A literature review. Applied Energy 162, 980–989.

Stadler, M., Groissböck, M., Cardoso, G., Marnay, C., 2014. Optimizing Distributed Energy Resources and building retrofits with the strategic DER-CAModel. Applied

Energy 132, 557–567.

Stadler, M., Kloess, M., Groissböck, M., Cardoso, G., Sharma, R., Bozchalui, M. C., Marnay, C., 2013. Electric storage in California's commercial buildings. Applied Energy 104, 711–722.

Stadler, M., Marnay, C., Siddiqui, A. S., Lai, J., Aki, H., 2009a. Integrated Building Energy Systems Design Considering Storage Technologies. Lawrence Berkeley National Laboratory.

Stadler, M., Marnay, C., Siddiqui, A. S., Lai, J., Coffey, B., Aki, H., 2009b. Effect of Heat and Electricity Storage and Reliability on Microgrid Viability: A Study of Commercial Buildings in California and New York States. Lawrence Berkeley National Laboratory.

Stadler, M., Siddiqui, A., Marnay, C., Aki, H., Lai, J., 2011. Control of greenhouse gas emissions by optimal DER technology investment and energy management in zero-net-energy buildings. European Transactions on Electrical Power 21 (2), 1291–1309.

Sullivan, M. J., Mercurio, M., Schellenberg, J., Jun 2009. Estimated Value of Service Reliability for Electric Utility Customers in the United States.

Sullivan, M. J., Mercurio, M. G., Schellenberg, J. A., Eto, J. H., Jul 2010. How to estimate the value of service reliability improvements. In: IEEE PES General Meeting. IEEE.

Sullivan, M. J., Schellenberg, J., Blundell, M., Jan 2015. Updated Value of Service Reliability Estimates for Electric Utility Customers in the United States. Lawrence Berkeley National Laboratory, Report No. LBNL-6941E.

Tollefson, G., Billinton, R., Wacker, G., 1991. Comprehensive bibliography on reliability worth and electrical service consumer interruption costs: 1980-90. IEEE Transactions on Power Systems 6 (4), 1508–1514.

Tollefson, G., Billinton, R., Wacker, G., Chan, E., Aweya, J., 1994. A canadian customer survey to assess power system reliability worth. IEEE Transactions on Power Systems 9 (1), 443–450.

Upadhyay, S., Sharma, M., Oct 2014. A review on configurations, control and sizing methodologies of hybrid energy systems. Renewable and Sustainable Energy Reviews 38, 47–63.

US Energy Information Administration, 2015. Natural Gas Prices.
URL http://www.eia.gov/dnav/ng/ng_pri_sum_dcu_SCA_m.htm

US Energy Information Administration, 2016. Short-term Energy Outlook (STEO) 2016. US Energy Information Administration.

von Appen, A. J., Marnay, B. C., Stadler, C. M., Momber, D. I., Klapp, E. D., Scheven, F. A. V., 2011. Assessment of the economic potential of microgrids for reactive power supply. 8th International Conference on Power Electronics - ECCE Asia, 809–816.

Wang, S., Li, Z., Wu, L., Shahidehpour, M., Li, Z., Aug 2013. New metrics for assessing the reliability and economics of microgrids in distribution system. IEEE Transactions on Power Systems 28 (3), 2852–2861.

Wilson, A., Jun 2017. Microgrid Deployment Tracker 2Q17. Navigant Consulting, Inc.

Wilson, R., Jul 2002. Architecture of Power Markets. Econometrica 70 (4), 1299–1340.

Woo, C.-K., Pupp, R. L., Feb 1992. Costs of service disruptions to electricity consumers. Energy 17 (2), 109–126.

Yokoyama, R., Niimura, T., Saito, N., 2008. Modeling and evaluation of supply reliability of microgrids including pv and wind power. In: 2008 IEEE Power and Energy Society (PES) General Meeting–Conversion and Delivery of Electrical Energy in the 21st Century.

Zachar, M., Daoutidis, P., Oct 2015. Understanding and predicting the impact of location and load on microgrid design. Energy 90, 1005–1023.

Zachar, M., Trifkovic, M., Daoutidis, P., Oct 2015. Policy effects on microgrid economics, technology selection, and environmental impact. Computers & Chemical Engineering 81, 364–375.

Zhang, D., Evangelisti, S., Lettieri, P., Papageorgiou, L. G., Jun 2015. Optimal design of CHP-based microgrids: Multiobjective optimisation and life cycle assessment. Energy 85, 181–193.

Zhou, P., Jin, R., Fan, L., May 2016. Reliability and economic evaluation of power system with renewables: A review. Renewable and Sustainable Energy Reviews 58, 537–547.

Zidan, A., Gabbar, H. A., Eldessouky, A., Dec 2015. Optimal planning of combined heat and power systems within microgrids. Energy 93, 235–244.